SHEDDING LIGHT INTO THE DARKNESS: USING MOLECULAR DATA TO RESOLVE WHALEFISH (CETOMIMIDAE) PHYLOGENETICS AND THE HISTORICAL DEMOGRAPHY OF POPULATIONS OF DEEP-PELAGIC FISHES

A Thesis

by

MAX D. WEBER

Submitted to the Office of Graduate and Professional Studies of
Texas A&M University
in partial fulfillment of the requirements for the degree of

MASTER OF SCIENCE

Chair of Committee,	Ron I. Eytan
Committee Members,	Jaime R. Alvarado Bremer
	R.J. David Wells
Intercollegiate Faculty Chair,	Anja Schulze

May 2020

Major Subject: Marine Biology

ABSTRACT

The deep-pelagic is the largest biome on planet Earth. Despite its size the animal life inhabiting the deep-pelagic is severely underrepresented in global marine biological records. Accordingly, many questions related to the demographic histories and taxonomic relationships of deep-pelagic fishes remain unanswered. We utilized molecular data to investigate taxonomic issues related to the family Cetomimidae (the whale fishes) and to infer the demographic histories of 13 species of deep-pelagic fishes.

Family Cetomimidae has long been plagued by taxonomic issues. Even the matching of male and female cetomimids has proven difficult due to striking sexual dimorphism within the family. We constructed maximum clade credibility trees and performed bGMYC analysis to better understand whale fish taxonomy.

Our Cetomimidae tree was largely in agreement with past morphological work. Areas of disagreement regarding morphological analyses included a clade comprising Cetostoma + Ditropichthys, as well as paraphyly within Gyrinomimus with respect to Cetomimus. Our bGMYC analysis revealed *Cetostoma regani* to be a cryptic species complex, comprised of two operational taxonomic units that diverged ~3.1 Ma ago. We identified two new putative Cetomimus species, as well. Finally, we were able to match all of our male samples to three different female species.

Reconstructions of historic demography shed light on how past ecological/evolutionary events impacted the population size of a given species. By understanding the past we can begin to understand how populations will behave in

response to current and future changes to their habitat. Mitochondrial and nuclear DNA markers were sequenced for 13 low-latitude deep-pelagic fish species representing eight families. Demographic histories were reconstructed using two sets of analyses. Historic population expansions were inferred for eight species using frequency-based statistics, while our extended Bayesian skyline plots (EBSPs) detected expansions in five of those eight species. Our EBSPs provided estimated dates of expansion that ranged from 80 ky ago to 270 ka ago. All of these dates appear to coincide with periods of warm sea surface temperature (SST) at approximately 41° of latitude in the North Atlantic, the northernmost range for many low-latitude deep-pelagic fishes.

DEDICATION

This work is dedicated my wife and parents.

ACKNOWLEDGEMENTS

I would like to thank my advisor Dr. Ron I. Eytan for his guidance through my graduate studies. Furthermore, Ron gave me the opportunity to work on the DEEPEND project, which was a truly awesome experience, and something I am incredibly grateful for. I would like to thank my committee members Dr. R.J. David Wells and Dr. Jaime Alvarado Bremer. My Masters project took many years to complete, but every time I was ready to move forward with the process they were eager to help me do so. I would like to thank everyone in the DEEPEND consortium who made it possible for me to collect my data and conduct this research. I would like to thank my lab mate Josh Carter for his support in my lab work. Finally, I must thank Travis Richards my fellow graduate student and DEEPEND researcher. Travis went on five research cruises with me, many times with the sole purpose of helping collect samples for genetic research. Without Travis's assistance in the field this research would not have been possible.

CONTRIBUTORS AND FUNDING SOURCES

Contributors

This work was supervised by a thesis committee consisting of Dr. Ron I. Eytan of the Marine Biology Department [advisor], Dr. Jaime Alvarado Bremer of the Marine Biology Department, and Dr. R.J. David Wells of the Marine Biology Deparment.

Dr. Tracey T. Sutton and Dr. Jon A. Moore identified the samples used throughout this thesis. I collected tissues in the field with the assistance of many DEEPEND consortium members, particularly April Cook, Dr. Ron I. Eytan, Nina Pruzinsky, Katie Bowen and Travis Richards. Lab work was aided by Josh Carter, Chase Lawson, and Jessica Alsing. Dr. Ron I. Eytan assisted in the cleaning and editing of sequences. All other work conducted for the thesis was completed by the student independently.

Funding Sources

Graduate study funding, provision of samples, and cost of labwork were provided by the Gulf of Mexico Research Iniative's DEEPEND Consortium.

NOMENCLATURE

Trachichthyoidei and Trachthyiformes. This was the name used in Moore (1993) to describe a clade consisting of the families Trachichthyidae, Monocentridae, Anomalopidae, Diretmidae, and Anoplogastridae. When used outside the context of Moore (1993) they refer to the original families identified by Moore as well as Berycidae.

Stephanoberycoidei and Stephanoberyiciformes. This was the name used in Moore (1993) to describe a clade comprised of the families Melamphaidae, Hispidoberycidae, Stephanoberycidae, Gibberichthyidae, Rondeletiidae, Barbourisiidae, Megalomycteride, and Cetomimidae. Subsequent molecular studies have shown that Berycidae is a member of this clade. When used outside the context of Moore (1993) they refer to the original families identified by Moore as well as Berycidae.

TABLE OF CONTENTS

Page

Page

Page

LIST OF FIGURES

Page

Page

LIST OF TABLES

Page

1. INTRODUCTION

1.1 Background

The deep-pelagic is traditionally defined as the marine habitat between 200 meters in depth to approximately 100 meters above the sea floor (Sutton 2013). Three distinct zones exist within the deep pelagic: the mesopelagic (200 -1000 m), bathypelagic (1000-4000 m), and abyssopelagic (4000-6000 m) (Speight and Henderson 2013). The deep pelagic constitutes approximately 95 percent of the ocean by volume, which covers 70 percent of the Earth's surface, making it the world's largest biome (Haedrich 1996; Robison 2009; Webb et al. 2010).

A number of unique abiotic factors characterize the deep-sea. Pressure increases by one atmosphere approximately every ten meters. The temperature is typically cold, 5 degrees Celsius or less by 1,000 meters, and it varies only slightly seasonally (Tyus 2011). Light levels can no longer support photosynthesis at 200 meters and light disappears entirely by 1000 meters (Haddock et al. 2010). Because photosynthesis cannot occur, the majority of energy sources must originate in shallower waters. Energy reaches this environment in the form of marine snow (detritus) or through vertically migrating organisms (Asper 1987; Hidaka et al. 2001).

Despite the enormous size of the deep-pelagic zone, its ecology is poorly understood, as less than 1 percent of the biome has been explored (Robison 2009). Furthermore, an analysis of the global database of marine biological records shows that deep-pelagic species are severely underrepresented, even when compared to deep-

benthic species (Webb et al. 2010). Scientific understanding of the deep-sea has lagged behind other environments for some time. The deep-sea was originally presumed to be a biological desert, primarily devoid of life. Accordingly, few scientific efforts were made to explore it (Webb et al. 2010). Since the Challenger expedition of 1872 our view of the deep-sea has changed dramatically (Webb et al. 2010; Sutton 2013); containing more than 5,200 described species of fishes, the deep-sea is more an oasis than a desert (Glover et al. 2019).

Fishes of the deep-sea are characterized by adaptations to this extreme environment. Bioluminescence is present in more than 80% of all deep-sea fish species, and is the only source of light in much of the deep-sea (Haddock et al. 2010; Widder 2010). Muscle mass and metabolic rate decreases with depth, as the need to escape sight-oriented predators become lower (Seibel and Drazen 2007; Sutton 2013).

1.1. Description of Key Deep-Water Fish Assemblages of the Gulf of Mexico

Myctophids (family Myctophiidae) are a species-rich group with approximately 250 described members (Catul et al. 2011; Davis et al. 2014). Myctophids are commonly known as lanternfishes, a name derived from their intrinsic bioluminescent organs, or photophores. The number and placement of photophores varies drastically by species and aids in species recognition (Herring 2007; Davis et al. 2014).

It has been suggested that myctophids are among the most numerically abundant vertebrates on the planet (Catul et al. 2011). Largely found in the mesopelagic, most species undergo a diel vertical migration. The predominant pattern is that of fish retreating to depth during the hours of daylight and entering shallower waters at night to

take advantage of the greater abundance of food (Catul et al. 2011). The number of fishes that participate in the daily migration is so large that the phenomenon first registered on sonar by the United States Navy, with the appearance of a false ocean floor, the deep scattering layer (DSL), that moved throughout the day (Barham 1966). This vertical migration is believed to be a major contributor of carbon and energy to deeper dysphotic waters (Sutton 2013).

Members of the family Stomiidae, commonly referred to as barbelled dragonfishes, are deep-sea inhabitants distributed circumglobally (Hastings et al. 2015). The family is represented by 28 genera and 294 species, making it one of the most diverse groups of deep-sea fishes. Dragonfishes are critically important ecologically in the deep-sea environment, as they are dominant upper trophic level predators in both the mesopelagic and bathypelagic (Sutton and Hopkins 1996; Sutton 2013; Hastings et al. 2015).

Stomiids exhibit a host of morphological traits that are suited to their ecological role as deep-sea predators. Many of these traits relate to modifications of the cephalic region to aid in feeding. Stomiids can open their jaw to angles exceeding 100 degrees, allowing them to swallow large prey, an important trait in an environment with exceedingly low prey densities (Kenaley 2012). A long jaw length, over 30 percent of the standard length in some species, also aids in the taking of large prey (Kenaley and Hartel 2005). Teeth are pointed and recurved to prevent the escape of prey (Paxton and Eschmeyer 1994). Mental barbels with an intrinsically bioluminescent tip are present in

most species and may serve to attract prey items (Gartner et al. 1997; Hastings et al. 2015).

The suborder Ceratioidei contains 160 described species of deep-sea anglerfishes that are primarily found in the bathypelagic (Pietsch 2005). This group possesses a number of derived characteristics such as extreme sexual dimorphism, male parasitism, and bioluminescent lures. Males are dwarfed by females and in many species live a parasitic life where they attach to females. The two will fuse together providing the male nourishment and the female sperm for reproduction (Pietsch 2005). Unlike stomiids and myctophids, anglerfishes not only utilize intrinsic bioluminescence, but they also rely on a bacterial symbiont to achieve bioluminescence. They house their symbionts in highly complex light organs on their esca, a structure derived from the first fin ray, and utilize bioluminescence as a means to attract prey (Herring 2007). Observations indicate these fishes are able to control the bacterial bioluminescence, presumably as a result of highly evolved process where secretions are released into the light organ to stimulate light emission (Pietsch 2009).

Cetomimidae is another dominant bathypelagic family, with more than 20 species. The cetomomids, or whale fishes, may be the most sexually dimorphic of any ray-finned fish families. Females are characterized by robust whale-shaped bodies, large horizontal mouths, extensive lateral line systems, and the lack of both external scales and pelvic fins (Paxton 1989; Johnson et al. 2009). Male are small (under 68 mm), elongated in shape, possessing large nasal organs, tiny horizontally oriented mouths, mosaic scales, and lacking pelvic fins (Johnson et al. 2009).

Several studies have uncovered strong ecological links between the deep pelagic and epipelagic surface waters. Myctophids are consumed by ceteaceans, birds, and pinnipeds when undergoing vertical migrations to shallower depths at night (Guinet et al. 1996). Varghese (2013) found that a deep pelagic fish from the family Stomiidae was one of five prey items most commonly consumed by the Indo-Pacific sailfish, *Istiophorus playtpterus*. A gut content analysis revealed that blue fin tuna (*Thunnus thynnus*) primarily feed on deep pelagic fishes from the families Stomiidae and Myctophidae in the Mediterranean (Battaglia et al. 2013). The newly discovered ecological importance of the deep pelagic to such economically important species highlights the importance of efforts to learn more about the environment.

1.2. Project Overview and Motivation

This research is a product of the "Deep Pelagic Nekton Dynamics of the Gulf of Mexico" (DEEPEND) Consortium, funded by the Gulf of Mexico Research Initiative. Six research cruises in the Northern Gulf of Mexico, from 2015-2018, were conducted to collect data to better understand the physical and biological characteristics of the deep pelagic zone in the Gulf of Mexico (GoM).

Fishes were obtained through trawls with a "Multiple Opening and Closing Net and Environmental Sensing System" (MOCNESS). This system is comprised of six nets that can be opened and closed independently by an operator, allowing for sampling to occur at discrete depth zones. Due to the rarity of the fishes collected on the cruises, mitochondrial cytochrome oxidase I (COI) was sequenced for 10 individuals for each putative species we collected. This marker is widely used to identify and barcode

species, and our COI sequences frequently represented the first molecular data available for these species. This sequence data provided us the opportunity to investigate larger questions that were previously impossible to answer, due to insufficient sample sizes.

In particular we wished to investigate the phylogenetic relationships of the family Cetomimidae and attempt to match male and female species within the family as it is characterized by extreme sexual dimorphism. To date only one male and female species have been matched, and the phylogenetic relationships within the group have been poorly resolved, due to an overall lack of samples and sequence data. We also sought to better understand the demographic histories of the fishes that reside in the deep pelagic of the GoM. The demographic histories of deep-pelagic fishes are currently unknown, and such knowledge is critical to understanding how the community responds to major environmental changes.

1.2 Objectives

There were two research objectives coming out of the DEEPEND project utilizing genetic data from deep-sea fishes:

1. For our first objective we utilized molecular data to investigate three areas of inquiry related to the family Cetomimidae (whale fishes).

    (i) What are the phylogenetic relationships between the families that comprise the clade Stephanoberycoidei?

    (ii) What are the phylogenetic relationships within the family Cetomimidae?,

    (iii) Can we match male and female cetomimid species?

2. For our second objective we utilized genetic data (mitochondrial cytochrome oxidase I (COI) and three nuclear DNA sequence markers) to answer the following questions related to demographic changes in thirteen deep pelagic fish species in the Gulf of Mexico.

    (i) Have there been detectable long-term effective population size changes in thirteen GoM deep pelagic fish species?

    (ii) What long-term environmental trends can explain the changes we infer?

1.3 References

Asper, V. L. 1987. Measuring the flux and sinking speed of marine snow aggregates. Deep Sea Research Part A. Oceanographic Research Papers 34:1-17.

Barham, E. G. 1966. Deep scattering layer migration and composition: observations from a diving saucer. Science 151:1399-1403.

Battaglia, P., F. Andaloro, P. Consoli, V. Esposito, D. Malara, S. Musolino, C. Pedà, and T. Romeo. 2013. Feeding habits of the Atlantic bluefin tuna, Thunnus thynnus (L. 1758), in the central Mediterranean Sea (Strait of Messina). Helgoland Marine Research 67:97.

Catul, V., M. Gauns, and P. Karuppasamy. 2011. A review on mesopelagic fishes belonging to family Myctophidae. Reviews in Fish Biology and Fisheries 21:339-354.

Davis, M. P., N. I. Holcroft, E. O. Wiley, J. S. Sparks, and W. L. Smith. 2014. Species-specific bioluminescence facilitates speciation in the deep sea. Marine Biology 161:1139-1148.

Gartner, J. V., R. E. Crabtree, and K. J. Sulak. 1997. Feeding At Depth. Pp. 115-193. Fish physiology. Elsevier, Cambridge, MA.

Glover, A., N. Higgs, and T. Horton. 2019. WoRDSS: World Register of Deep-Sea Species. http://www.marinespecies.org/deepsea/aphia.php?p=tax details&id=11676

Guinet, C., Y. Cherel, V. Ridoux, and P. Jouventin. 1996. Consumption of marine resources by seabirds and seals in Crozet and Kerguelen waters: changes in relation to consumer biomass Antarctic Science 8:23-30.

Haddock, S. H., M. A. Moline, and J. F. Case. 2010. Bioluminescence in the sea. Annual review of marine science 2:443-493.

Haedrich, R. 1996. Deep-water fishes: evolution and adaptation in the earth's largest living spaces. Journal of Fish Biology 49:40-53.

Hastings, P. A., H. J. Walker, and G. R. Galland. 2015. Fishes: a guide to their diversity. University of California Press, Berkeley, CA.

Herring, P. J. 2007. Sex with the lights on? A review of bioluminescent sexual dimorphism in the sea. Journal of the Marine Biological Association of the United Kingdom 87:829-842.

Hidaka, K., K. Kawaguchi, M. Murakami, and M. Takahashi. 2001. Downward transport of organic carbon by diel migratory micronekton in the western equatorial Pacific:: its quantitative and qualitative importance. Deep Sea Research Part I: Oceanographic Research Papers 48:1923-1939.

Johnson, G. D., J. R. Paxton, T. T. Sutton, T. P. Satoh, T. Sado, M. Nishida, and M. Miya. 2009. Deep-sea mystery solved: astonishing larval transformations and extreme sexual dimorphism unite three fish families. Biology Letters 5:235-239.

Kenaley, C. P. 2012. Exploring feeding behaviour in deep-sea dragonfishes (Teleostei: Stomiidae): jaw biomechanics and functional significance of a loosejaw. Biological Journal of the Linnean Society 106:224-240.

Kenaley, C. P. and K. E. Hartel. 2005. A revision of Atlantic species of Photostomias (Teleostei: Stomiidae: Malacosteinae), with a description of a new species. Ichthyological Research 52:251-263.

Paxton, J. R. 1989. Synopsis of the whalefishes (family Cetomimidae) with descriptions of four new genera. Records of the Australian Museum 41:135-206.

Paxton, J. R. and W. N. Eschmeyer. 1994. Encyclopedia of fishes. University of New South Wales Press, Ranwick, Australia.

Pietsch, T. W. 2005. Dimorphism, parasitism, and sex revisited: modes of reproduction among deep-sea ceratioid anglerfishes (Teleostei: Lophiiformes). Ichthyological Research 52:207-236.

Pietsch, T. W. 2009. Oceanic Anglerfishes: Extraordinary Diversity in the Deep Sea. University of California Press, Berkeley, CA.

Robison, B. H. 2009. Conservation of deep pelagic biodiversity. Conservation Biology 23:847-858.

Seibel, B. A. and J. C. Drazen. 2007. The rate of metabolism in marine animals: environmental constraints, ecological demands and energetic opportunities. Philosophical Transactions of the Royal Society of London B: Biological Sciences 362:2061-2078.

Speight, M. R. and P. A. Henderson. 2013. Marine Ecology: Concepts and Applications. Wiley, Hoboken, NJ.

Sutton, T. 2013. Vertical ecology of the pelagic ocean: classical patterns and new perspectives. Journal of Fish Biology 83:1508-1527.

Sutton, T. T. and T. L. Hopkins. 1996. Trophic ecology of the stomiid (Pisces: Stomiidae) fish assemblage of the eastern Gulf of Mexico: Strategies, selectivity and impact of a top mesopelagic predator group. Marine Biology 127:179-192.

Tyus, H. M. 2011. Ecology and conservation of fishes. CRC press, Boca Raton, FL.

Varghese, S. P., V. S. Somvanshi, and D. K. Gulati. 2013. Ontogenetic and seasonal variations in the feeding ecology of Indo-Pacific sailfish, *Istiophorus platypterus* (Shaw, 1792) of the eastern Arabian Sea. Indian Journal of Geo-Marine Sciences 42:593-605.

Webb, T. J., E. V. Berghe, and R. O'Dor. 2010. Biodiversity's big wet secret: the global distribution of marine biological records reveals chronic under-exploration of the deep pelagic ocean. PLoS ONE 5:e10223.

Widder, E. A. 2010. Bioluminescence in the ocean: origins of biological, chemical, and ecological diversity. Science 328:704-708.

2. PHYLOGENETIC RELATIONSHIPS OF THE WHALE FISHES (FAMILY CETOMIMIDAE) AND NEW SPECIES LEVEL MATCHES OF MALES AND FEMALES

2.1 Introduction

2.1.1 Description of Family Cetomimidae

With nine recognized genera and approximately 15-20 currently recognized species, the family Cetomimidae (whale fishes) is one of the dominant bathypelagic families and may be the most abundant fish family below 1800 meters (Colgan et al. 2000; Paxton et al. 2016). Most species are small, under 200 mm standard length, however one individual from a species in the genus *Gyrinomimus* measured 390 mm in length (Paxton 1989). Inhabiting all of the world's oceans, Paxton (1989) identified two patterns of distribution for whale fishes using the four most commonly collected species. *Cetostoma regani* and *Ditropichthys storeri* have cosmopolitan distributions between fifty degrees north and forty degrees south, while two *Gyrinomimus* species have a North Pacific distribution between thirty-nine and fifty-two degrees and a circumglobal distribution in the Southern Ocean between thirty-two and seventy-two degrees south.

Cetomimids were long a source of mystery, as collections were historically comprised entirely of mature females despite the existence of more than 600 specimens (Paxton 1989). The family was defined by three synapomorphies. Whale fishes possess gill rakers in some form other than elongate and flattened and lacked both pelvic fins and pleural ribs (Paxton 1989). Other notable characteristics included a large horizontal mouth for feeding on large prey items, small eyes, whale-shaped body, lack of external scales, and extensive lateral line system (Johnson et al. 2009).

It is now known that two other deep-sea fish families, Megalomycteridae (bignose fishes) comprised entirely of males, and Mirapinnidae (tapetails) are, respectively, male and larval members of the family Cetomimidae (Johnson et al. 2009). This is astonishing given the number of morphological differences between males, females, and larvae of the family. Cetomimid males (formerly Megalomycteridae) are small (under 68 mm), elongated in shape, possess large nasal organs, tiny horizontally oriented mouths, mosaic scales, and lack pelvic fins (Johnson et al. 2009). Mirapannidae (hairyfish/tapetails) are characterized by a lack of scales and lateral lines with large mouths for copepod feeding, as well as vertically oriented fins and jaws (Bertelsen and Marshall 1956; Johnson et al. 2009)

2.1.2 How Three Families Became One

Gosline (1971) was the first to recognize a close relation between Megalomycteridae and Cetomimidae, going as far as to suggest that megalomycterids may be in fact male cetomimids. In a 1974 review Robins asserted that some of the mirappiniform fishes are prejuvenile cetomimids, but no further evidence or discussion was given (Robins 1974). De Sylva and Eschmeyer (1977) provided morphological evidence that specimens from the family Kasidoroidae (described in 1975 and placed in the order Mirapinniformes) were actually juvenile fishes from the family Gibberichthyidae. The authors further described that metamorphosis in deep-water fishes is poorly known, and "bizarre transformations involving more than one metamorphosis may be common in certain fish groups." Given the previous classification of Kasidoroidae as Mirapinniformes, De Sylva and Eschmeyer (1977)

suggested that the identity of Rousauridae, Megalomycteridae, Mirappinidae, and Eutaeniophoridae should be reexamined, as they may be "prejuvenile stages of cetomimid, berycoid, or other fishes".

Paxton (1989) rejected the notion that Megalomycteridae and Mirapinnidae were male and pre-juvenile cetomimids, based on several lines of evidence. The fin ray counts of only one of four megalomycterid genera match any of the nine cetomimid genera. Mirappiniformes differ from cetomimids (adult females) in jaw shape/size, caudal ray fin count, and the possession of a pelvic fin. Furthermore, the largest Mirappiniformes were larger in size than the smallest cetomimids. An investigation by Moore (1993) into the phylogenetic relationships of the Trachichthyiformes (Trachichthyoidei and Stephanoberycoidei) using osteology and soft anatomy did not find any evidence to reject Paxton's claims. Instead, Moore placed Mirappinidae as sister to Megalomycteridae forming a clade that was in turn sister to Cetomimidae. All three families were united by the distribution of red muscle.

It was not until 2003 that any new evidence was uncovered to reveal the relationship of the three families. Miya et al. (2003) sequenced whole mitogenomes from one hundred fishes to explore the phylogenetic relationships of higher teleost fishes. Interestingly, one sample included in study, *Parataeniophorus sp*. (Family Mirapinnidae) was nearly identical to the *Cetostoma regani* sample (Family Cetomimidae) used in the study, only differing by approximately 0.04% in all positions. Unfortunately, the *Parataeniophorus* specimen was small and the entire body was used for extraction, leaving no voucher. Miya et al. (2003) suggested that Mirapinnidae may

actually be larval cetomimids, citing a similar phenomenon in the deep-sea family Giganturidae, as giganturid larvae had been classified as members of the independent family Rosauridae until 1991 (Johnson and Bertelsen 1991). Paxton and Johnson (2005) questioned these results based on extreme morphological differences between the groups and the lack of a voucher specimen. It was believed "impossible anatomically" for Parateniophorus to transform into a cetomimid.

Finally, new specimens from the Gulf of Mexico provided the necessary vouchers and molecular evidence to solve this mystery (Johnson et al. 2009). Whole mitogenomes from fifteen species were used to create a maximum likelihood tree. This was in turn used as a backbone constraint for the construction of subsequent maximum likelihood trees for thirty-six 16s rRNA sequences. The sequences belonged to 16 putative species from the five "whale fish" families as well as two melamphaids. According to the molecular results, Mirapannidae were indeed larval whale fishes. Furthermore, Megalomycteridae (bignose fishes) known by only sixty-five specimens (all male) were male cetomimids. New transitioning samples from the juvenile stage provided additional morphological evidence in support of this conclusion.

While the maximum likelihood tree confirmed that males of the species *Ataxolepis apus* were embedded within the genera *Cetomimus* and *Gyrinomimus*, it did not link them to any particular species (Johnson et al. 2009). *Parataeniophorus gulosus* (larvae) was linked to *Cetostoma regani*. An incompletely developed nasal organ and good spermatogenic tissue suggested it would develop into a male, providing the first

tentative link of a male and female species. Unfortunately no adult male specimen was available for description.

In the most recent work on the subject, Paxton et al. (2016) wrote that of the eight known species of males, only three have been linked to females. The first species match was made for *Cetostoma regani*, with one known male specimen. The other two males have been linked to the *Cetostoma* and *Gyrinomimus* clade, but no species from either genus have been linked to a male.

Johnson et al. (2009) stated that the, "Next challenge is to link the three life stages of each species." With fourteen new male specimens collected and sequenced on the DEEPEND cruises occurring between May 2015 and August 2018, we have a unique opportunity to make more species-level matches between male and female cetomimids. Since this has been only accomplished for one species at present, it would be an invaluable contribution from the DEEPEND consortium.

2.1.3 Phylogenetic Uncertainty within the Family Cetomimidae

Our understanding of the phylogenetic relationships within the family Cetomimidae is also characterized by a history of uncertainty. Paxton (1989) provided a detailed description of each genus and their relationships using a number of morphological traits including gill arches, head laterosensory canals, lateral line scales, cavernous tissue, anal lappets, and the subpectoral organ. Nine genera were identified in total. *Rondeletia* and *Barbourisia* were used as outgroups for the polarizations of thirty-nine traits to determine phylogenetic relationships within the family Cetomimidae (see Figure 1). *Procetichthys* was identified as the basal member of the cetomimids,

followed by *Ditropichthys* and then a clade comprised of *Cetichthys* and *Notiocetichthys*. Paxton described the relationship between the next five genera as equivocal with the exception of *Cetomimus* and *Gyrinomimus*, which were identified as sister genera based on their lateral lines. Paxton's working hypothesis for these five genera was that *Danacetichthys* and *Cetostoma* were sister groups to the remaining three genera, based on the gill-raker tooth plate shape and extent of the fourth gill slit.

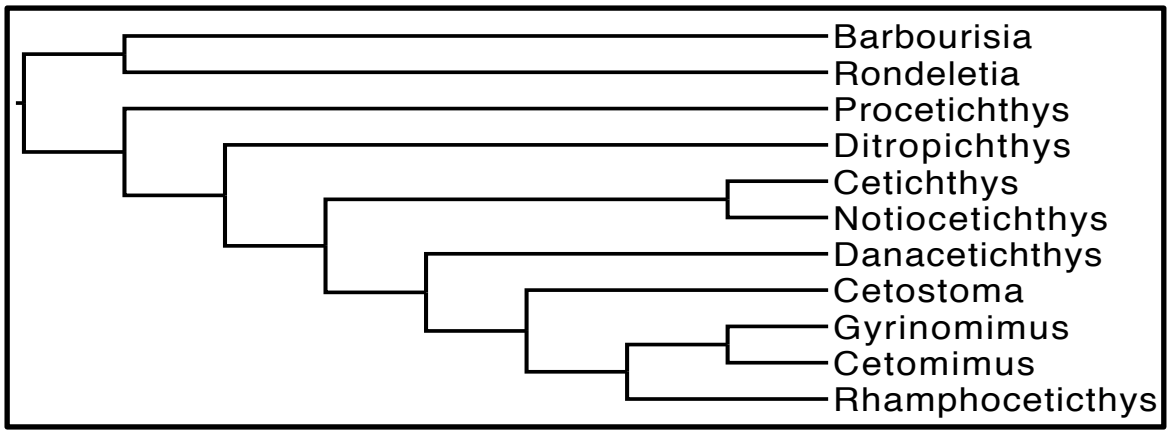

Figure 1. Cetomimidae Phylogeny adapted from Paxton (1989). The tree is based on morphology.

Colgan et al. (2000) questioned the phylogenetic relationships put forth by Paxton (1989). Colgan et al. (2000) used the 12s DNA sequence marker (30 sequences) and 16s rDNA (39 sequences) to investigate relationships within the family Cetomimidae and within the Stephanoberyciformes/Beryciformes as a whole (see Figure 2). Eleven individuals from the family Cetomidae were included in the study representing four genera (*Cetostoma*, *Cetomimus*, *Ditropichthys*, and *Gyrinomimus*). The results of the 16s and combined analyses suggested *Cetostoma* was sister to *Ditropichthys* rather than the *Cetomimus*/*Gyrinomimus* clade. Also of note, while *Cetomimus* was monophyletic in the 16s and combined trees, *Gyrinomimus* was paraphyletic with respect to *Cetomimus*. Three clades were evident: *Gyrinomimus cf myersi*, *Gyrinomimus sp R* + *Gyrinomimus grahami*, and *Gyrinomimus sp. R* + *Gyrinomimus sp L*. This was an unexpected result as the two genera were clearly defined using morphology. Paxton (1989) characterized *Cetomimus* as possessing domed vomer and *Gyrionmimus* by enlogated jaw teeth. Colgan et al. (2000) wrote that a revision of *Gyrinomimus* was underway by Paxton based on morphology. Within the revision three species groups were recognized, largely in line with the results of this study.

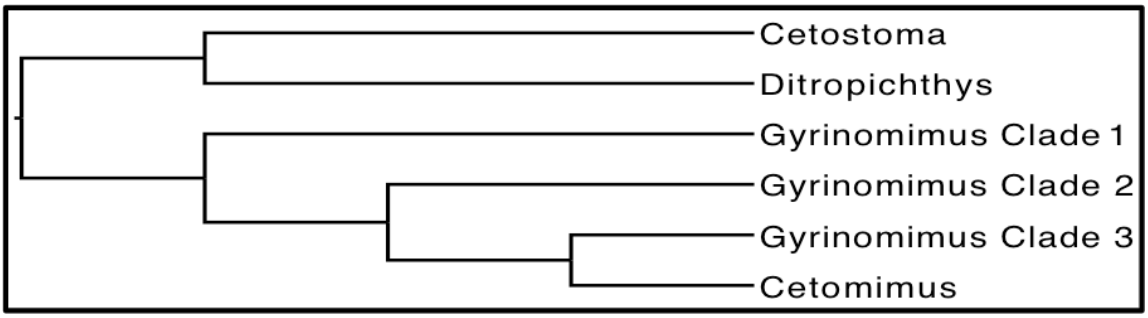

Figure 2. Cetomimidae Phylogeny adapted from Colgan et al. (2000). The tree is based on 12s and 16s combined analysis.

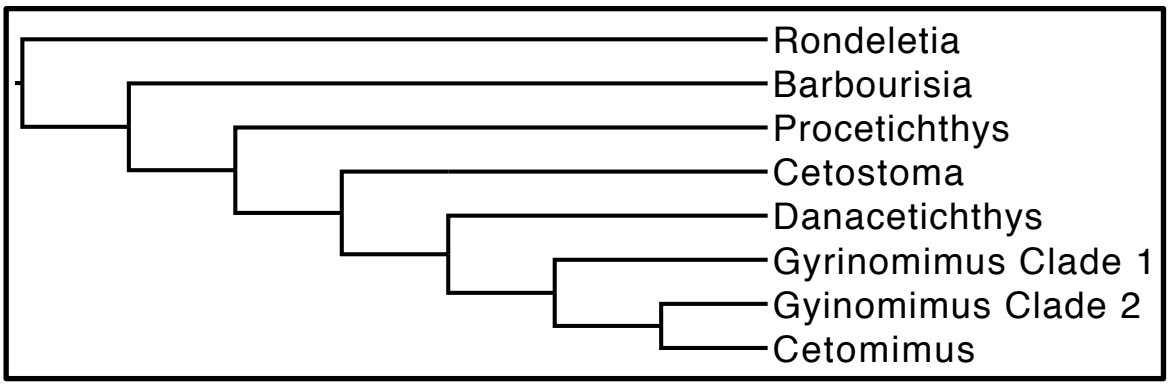

Figure 3. Cetomimidae Phylogeny adapted from Johnson et al. (2009). The tree is based on whole mitogenomes and 16s rRNA. The study did not include Ditropichthys, Cetichthys, Notiocetichthys, or Rhamphocetichthys.

The maximum likelihood tree from Johnson et al. (2009) (described in the previous section) included seven putative cetomimid species from five genera (See Figure 3). The placement of *Procetichthys* as the primitive sister to all other member of Cetomimidae was in agreement with the morphological assessment by Paxton (1989). However, the molecular evidence pointed to paraphyly within *Gyrinimomus* with respect to *Cetomimus*. Only two species from *Gyrinomimus* were included, so further clarification on the number and composition of the *Gyrinomimus* species groups was not provided.

We compiled a COI dataset from the DEEPEND project that included twelve putative species and five currently recognized genera. COI sequences from two additional *Gyrinomimus* species, one additional *Cetomimus* species, one species from the genus *Danacetichthys*, and one species from the genus *Procetichthys* were downloaded from GenBank and included as well. We used this dataset to investigate the phylogenetic relationships of the family *Cetomimidae*. No sequences were available for the three remaining genera. This is the most complete phylogenetic investigation into the family to date. We tested for paraphyly within *Gyrinomimus* with respect to *Cetomimus* and compared the topology to that of Paxton (1989), Colgan et al. (2000), and Johnson et al. (2009) (Figures 1-3).

2.1.4 Phylogenetic Uncertainty in the Stephanoberyciformes and Beryciformes

Like the relationships within the family Cetomimidae, the relationships between Cetomimidae and the other families comprising the Stephanoberyciformes and Beryciformes are unsettled. Moore (1993) performed phylogenetic analysis on the

"Trachichthyiformes" (Beryiciformes and Stephanoberyciformes) using both osteology and soft anatomy (See Figure 4 for Higher Level Phylogenetic Relationships and Figure 5 for Phylogenetic Relationships within Stephanoberycoidei). Moore proposed a monophyletic "cetomimoid" clade comprised of Rondeletiidae, Barbourisiidae, Megalomycteridae (now Cetomimidae), and Cetomimidae rejecting Gosline's (1971) earlier assertion that this group was polyphyletic. Another monophyletic clade containing families Hispidoberycidae, Stephanoberycidae, and Giberichthyidae was sister to the "cetomimoids". Melamphaidae was sister to both of the groups. Moore (1993) assigned the name Stephanoberycoidei for these eight families. Another five families (*Trachichthyidae*, *Monocentridae*, *Anomalopidae*, *Diretmidae*, and *Anoplogastridae*) were named Trachichthyoidei, which combined with Stephanoberycoidei to from the Trachichthyiformes. Holocentridae was absent from this group and placed as sister to "higher percomorphs".

Colgan et al. (2000) supported the notion of a monophlyetic clade comprised of Barbourisiidae, Rondeletiidae, and Cetomimidae using 12s rDNA (Hispidoberycidae, Stephanoberycidae, and Gibberichthyidae were not included in this study). 16s rDNA did not support this hypothesis, however only one extra step was required to make the 16s results monophyletic. The combined results supported the assertion of Moore (1993) that the "cetomimoids", Berycidae+Melamphaidae, and the rest of the Beryciformes excluding Holocentridae form a monophyletic group.

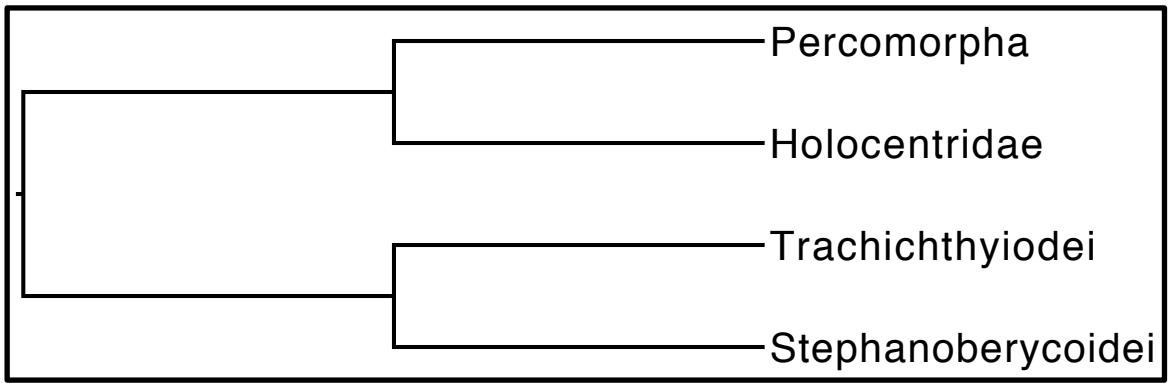

Figure 4. Higher level relationships of Trachichthyoidei, Stephanoberycoidei, Holocentridae and Percomorpha. This arrangement is adapted from Moore (1993) and Betancur et al. (2013), with the caveat that Moore did not place family Berycidae within Stephanoberycoidei.

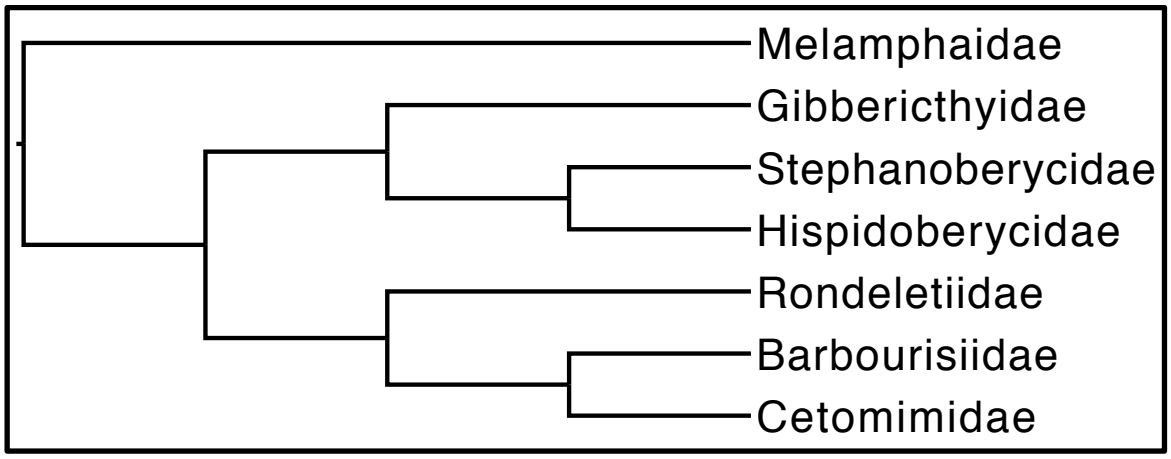

Figure 5. Phylogenetic Relationships within Stephanoberycoidei adapted from Moore (1993). Based on morphology.

Miya et al. 2003 used whole mitogenomes to investigate phylogenetic patterns of higher teleosts (Figure 6 shows the resulting tree). No samples from the families Barbourisiidae were included, but the results suggested that Rondeletiidae and Cetomimidae are closely related, and did nothing to harm the notion of monophyletic "cetomimoid" clade. Unlike Moore (1993) and Colgan et al. (2000) the results suggested that the "Trachichthyoidei" of Moore split from Percomorpha, Holocentridae, and the Stephanoberyciformes. Percomorpha is sister to a clade containing Holocentridae and the Stephanoberyciformes. Miya et al. (2003) noted that several observations indicate that mitogenome data alone may not be able to resolve the higher level relationships of Trachichthyoidei, Stephanoberycoidei, Holocentridae and Percomorpha.

In a follow up to the previous study, Miya et al. (2005) once again employed whole mitogenomes from 102 species of fish (Figure 7 shows the resulting tree). The resulting phylogeny for the Stephanoberyciformes and Beryciformes looked strikingly different. Miya et al. (2005) named a clade Berycorpha, which was comprised of two clades: Trachichthyoidei and Stephanoberycoidei+Holocentridae.

Near et al. (2013) explored the phylogenetic relationships throughout the spiny-ray fish tree of life (Figure 8 shows the resulting tree). A total of 520 species, ten nuclear genes, and thirty-seven fossil age constraints were employed. Two species from Cetomimidae, one species from Rondeletiidae, and one species from Barbourisiidae were included in the study. The results suggest that these three families do not form a monophyletic "cetomimoid" clade as proposed by Moore (1993). In the ultrametric tree,

Acanthochaenus luetkenii of the family Stephanoberycidae, diverges from Barbourisiidae after Rondeletiidae. A "Beryciformes" clade was identified that was sister to Percomorpha, and includes Trachichthyoidei, Stephanoberycoidei, and Holocentridae. Within the clade, Holocentridae is the first to split and is sister to Trachichthyoidei and the Stephanoberycoidei).

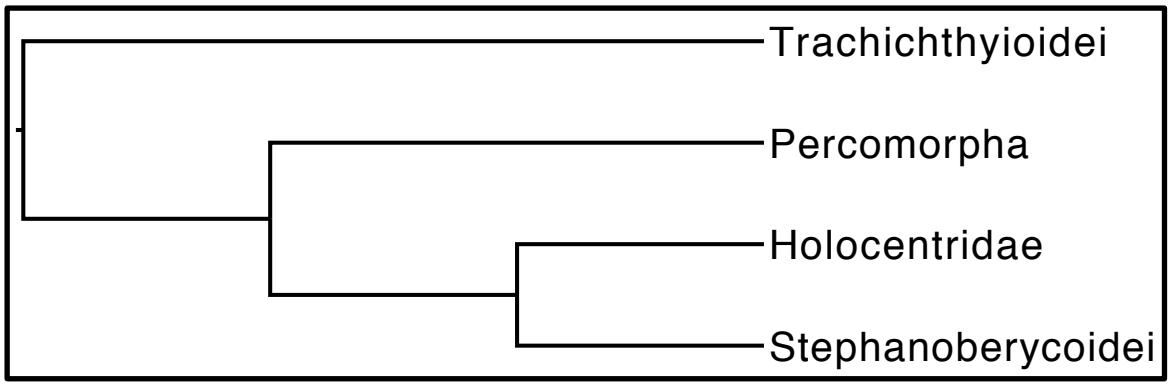

Figure 6. Higher level relationships of Trachichthyoidei, Stephanoberycoidei, Holocentridae and Percomorpha. This arrangement is adapted from Miya et al. (2003), Dornburg et al. (2017), and Hughes et al. (2018).

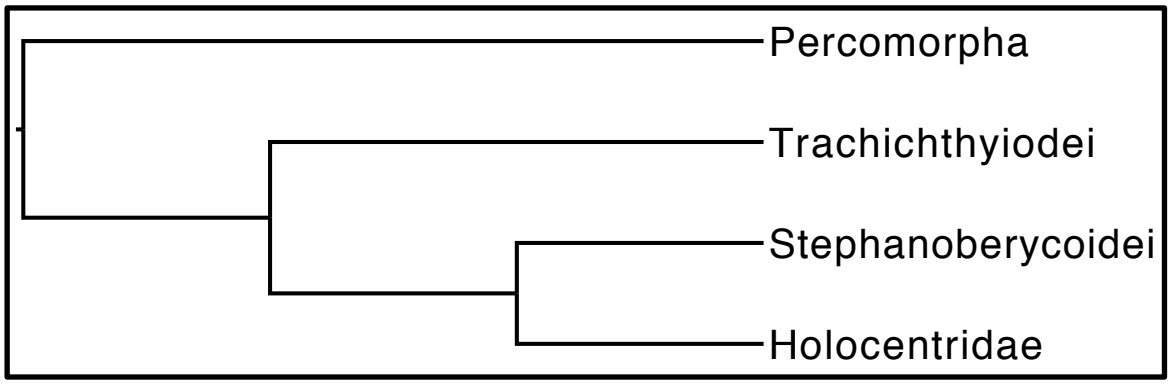

Figure 7. Higher level relationships of Trachichthyoidei, Stephanoberycoidei, Holocentridae and Percomorpha. This arrangement is adapted from Miya et al. (2005).

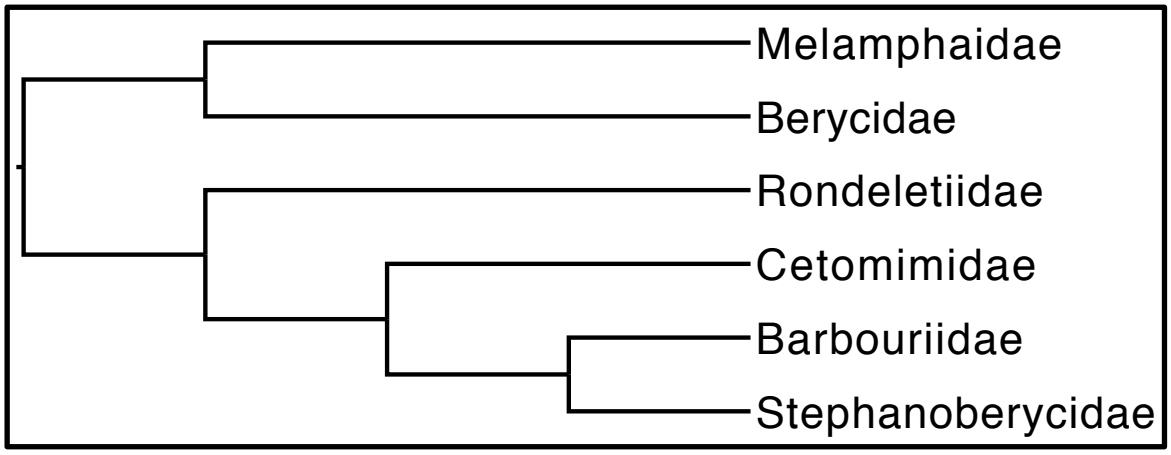

Figure 8. Phylogenetic Relationships within Stephanoberycoidei adapted from Near et al. (2013). Based on ten nuclear markers.

Betancur et al. (2013) sequenced twenty-one markers (20 nuclear and one mitochondrial) for 1410 bony fishes, two tetrapods, and two chondrichthyan outgroups to explore phylogenetic relationships within the bony fishes (Figure 4 shows the resulting tree). The results pointed to the existence of a "Beryciformes" clade consisting of Trachichthyoidei and Stephanoberycoidei. Holocentridae is outside this clade and elevated to the "Holocentriformes" which is sister to Percomorpha.

Two recent studies using nuclear DNA data have arrived at similar conclusions regarding the relationships of Percomorpha, the Beryciformes, and Stephanoberyciformes. Dornburg et al. (2017) used 132 loci and employed techniques to account for GC bias convergence to identify the sister group of Percomorpha (Figure 6 shows the resulting tree). The Trachichthyiformes appeared to split from a clade containing Percomorpha, Holocentridae, and the Stephanoberyciformes. Holocentridae and the Stephanoberyciformes are sister to Percomorpha. Within that clade Holocentridae is sister to the Stephanoberyciformes. Hughes et al. (2018) employed the use of 1,105 orthologous exons from 144 genomes and 159 transcriptomes to investigate phylogenetic relationships of the ray-finned fishes, and generate a maximum likelihood tree (Figure 6 shows the resulting tree). Gene genealogy interrogation (GGI) was applied to problem areas within the tree. The resultant topology of the GGI analysis for Percomorphacea, the Trachichthyiformes (Trachichthyoidei), Beryciformes (Stephanoberycoidei), and Holocentridae was identical to that of Dornburg et al. (2017).

It appears as though the most recent studies employing vast numbers of loci for phylogenetic analysis are beginning to converge on a hypothesis for the relationship

between Percomorphacea, the Trachichthyiformes, the Beryciformes, and Holocentriformes. It is unlikely our COI data will be able to improve on these results. Phylogenetic relationships within the Stephanoberyciformes are still poorly resolved, however. In the previously mentioned studies only Moore (1993) and Near (2013) included the family Stephanoberycidae, and they arrived at strikingly different conclusions. *Gibberichthys* was only included in Moore's (1993) analysis. We will use COI data to attempt to better resolve the relationships within the Stephanoberyciformes, and test for the existence of Moore's (1993) monophyletic "cetomimoid" clade by including all of our Cetomimidae sequences, as well as one representative sequences from each genera in the families Melamphaidae, Stephanoberycidae, Gibberichthyidae, Rondeletiidae, and Barbourisiidae.

2.1.5 Objectives

The DEEPEND project has provided a large number of new cetomimid samples including males, females, and undescribed species. We sought to use our mitochondrial COI data and perform phylogenetic analyses to answer three questions. (1) Can new species level matches be made for more male and female whale fish species? (2) Do our results support the previous conclusions drawn by Paxton (1989), Colgan et al. (2000), and/or Johnson et al. (2009) regarding the intrafamilial relationships of the family Cetomimidae? Finally, (3) what are the phylogenetic relationships between the families that comprise the clade Stephanoberycoidei?

2.2 Methods

2.2.1 Sampling

Samples were taken during six different research cruises from 2015-2018. Fishes were obtained through trawls with a "Multiple Opening and Closing Net and Environmental Sensing System" (MOCNESS). This system is comprised of six nets that can be opened and closed independently by an operator, allowing for sampling to occur at discrete depth zones. Upon retrieval, samples were identified at sea. Tissue was removed from lateral muscle or the caudal peduncle and placed in 95 % ethanol for preservation. Small samples (~ $1cm^3$) were preserved whole in ethanol, while larger samples were fixed in 10% formalin after tissue biopsy.

2.2.2 Sequencing

Approximately one mm^3 of tissue was removed from our samples and placed into a 96 well plate. These tissues were shipped to the Canadian Centre for DNA Barcoding (CCDB) for the sequencing of mitochondrial cytochrome oxidase I (COI) in their automated pipeline. Samples producing sequences that were too short (under 500 base pairs in length), showed sign of contamination, or that failed outright were extracted in our lab using the QIAGEN DNeasy Blood & Tissue Kit (Qiagen, Valencia, CA).

Polymerase Chain Reaction (PCR) was attempted using different sets of custom forward and reverse COI primers. (See Appendix Table A-1 for list of COI primers used). The PCR products were cleaned using the PEG cleanup method (Glenn 2019) DNA pellets were rehydrated with 22 µl of sterile water and the concentration of DNA was quantified using a Cytation 5 plate reader. 0.8 µl of the forward or reverse primer

was added to each well, along with 15 ng of DNA for every 200 base pairs of the amplified sequence, and enough autoclaved water to achieve a total of 18 µl of liquid. The plates were shipped to the Keck DNA Sequencing Lab at Yale University for Sanger sequencing. Sequences were cleaned and edited using Sequencher version v5.1 (Genecodes 2000). The cleaned sequences were aligned using MAFFT in Geneious v9.1.8 (Kearse et al. 2012).

2.2.3 Intrafamilial Relationships of Cetomimidae

In order to assess the intrafamilial relationships of the family Cetomimidae, all COI sequences obtained in DEEPEND were compiled along with one COI sequence from the five other Cetomimid species with COI sequences uploaded to Genbank (*Cetomimus sp. AMS, Gyrinomimus myersi, Gyrinomimus sp. UWNC, Danacetichthys galanethus*, and *Procetichthys kreffti*) (See Table A-2 for Accession Numbers). One COI sequence each from *Barbourisia rufa* and *Rondeletia bicolor* were added to the dataset to serve as outgroups. The sequences were aligned and trimmed in Geneious v9.1.8 (Kearse et al. 2012). Identical sequences were pruned, as they lead would lead to over partitioning in our downstream bGMYC analysis (Reid 2014).

PartitionFinder v2 (Lanfear et al. 2012) was used to identify the optimal partitioning scheme and substitution models for this dataset. A NEXUS file containing the sequences was uploaded to BEAUTI, part of the BEAST v2.4.7 package (Bouckaert et al. 2014). Partitions and substitution models were set according to the PartitionFinder results. We set a most recent common ancestor prior at 11.717 million years, with a normal distribution, for a clade containing *Ditropichthys* and *Cetostoma*, but did not

enforce monophyly, in order to age calibrate our tree. This calibration was based on our results from our secondarily calibrated tree in section 3 (See Appendix Figure A4). An uncorrelated log normal clock and a birth-death tree prior were set to run for 50,000,000 generations, sampling every 1,000 in order to generate an ultrametric tree in BEAST. We checked for convergence in Tracer v 1.7.1 (Rambaut et al. 2018) and used TreeAnnotator (part of the BEAST v2.4.7 package) to generate a maximum clade credibility tree that was visualized in FigTree v1.4 (Rambaut 2012).

We next employed a species or operational taxonomic units (OTUs) discovery method, to assess whether or not any of our male and female specimens belonged to the same out, and identify any cryptic speciation present in the dataset. OTUs were determined using a Bayesian general mixed Yule coalescent model (GMYC) that does not rely on any a priori knowledge of taxonomic distinctions. The GMYC approach is a more robust method for identifying OTUs than more commonly used analyses such as the BIN method, which often fail to accurately reflect real-world patterns of diversity (Barley and Thomson 2016). The model is paired with ultrametric trees created using DNA sequence data, and determines whether any given branching point is a divergence event (between species) or a coalescent event (within species) based on the differing rates of these processes. In this manner it can delimit OTUs based on evolutionary process and not a simple threshold (Pons et al. 2006; Reid 2014). bGMYC was run with both a single threshold approach on maximum clade credibility tree and maximum threshold approach on 100 trees using the R package bGMYC (Reid 2014) (see Figure 10). We used the burnin and threshold settings suggested in the bGMYC instructions

provided with the program. The bGMYC run was set to search for between 2 and 26 OTUs (there were 26 sequences in total).

2.2.4 Phylogenetic Relationship within the Stephanoberyciformes

We compiled a dataset including one COI sequence for every genus in the order Stephanoberyciformes when available (see Table 1 for breakdown of families, genera, and sequences in the order). Whenever possible, DEEPEND sequences were used. *Polymixia lowei* and *Anoplogaster cornuta* were included and set as outgroups. As before, PartitionFinder v2 (Lanfear et al. 2012) was used to identify the optimal partitioning scheme and substitution models for this dataset. Partitions and substitution models were set according to the PartitionFinder results. An uncorrelated log normal clock and a birth-death tree prior were set to run for 50,000,000 generations, sampling every 1,000 in order to generate an ultrametric tree in Beast. We checked for convergence in Tracer v 1.7.1 (Rambaut et al. 2018) and used TreeAnnotator (part of the BEAST v2.4.7 package) to generate a maximum clade credibility tree that was visualized in Figtree v1.4 (Rambaut 2012). A monophyletic prior was set for the family Cetomimidae to improve the running of the chain.

Table 1. Genera and sequence availability for Stephanoberycoidei.

Family	Genus	Sequence Available
Stephanoberycidae	*Abyssoberyx*	No
Stephanoberycidae	*Acanthochaenus*	Yes
Stephanoberycidae	*Malacosarcus*	No
Stephanoberycidae	*Stephanoberyx*	No
Gibberichthyidae	*Gibberichthys*	Yes
Barbourisiidae	*Barbourisia*	Yes
Rondeletiidae	*Rondeletia*	Yes
Hispidoberycidae	*Hispidoberyx*	No
Cetomimidae	*Gyrinomimus Clade 1*	Yes
Cetomimidae	*Gyrinomimus Clade 2*	Yes
Cetomimidae	*Gyrinomimus Clade 3*	Yes
Cetomimidae	*Cetostoma*	Yes
Cetomimidae	*Ditropichthys*	Yes
Cetomimidae	*Danacetichthys*	Yes
Cetomimidae	*Procetichthys*	Yes
Cetomimidae	*Cetomimus*	Yes
Cetomimidae	*Cetichthys*	No
Cetomimidae	*Notiocetichthys*	No
Cetomimidae	*Rhamphocetichthys*	No
Melamphaidae	*Melamphaes*	Yes
Melamphaidae	*Poromitra*	Yes
Melamphaidae	*Scopeloberyx*	Yes
Melamphaidae	*Scopelogadus*	Yes
Melamphaidae	*Sio*	No
Berycidae	*Beryx*	Yes
Berycidae	*Centroberyx*	Yes

2.3 Results

2.3.1 Phylogenetic Relationships within the Family Cetomimidae

We sequenced and compiled a dataset that included fifty-two sequences from the family Cetomimidae representing six recognized genera to investigate phylogenetic relationships within the family Cetomimidae (Table 1). After pruning identical sequences to improve the accuracy of our bGMYC analysis, we were left with twenty-four sequences. The sequences were trimmed to a length of 579 base pairs, giving us 163 variable sites representing 212 mutations and 24 parsimony informative sites. The greatest raw pairwise sequence divergence within the family was found between *Procetichthys kreffti* and *Danacetichthys galathenus* at 20.21%. Within the genus *Gyrinomimus* pairwise divergence was as high as 12.09% between two samples and there was 4.15% pairwise between the two *Cetostoma regani* sequences used in tree construction. The twenty-four sequences were used in the construction of an ultrametric tree.

Our maximum clade credibility tree of family Cetomimidae places *Procetichthys* as the most primitive cetomimid and sister to all others, diverging 33.506 million years ago (Figure 9). *Ditropichthys* and *Cetostoma* are the next most primitive genera and form a clade. *Danacetichthys* diverged from the remaining genera ~14.954 million years ago. *Gyrinomimus* appears to be paraphyletic with respect to *Cetomimus*, forming three clades comprised of 1) *Gyrinomimus bruuni*, 2) *Gyrinomimus myersi* + *Gyrinomimus sp UWNC* and 3) *Gyrinomimus parri.* The clades diverged 10.111 and then 4.067 million years ago, respectively. *Cetomimus* is the most derived genus in our tree. Most of the

nodes at the species level are well resolved and have posterior values of greater than 95%. However, the node between *Gyrinomimus myersi* + *Gyrinomimus sp UNC* and the node between *Cetomimus* + *Gyrinomimus parri* have posterior values of 54.1% and 60.5%, respectively. This may indicate some uncertainty in the existence and/or species composition of the three *Gyrinomimus* clades we identified.

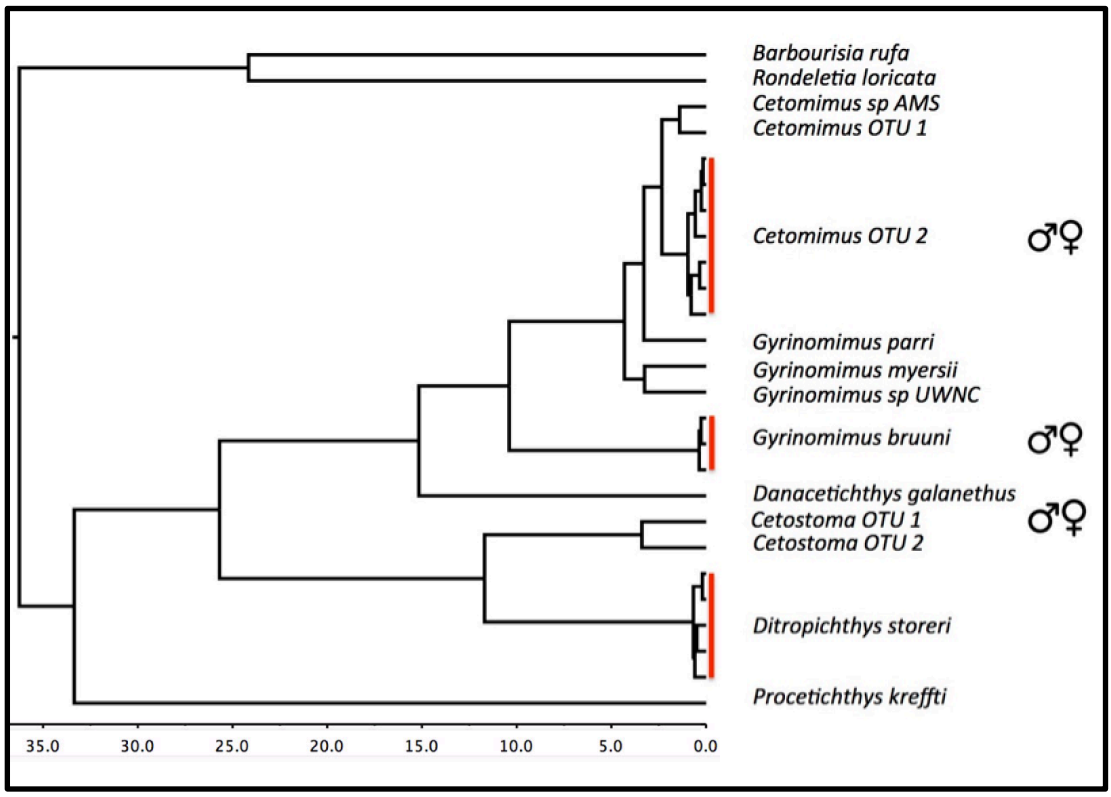

Figure 9. Maximum Clade Credibility Tree for family Cetomimidae. The red lines show sequences that belong to the same species or OTU based on our bGMYC analysis. Species/OTUs containing both male and female specimens are indicated by the male and female symbols.

Table 2. Summary of the cetomimid OTUs identified by bGMYC analysis.

Species/OTU	Origin of Sequence(s)	# of Haplotypes	# of Sequences	Sex of Samples
Cetomimus sp AMS	GenBank	1	1	Female
Cetomimus OTU 1	This study	1	1	Female
Cetomimus OTU 2	This study	5	18	Male and Female
Gyrinomimus parri	This study	1	1	Female
Gyrinomimus myersii	GenBank	1	1	Female
Gyrinomimus sp UWNC	GenBank	1	1	Female
Gyrinomimus bruuni	This study	3	6	Male and Female
Danacetichthys galanethus	GenBank	1	1	Female
Cetostoma OTU 1	This study	1	4	Male and Female
Cetostoma OTU 2	This study	1	7	Female
Ditropichthys storeri	This study	4	10	Female
Procetichthys kreffti	GenBank	1	1	Female

There are most likely twelve cetomimid OTUs within our dataset according to the bGMYC analysis (Figure 9, Figure 10, and Table 2). Our results were largely in agreement with current taxonomy regarding described female species. *Cetostoma regani* however, was identified as two as a cryptic species complex comprised of two OTUs, which we will refer to as *Cetostoma OTU 1* and *Cetostoma OTU 2*. This is not surprising given the more than four percent pairwise divergence between sequences noted earlier. According to our maximum clade credibility tree the two OTUs diverged approximately 3.1 million years ago. One *Gyrinomimus* sample identified as *Gyrinomimus sp* was found to belong to *Gyrinomimus bruuni*. We had numerous sequences identified as *Cetomimus sp*. All but one formed a single OTU, which we will refer to as *Cetomimus OTU 2*. The other sequence was identified as a singleton OTU, *Cetomimus OTU 1*.

2.3.2 Male and Female Matching

The dataset we compiled included fourteen male sequences in total. One male cetomimid sample is identical to three female *Cetostoma OTU 1* samples. Another male sample is identical to three individuals identified as *Gyrinomimus bruuni* females. Two more male sequences were placed in the *Gyrinomimus bruuni* OTU by the bGMYC analysis (Figure 10). The remaining male samples were linked by bGMYC with four female specimens in the *Cetomimus OTU 2*. No male sequences were left unlinked to a female OTU/species. Table 2 and Figure 9 summarize the female species/OTUs included in this study and show which species we have matched to at least one male specimen.

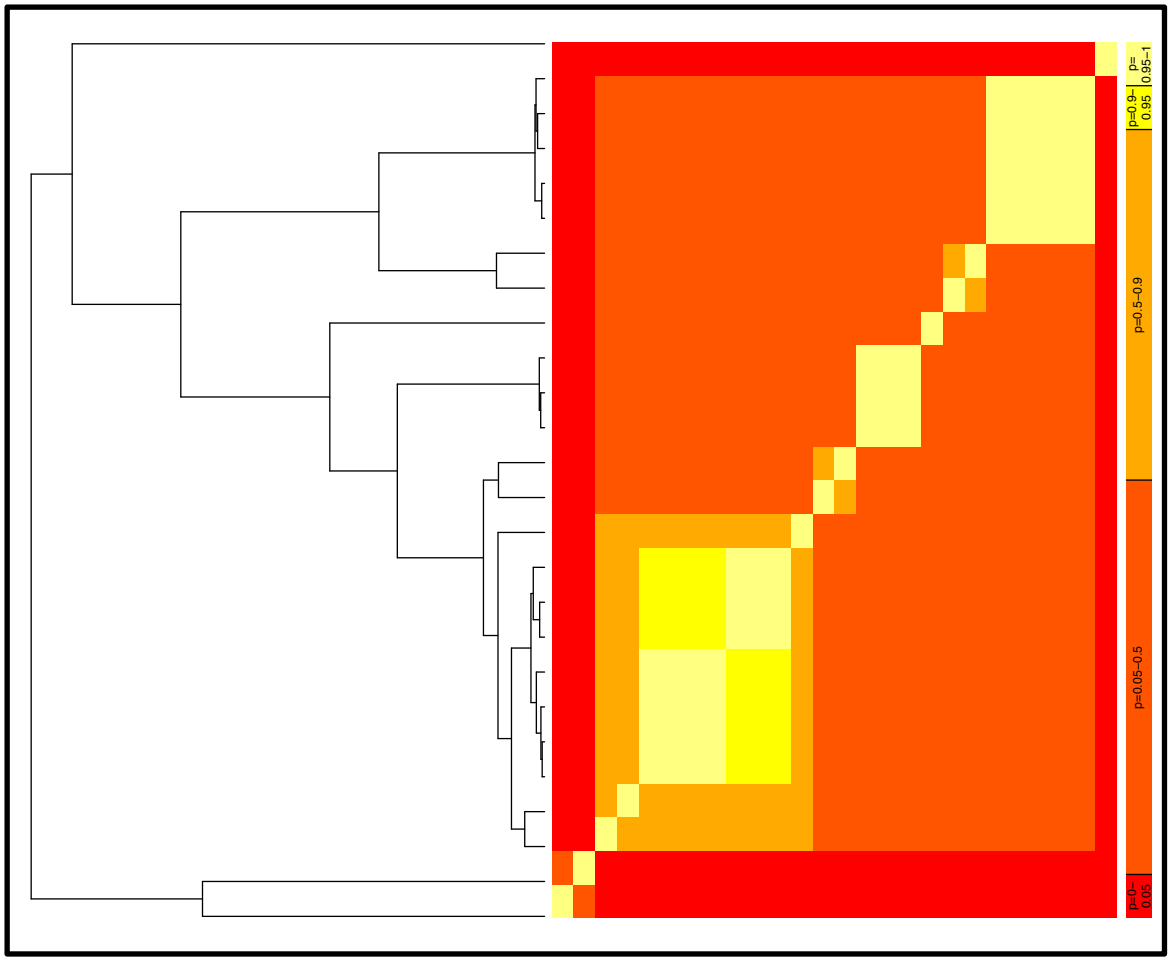

Figure 10. bGMYC Analysis for our Cetomimidae maximum clade credibility tree (see figure 9). The colors indicate the probability of neighboring tips belonging to the same OTU. The key on the right lists the probability represented by each color. Light yellow is the most likely (p = 0.96-1.00) and red is least likely (p = 0.00-0.05).

2.3.3 Phylogenetic Relationships within Stephanoberycoidei

We were able to sequence and compile a dataset that included samples from seven of the eight families in Stephanoberycoidei. Only Hispidoberycidae was unavailable. Our dataset included one sequence from eighteen of the twenty-six genera in Stephanoberycidae (we are treating the three *Gyrinomimus* clades as three distinct genera). The sequences were trimmed to 579 base pairs in the length, resulting in 231 variable sites, 206 parsimony informative sites, and an estimated 393 mutations.

Our maximum clade credibility tree recovered two major clades within Stephanoberycoidei with a posterior value of 1.0 (see Figure 11). The first clade is comprised Melamphaidae and Berycidae. The second clade contains Stephanoberycidae, Gibberichthyidae, Barbourisiidae, Rondeletiidae, and Cetomimidae. Within this clade, Stephanoberycidae is the most primitive and sister to the rest. This node has a posterior value of 100%. The maximum clade credibility tree suggests Cetomimidae+Barbourisiidae diverged from Gibberichthyidae+Rondeletiidae next. This branching event has low support however, with a posterior value of only .45.

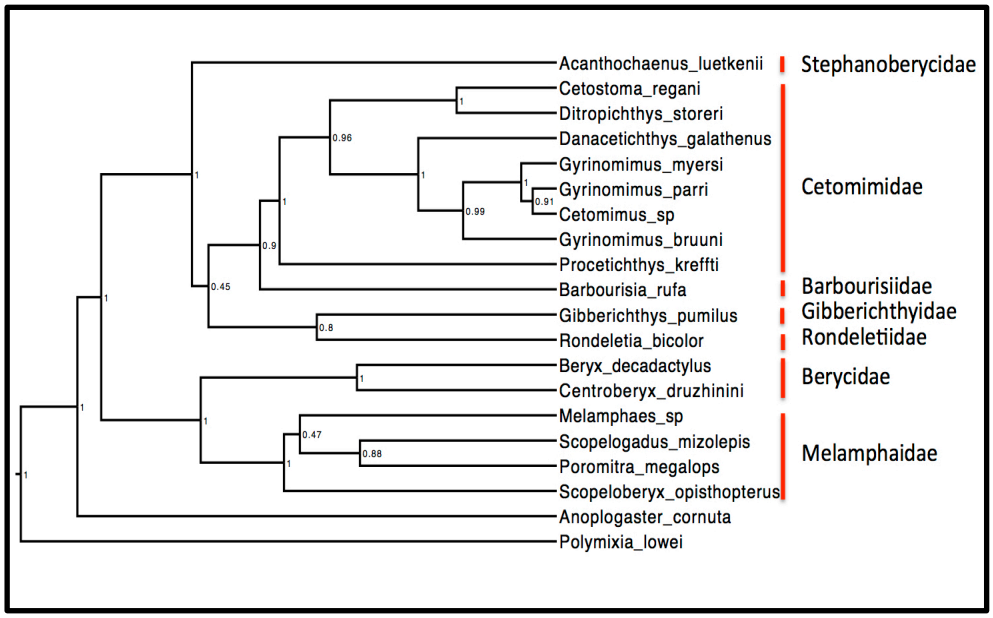

Figure 11. Maximum clade credibility tree for Stephanoberycoidei. The red lines indicate sequences from the same family. Posterior values are displayed at each node.

2.4 Discussion

2.4.1 Phylogenetic Genetic Relationships within the Family Cetomimidae

Our Cetomimidae maximum clade credibility tree (Figure 9) was the most complete phylogenetic investigation of the family to date. The tree largely agreed with past work done using both morphology and molecular evidence. Our placement of *Procetichthys kreffti* as the most ancestral genus within the family, and sister to the rest is in agreement with Paxton (1989) and Johnson (2009) (Figures 1 and 3).

The next clade in our tree *Cetostoma* + *Ditropichthys* was identified in the only other molecular investigation to include *Diropichthys*, Colgan et al. (2000) (Figure 2). It stands in contrast, however, to Paxton's (1989) tree based on morphological characters. The placement of *Ditropichthys* agreed with Paxton (1989), but *Cetostoma* was identified as a more derived genus and sister to *Grinomimus* + *Cetomimus* and *RhamphocetichthysCetichthys* and *Notiocetichthys* sequences were unavailable, but should be the next clade to diverge according to Paxton (1989). Given their absence, Paxton's (1989) would place *Danacetichthys* next, as found in our tree and that of Johnson et al. (2009).

Like Colgan et al. (2000) and Johnson et al. (2009), we identified paraphyly within *Gyrinomimus* with respect to *Cetomimus*. Colgan et al. (2000) identified three unique *Gyrinomimus* "species groups" or clades, while Johnson et al. (2009) found two (fewer *Gyrinomimus* species were used in Johnson et al. (2009). Our maximum clade credibility tree included three *Gyrinomus* clades. The first of these clades to diverge in the Colgan et al. (2000) 16s tree included *Gyrinomimus bruuni*, in agreement with our

findings. The second *Gyrinomimus* clade to diverge in Colgan et al. (2000) included *Gyrinomimus grahami* and *Gyrinomimus sp R*. COI sequences are not avaialable for either of these species, so they are not absent from our tree. *Gyinomimus myersi* belonged to the final *Gyrinomimus* clade and was sister to *Cetomimus* in the 16s tree (Colgan et al. 2000). *Gyrinomimus myersi* is placed in our second *Gyrinomimus* clade, however, and our clade containing *Gyrinomimus parri* is sister to *Cetomimus*. This disagreement brings up two possibilities. There may be four *Gyrinomimus* clades, and the absence of *G. grahami* and *G. sp R,* from our dataset prevented the identification of four clades. The other possibility is that there is simply uncertainty in the order of divergence for *Gyrinomimus clade 2* and *3*. Colgan et al. (2000) noted that Paxton was in the process of revising *Gyrinomimus* based on morphology and that three species groups were recognized. This work would help to verify the clade delimitation that we identified. The future inclusion of multiple nuclear markers and more *Gyrinomimus* species would also increase the reliability of our conclusions regarding *Gyrinomimus*.

Our maximum clade credibility tree is the most comprehensive cetomimid tree based on molecular data to date. Despite this fact, we are still missing sequences from three genera. The sequencing of these species would help to better resolve the current hypotheses regarding their position within the family based on morphology. Furthermore, the inclusion of more genes would aid in increasing posterior support for areas of taxonomic uncertainty

2.4.2 Phylogenetic Genetic Relationships within Stephanoberycoidei

We constructed a second maximum likelihood tree to investigate phylogetnetic relationships within Stephanoberycoidei. Similar to our previous dataset, this was the most taxonomically complete investigation to date. Like Near et al. (2013) we identified a strongly supported clade comprised of Melamphaidae and Berycidae. The rest of our tree (Figure 11) resembles neither of the trees built by Near et al. (2013) or Moore (1993) with molecular and morphological evidence, respectively.

Moore proposed a monophyletic "cetomimoid" clade that included Rondeletiidae, Barbourisiidae, and Cetomimidae, while Near et al. (2013) found a clade containing these three genera + Stephanoberycidae. Gibberichthyidae was not included in their analysis, which could have affected their phylogenetic inferences (Near et al. 2013). Our tree identified a clade comprising Rondeletiidae, Barbourisiidae, Cetomimidae and Gibbericthyidae instead of Stephanoberycidae. Unfortunately, posterior support on the nodes was low, casting some doubt on the topology we recovered. Regardless, it would appear as though the monophyletic "cetomimoid" clade proposed by Moore may not be accurate. Either Gibberichthyidae or Stephanoberycidae may be members of a clade containing Barbourisiidae, Cetomimidae, and Rondeletiidae.

In the future, Hispidoberycidae must be sequenced and included in phylogenetic investigations into Stephanoberycoidei, something that has not been done up to this point. Furthermore, a next generation sequencing approach, or the inclusion of additional genes, may help to resolve the uncertain phylogenetic relationships within the group as it has done for the relationships between Stephanoberycoidei, Percomorphacea,

Trachichthyoidei, and Holocentridae. This would be particularly beneficial in strengthening posterior support for the relationships within the clade that diverges from Berycidae + Melamphaidae.

2.4.3 Matching of Males and Females

Johnson et al. (2009) stated that the, "Next challenge is to link the three life stages of each species." To date, only one male specimen from the family Cetomimidae has been linked to a female at the species level: *Cetostoma regani* (Paxton et al. 2016). Our bGMYC analysis identified one more male specimen that was identified as *Cetostoma OTU 1*. Because *Cetostoma regani* is a cryptic species, we do not currently know to which OTU the previous male specimen belongs. It may be a new species level match between male and female specimens or it may represent the second male voucher for the species.

It was known that majority of the male samples previously sequenced belonged to the clade containing *Gyrinomimus* + *Cetomimus*, however matches at the species level were elusive (Johnson et al. 2009; Paxton et al. 2016). Our 13 other male samples fell into this clade as well. Fortunately, we were able to match all of our remaining male samples to two different female species/OTUs, the firsrt matching to a named species, *Gyrinomimus bruuni*. The second is an unnamed OTU, *Cetomimus OTU 2*. It is now of great importance for morphological work to performed. The *Cetomimus OTU 2* was identified as *Cetomimus sp*, but several new *Cetomimus* species have been described (Paxton et al. 2016). We need to check to see if any of these newly described match our *Cetomimus OTU 2*. If not, a species description including both the males and females

can be written. The morphology of *Gyrinomimus bruuni* males must also be described. Given the scarcity of cetomimid samples and the historic confusion regarding the relations between males and females, the matching of so many male and female samples is an especially exciting result.

2.5 Conclusions

In summary, we have provided further evidence as to the phylogenetic relationship within Cetomimidae, as well as between Cetomimidae and the other families comprising the Stephanoberyciformes. Our work supports a sister clade identified by Colgan et al. (2000), comprised of *Ditropichthys* and *Cetomimidae*. We found paraphyly within *Gyrinomimus* with respect to *Cetomimus,* in agreement with Colgan et al. (2000) and Johnson et al. (2009). Our results suggest the possibility of three or four species groups within *Gyrinomimus*. The Cetomimidae bGMYC tree also identified the existence of a cryptic Cetostoma OTU, which must now be described. While definitive phylogenetic relationships within the Stephanoberyciformes remain elusive, we found no support for the monophyletic "cetomimoid" clade of Cetomimidae + Rondeletiidae + Barbourisiidae suggested by Moore (1993). Next generation sequencing or the sequencing of multiple nuclear markers will help to resolve uncertainty on the phylogentic relationships within the Stephanoberyciformes. Finally, we were able to match all of our male samples to female species/OTUs. This is a particularly exciting product of the DEEPEND Consortium, as this has only been done for one male voucher previously. Our next step is to perform the morphological work necessary to describe the males and the unnamed female OTU

2.6 References

Barley, A. J. and R. C. Thomson. 2016. Assessing the performance of DNA barcoding using posterior predictive simulations. Molecular Ecology 25:1944-1957.

Bertelsen, E. and N. Marshall. 1956. The Mirapinnati, a new order of fishes. Dana Report 42:1-35.

Betancur-R, R., R. E. Broughton, E. O. Wiley, K. Carpenter, J. A. López, C. Li, N. I. Holcroft, D. Arcila, M. Sanciangco, and J. C. Cureton Ii. 2013. The tree of life and a new classification of bony fishes. PLoS currents 5.

Bouckaert, R., J. Heled, D. Kühnert, T. Vaughan, C.-H. Wu, D. Xie, M. A. Suchard, A. Rambaut, and A. J. Drummond. 2014. BEAST 2: a software platform for Bayesian evolutionary analysis. PLoS computational biology 10:e1003537.

Colgan, D., C.-G. Zhang, and J. Paxton. 2000. Phylogenetic investigations of the Stephanoberyciformes and Beryciformes, particularly whalefishes (Euteleostei: Cetomimidae), based on partial 12S rDNA and 16S rDNA sequences. Molecular Phylogenetics and Evolution 17:15-25.

De Sylva, D. P. and W. N. Eschmeyer. 1977. Systematics and biology of the deep-sea fish family gibberechthyidae, a senior synonym of the family Kasidoroidae. 41.6:215-231.

Dornburg, A., J. P. Townsend, W. Brooks, E. Spriggs, R. I. Eytan, J. A. Moore, P. C. Wainwright, A. Lemmon, E. M. Lemmon, and T. J. Near. 2017. New insights on the sister lineage of percomorph fishes with an anchored hybrid enrichment dataset. Molecular Phylogenetics and Evolution 110:27-38.

Genecodes. 2000. Sequencher version 4.1. 1 b1. Genecodes Corporation, Ann Arbor, MI, USA.

Glenn, T. 2019. PEG Precipitation of PCR products. http://labs.mcdb.lsa.umich.edu/labs/olsen/files/PCR.pdf

Gosline, W. A. 1971. Functional morpholgy and classification of teleostan fishes. University Press of Hawaii, Honolulu, Honolulu, HI.

Hughes, L. C., G. Ortí, Y. Huang, Y. Sun, C. C. Baldwin, A. W. Thompson, D. Arcila, R. Betancur-R, C. Li, and L. Becker. 2018. Comprehensive phylogeny of ray-finned fishes (Actinopterygii) based on transcriptomic and genomic data. Proceedings of the National Academy of Sciences 115:6249-6254.

Johnson, G. D., J. R. Paxton, T. T. Sutton, T. P. Satoh, T. Sado, M. Nishida, and M. Miya. 2009. Deep-sea mystery solved: astonishing larval transformations and extreme sexual dimorphism unite three fish families. Biology Letters 5:235-239.

Johnson, R. K. and E. Bertelsen. 1991. The fishes of the family Giganturidae: systematics, development, distribution and aspects of biology. Dana Report:1-45.

Kearse, M., R. Moir, A. Wilson, S. Stones-Havas, M. Cheung, S. Sturrock, S. Buxton, A. Cooper, S. Markowitz, and C. Duran. 2012. Geneious Basic: an integrated and extendable desktop software platform for the organization and analysis of sequence data. Bioinformatics 28:1647-1649.

Lanfear, R., B. Calcott, S. Y. Ho, and S. Guindon. 2012. PartitionFinder: combined selection of partitioning schemes and substitution models for phylogenetic analyses. Molecular biology and evolution 29:1695-1701.

Miya, M., T. P. Satoh, and M. Nishida. 2005. The phylogenetic position of toadfishes (order Batrachoidiformes) in the higher ray-finned fish as inferred from partitioned Bayesian analysis of 102 whole mitochondrial genome sequences. Biological Journal of the Linnean Society 85:289-306.

Miya, M., H. Takeshima, H. Endo, N. B. Ishiguro, J. G. Inoue, T. Mukai, T. P. Satoh, M. Yamaguchi, A. Kawaguchi, and K. Mabuchi. 2003. Major patterns of higher teleostean phylogenies: a new perspective based on 100 complete mitochondrial DNA sequences. Molecular Phylogenetics and Evolution 26:121-138.

Moore, J. A. 1993. Phylogeny of the Trachichthyiformes (Teleostei: Percomorpha). Bulletin of Marine Science 52:114-136.

Near, T. J., A. Dornburg, R. I. Eytan, B. P. Keck, W. L. Smith, K. L. Kuhn, J. A. Moore, S. A. Price, F. T. Burbrink, and M. Friedman. 2013. Phylogeny and tempo of diversification in the superradiation of spiny-rayed fishes. Proceedings of the National Academy of Sciences 110:12738-12743.

Paxton, J. and G. Johnson. 2005. Cetomimidae: Whalefishes; Mirapinnidae: tapetails & hairyfish; Megalomycteridae: bignose fishes. Pp. 1089-1102. Early stages of Atlantic fishes. CRC Press, Boca Raton, FL.

Paxton, J., T. Trinski, and G. D. Johnson. 2016. Cetomimidae. FAO, Rome, Italy.

Paxton, J. R. 1989. Synopsis of the whalefishes (family Cetomimidae) with descriptions of four new genera. Records of the Australian Museum 41:135-206.

Pons, J., T. G. Barraclough, J. Gomez-Zurita, A. Cardoso, D. P. Duran, S. Hazell, S. Kamoun, W. D. Sumlin, and A. P. Vogler. 2006. Sequence-based species delimitation for the DNA taxonomy of undescribed insects. Systematic biology 55:595-609.

Rambaut, A. 2012. FigTree v1. 4.

Rambaut, A., A. Drummond, D. Xie, G. Baele, and M. Suchard. 2018. Posterior summarisation in Bayesian phylogenetics using Tracer 1.7. Systematic biology 67:901-904.

Reid, N. 2014. bGMYC: a Bayesian MCMC implementation of the general mixed Yule-coalescent model for species delimitation. R Package Version, 1.

Robins, C. 1974. Review: fishes of the western North Atlantic. part 6. Copeia:574-576.
\

3. HISTORIC FLUCTUATIONS OF EFFECTIVE POPULATION SIZES OF AN ASSEMBLAGE OF GULF OF MEXICO DEEP-PELAGIC FISHES

3.1 Introduction

Historic fluctuations in effective population sizes often reveal the effects of major evolutionary and ecological phenomena on the genetic diversity of a population or a species, such as geologic events and climatic oscillations (Almada, Almada, Francisco, Castilho, & Robalo, 2012; Avise, Avise, Fisher, & Brick, 2000; Eytan & Hellberg, 2010; W. Grant & Bowen, 1998; William Stewart Grant, 2015; Henriques, Potts, Santos, Sauer, & Shaw, 2014; Robalo et al., 2012). These changes in population sizes can be inferred through the use of genetic data. Detecting changes in demography helps to elucidate processes affecting the genetic diversity of a species and its ability to respond to environmental disturbance. However, while the historical demography of certain faunal assemblages has been thoroughly studied, others have not. This is because the effort and cost needed to collect sufficient material from certain habitats for population genetic analyses is high. The deep-pelagic is a difficult environment to sample, requiring extensive ship time and specialized collection gear.

Knowledge of the demographic history of Gulf of Mexico (GoM) deep-pelagic fishes is lacking, and predictions about which environmental factors may have influenced past population size changes of these fishes are difficult to make. This information is critical given the ecological importance of midwater fishes. The deep-pelagic comprises approximately 95% of the ocean by volume, and the biomass of deep-

pelagic fishes is at minimum ~1,000 million tons, several orders of magnitude larger than the total global commercial fisheries landings (Gjøsaeter & Kawaguchi, 1980; Irigoien et al., 2014; T. Sutton, 2013). Furthermore, deep-pelagic fishes are important prey items for numerous commercially targeted species (Battaglia, 2013; Varghese, Somvanshi, & Gulati, 2013).

Global climate conditions have varied greatly since the beginning of the Quaternary, approximately 2.4 million years ago (Hewitt, 2000). This period has been characterized by periodic glaciation, leading to alterations in global currents, oceanic temperatures, and sea level (Becquey & Gersonde, 2002; Clark et al., 2006; Clark et al., 2009; Mix, Bard, & Schneider, 2001; Otto-Bliesner et al., 2007; Ruddiman, Raymo, Martinson, Clement, & Backman, 1989). Severe glaciation events have led to the creation of small and isolated refuges where climatic conditions are conducive to the survival of a species (Canino, Spies, Cunningham, Hauser, & Grant, 2010; Maggs et al., 2008; Provan & Bennett, 2008; Stewart, Lister, Barnes, & Dalén, 2009). Range expansions and contractions greatly affect population size and species abundance (Avise et al., 2000; Nye, Link, Hare, & Overholtz, 2009). During these times, the reduction in available habitat may lead to a population bottleneck (Bernatchez, Dodson, & Boivin, 1989). Following the glaciation events, new habitat becomes available and then populations can expand once again (Bernatchez et al., 1989; Hewitt, 2000). Accordingly, many marine fishes are believed to have experienced population expansions following the most recent glacial maximum 21,000 years ago (Almada et al., 2012; Avise et al., 2000; Eytan & Hellberg, 2010; W. Grant & Bowen, 1998; William

Stewart Grant, 2015; Henriques et al., 2014; Robalo et al., 2012). Several studies have uncovered strong evidence of recent genetic bottlenecks attributed to changes in the marine environment, but with the added caveat that taxonomically and ecologically similar species do not always share these same demographic trends (Eytan & Hellberg, 2010; Moore & Chaplin, 2014; Sakuma, Ueda, Hamatsu, & Kojima, 2014).

Investigations into historic changes in the population size of deep-sea organisms are few and have focused on benthic species. Etter et al. (2005) suggested that deep-sea bivalve population sizes have remained relatively stable through time with a few recent fluctuations. On the other hand, Sakuma et al. (2014) found that two closely related deep-sea benthic fishes exhibited distinct patterns of historic population size: one has greatly expanded since the last glacial maxima while the other maintained a consistent large population throughout. Varela et al. (2012) inferred a population size increase in the deep-sea benthic fish species, *Hoplostethus atlanticus*, approximately 100,000 years ago. It is therefore likely that while the population sizes of some deep pelagic fishes have remained relatively stable in the face of historic changes in climate, others may have been affected greatly. Thus, although there is evidence for effects on benthic organisms in the deep-sea, the consequences of climactic change on the demography of deep-pelagic organisms is poorly understood.

In order to predict how deep-pelagic fish populations have changed over time, a mechanism of population control must be identified. Based on the stability of the environment over space and time, it is unlikely that physical conditions at depth would be the primary driver of population dynamics in deep-pelagic fishes (Clark et al., 2009;

Levitus et al., 2012; Robison, 2009). While deep-pelagic fishes are characterized as those living below 200 meters, many species inhabit the epipelagic at different stages of their life both as adults and larvae (Hsieh, Kim, Watson, Di Lorenzo, & Sugihara, 2009; Johnson et al., 2009). Because sea surface conditions are more variable than those at depth, the obligate use of surface waters could strongly influence species distribution patterns and in turn, the population sizes of deep-pelagic fishes (Becquey & Gersonde, 2002; Clark et al., 2006; Clark et al., 2009; Ruddiman et al., 1989).

The use of surface waters in adult deep-pelagic fishes is limited to species that undergo diel vertical migration, and differences in the vertical migratory habits of deep-pelagic fishes may be a key predictor of the degree to which climatic changes affect deep-sea fish population over time. Hsieh et al. (2009) analyzed changes in the geographic distribution of pelagic fishes over 50 years. They found that the distribution of vertically migrating mesopelagic fishes was more likely to vary in response to environmental change, primarily fluctuations in temperature, than non-vertically migrating mesopelagic fishes. This could be a result of significantly greater heating in the upper ocean than deep waters, which vertical migrators visit on a daily basis. If the changes in surface waters are no longer tolerable to the vertically migrating fishes these species can no longer persist in their former range. Their range may simply contract or it may shift latitudinally, a phenomenon that has been observed in numerous marine fish species (Dulvy et al., 2008; Nye et al., 2009). Because range expansions and contractions greatly affect population sizes and species abundances, deep pelagic fishes may exhibit two generalized patterns of historical population change (Avise et al., 2000;

Nye et al., 2009). One is that vertical migrators will be characterized by recent population expansions and/or contractions, but the population size of non-vertical migrators will be relatively stable over time.

Alternatively, the larval characteristics of deep-pelagic fishes may have a greater impact on population dynamics than the migratory behavior of their adult forms. While adult deep-pelagic fishes differ greatly in their use of surface waters, the majority of deep-pelagic fish families have pelagic larvae that inhabit the variable upper 200 meters of the water column (Bowlin, 2016; Johnson et al., 2009; Moser, 1996; T. T. Sutton, 2013).

The extent to which the larval phase may influence population dynamics can be evidenced in the distribution patterns exhibited by deep-pelagic fishes. Mesopelagic and bathypelagic fishes frequently possess circum-global populations (Catul, Gauns, & Karuppasamy, 2011; Gaither, Bowen, Rocha, & Briggs, 2016; Miya & Nishida, 1996; Sutton & Hopkins, 1996) (See Appendix Table A2 for distribution of species included in this study). Their ranges typically exhibit strong latitudinal boundaries and can broadly be characterized as low-latitude/tropical or high-latitude/polar in distribution with a transition zone at approximately 40 degrees North and South (Olson, 2001; Pearcy, 1991; Randall, 1981). Even non-vertically migrating bathypelagic families such as the whale fishes fit this pattern (Paxton, 1989). It seems unlikely that this distribution can be explained by physiological constraints on adults of these species given the latitudinal homogeneity of the environment at the depths they reside (Helfman, Collette, Facey, & Bowen, 2009; Tyus, 2011).

Rather, it would be more likely that the physiological tolerances of the larvae inhabiting surface waters place constraints on deep-pelagic fish ranges. Numerous studies have pointed to environmental factors in the surface waters such as temperature and salinity as being primary predictors of larval species distributions (Ahlstrom, 1969; Netburn & Koslow, 2018; Sassa, Kawaguchi, Oozeki, Kubota, & Sugisaki, 2004; Urias-Leyva et al., 2018). In transition zones between tropical and subpolar regions, the dominant larval assemblage has been shown to vary annually based on sea surface temperatures (Ahlstrom, 1969; Hsieh et al., 2009). Aceves-Medina et al. (2004) found that the distribution of larvae was congruent with that of the adults. If the physiological tolerances of surface water dwelling larvae do indeed dictate range sizes, long-term changes in sea surface conditions (particularly changes in temperature) could lead to significant changes in the ranges and population sizes of these species. If true, increases in sea surface temperature (SST) would be expected to lead to an increase in suitable habitat and population sizes for the tropical species included in this study as it would shift the maximum extent of their range poleward. The cooling of SST would have the opposite effect.

To better understand the demography of deep-pelagic fishes, we answered the following questions: (1) Has there been historical changes in genetic effective population sizes in deep-pelagic fishes of the Gulf of Mexico? (2) Can these patterns be explained by long-term changes in sea surface temperature? and if so (3) Are these patterns the result of adult migratory habits or the effects of sea surface temperature fluctuations on shallow-dwelling larvae?

To investigate these questions, we collected a DNA sequence dataset of both mitochondrial and nuclear genes for thirteen fish species present in the GoM deep-pelagic environment. These species represent eight families, and differ greatly in life history characteristics (Appendix Tables A-4 and A-5). The inclusion of a large number of unrelated species provides greater power to establish demographic trends in deep-pelagic fish assemblages.

If population size changes are inferred in species that vertically migrate, but are absent from species that do not do so, it would suggest that the adult migratory habits of deep-pelagic fishes is the main determinant of their demographic histories. If this was not found to be the case, reconstructions of historic SST at 41°N (the northern extent of many low-latitude midwater ranges) could help determine whether the larval phase controls population size. This would be evidenced if population expansion correlated to periods of warm SST at this latitude. These results provide insights into the biological and environmental factors that influence population size dynamics in deep-pelagic fishes, which as a group is both ecologically critical and poorly understood.

3.2 Methods

3.2.1 Selection of Nuclear Markers

In addition to the mitochondrial gene *cytochrome oxidase* I (*COI*), we generated DNA sequence data from three nuclear DNA exons for use in the demographic analyses. The inclusion of multiple loci allowed for replicate samples of a species demographic history that could be missed by the use of only one gene (Eytan & Hellberg, 2010). This is particularly important when interpreting frequency-based test results. Significant results can be indicative of either demographic changes or departures from neutrality. Differing selective forces may be acting independently on each locus, while demography should affect any neutral site uniformly (Heled & Drummond, 2008; Li, 2010).

Finding a suitable nuclear marker proved difficult, as our thirteen species were distributed across the fish tree of life and spanned over one hundred million years of evolution (Near et al., 2013). PCR trials were performed using nested exon primers, because coding regions are more readily conserved, meaning that they would be more likely to amplify distantly related species. Three genes, PLAG, ENC, and MYH, were successfully amplified and sequenced for a large proportion of the study species (See Appendix Tables A1, A4, and A5 for Primer Sequences). We Sanger-sequenced all species that that produced appropriately sized PCR products on an ABI 3730 capillary sequencer. Prior to sequencing, all PCR products were cleaned using a standard PEG protocol (Glenn 2019).

3.2.2 Frequency Based Analyses

We performed demographic analyses on every species with at least one nuclear marker (for a minimum of ten individuals) in addition to the mitochondrial COI sequence, for a total of 13 species. Our first set of analyses were frequency-based where the number and distribution of segregating sites in an alignment of DNA sequences provided information on a species' demography such as the presence of population growth, population structure, positive selection, and balancing selection (Innan, Zhang, Marjoram, Tavaré, & Rosenberg, 2005; Rogers & Harpending, 1992; Rosendahl, Mcgee, & Morton, 2009; Watterson, 1975).

We calculated Tajima's D, Fu's F_s, and R_2 for each nuclear and mitochondrial marker (Fu, 1997; Ramos-Onsins & Rozas, 2002; Tajima, 1989). Comparisons of the statistical power of frequency-based tests have shown that F_s and R_2 are the most capable of detecting population growth (Ramos-Onsins & Rozas, 2002). They are complementary to one another as well, with F_s excelling at population growth detection in large sample sizes, while R_2 performs better with small sample sizes. A significant and large negative Fs value suggests population growth, while a significant and small positive R2 value indicates population growth. Tajimas's D points to population growth and/or a selective sweep when significant and negative. All of the frequency-based tests were performed in DNAsp v6 (Rozas et al., 2017). Ambiguity codes were replaced with Ns to allow for calculation in DNAsp. Tajima's D is a two-tailed test, so significance was initially determined by the test itself. The significance of all three tests was also

determined using coalescent simulations with 1000 replicates implemented in DNAsp. Other statistics, such haplotype diversity (Hd) and Pi were recorded, as well.

3.2.3 Gene Tree Based Analyses

The second set of tests makes use of the topologies and branch lengths of gene trees to infer changes in population size over time using the coalescent. We performed these analyses in BEAST v2.4.7 (Bouckhaert et al. 2016) to generate Extended Bayesian skyline plots (EBSPs) to show changes in population size over time. EBSPs utilize coalescent theory and a Markov Chain Monte Carlo Algorithm to infer and visualize demographic changes in a dataset. The Bayesian skyline plot is preferable to earlier skyline plot methods as it models both genealogy and demographic history simultaneously, which reduces error rates from uncertainty in estimates of node time (Heled & Drummond, 2008; Ho & Shapiro, 2011).

3.2.4 Calculation of the Clock Rate

Secondarily calibrated ultrametric trees were constructed in BEAST to calculate species-specific clock rates. Near et al. (2013) investigated the patterns of lineage diversification in spiny ray fishes using 520 species, 37 fossil calibrations, and 10 genes. Divergence dates from lineages taxonomically related to our study species served as priors on nodes calibrated with normal distributions matching the posterior estimates of divergence times obtained from the Near *et al*. tree (See Appendix Tables A-8 to A-12 for calibrations used).

COI sequences were generated for this study, but some were obtained from GenBank for those species not present in our dataset but included in the Near et al.

paper. In these cases, five sequences were downloaded for each species from GenBank when available and pairwise comparisons of these sequences were examined to ensure that there was no evidence of misidentifications between samples, which would be indicated by large intraspecific DNA sequence divergences. This could indicate that identification errors were present in the GenBank database. Once confident in the taxonomic identity of the sequences, one sequence from each species was compiled in a NEXUS file using Geneious v9.1.8 (Kearse et al., 2012). The list of samples used in the final tree construction and their accession number is present in Appendix Tables A11-A15.

Partition schemes and substitution models were determined using PartitionFinder v2 (Lanfear, Calcott, Ho, & Guindon, 2012). A relaxed, uncorrelated log-normal clock was set to allow for variation in rates between lineages. Most recent common ancestor priors were set with normal distributions according to the results from Near et al. (2013) (Tables A-8 to A-12). We used a Birth Death Model with a chain length of 50,000,000 sampling every 1,000 generations. After each run the log files were examined in Tracer v 1.7.1 (A Rambaut, Drummond, Xie, Baele, & Suchard, 2018) to ensure convergence.

The Stomiiformes and Gempylidae trees did not converge due to poor substitution model fit on one of the three partitions. The substitution models for the poorly running partitions were replaced with bModeltest (R. R. Bouckaert & Drummond, 2017). bModeltest does not require a substitution model to be set prior to running. Rather, different substitution models and gamma-distributed rate heterogeneity

are explored throughout the run to infer the model of best fit. After this change was made, the Stomiiformes and Gempylidae trees converged properly.

A maximum clade credibility tree was constructed using Tree Annotator (part of the BEAST package) with a burnin of 25% of the posterior set of trees. The maximum clade credibility tree was visualized in FigTree v 1.4 (Andrew Rambaut, 2012). Five trees were constructed in total (Appendix Figures A-1 to A-5). Divergence dates between our study species and their sister species were recorded.

We then calculated the *COI* clock rate for each species. To do this in a Bayesian framework we created another set of ultrametric trees for each study species that included their sister species (from the previous set of secondarily calibrated trees). A dataset was compiled using all available COI sequences for the each species. Once again, we ran these trees in BEAST under a Birth Death Model. The substitution models were set according to PartitionFinder. We set a strict clock with a MRCA prior date taken from our previous set of trees (Appendix Figures A-1 through A-5). Trees were run with chain length of 50,000,000. Log files were inspected in Tracer for convergence and the clock rate was recorded. This process was repeated for our nuclear markers in order to determine an initial clock rate to set in our EBSP runs.

3.2.5 Extended Bayesian Skyline Plot Construction

All available genes were included in the analysis for each species. We were unable to find one method of extended Bayesian skyline plot (EBSP) construction that would lead to convergence for every single species present in this study. Instead, we

constructed two different EBSPs using two different approaches for each species. The six methods are outlined below.

In EBSP construction method 1, the optimal partitioning scheme and model of evolution were determined for each species and marker set using Partition Finder v2.0 (Lanfear et al., 2012). Partition schemes and substitution models were set according to the Partition Finder results, and the chain length was set to 50,000,000 sampling every 1,000. A strict clock was set for each of the markers, and *COI* rates from previously described clock rate calculation were used. The initial nuclear rates were taken from Appendix table A-18. The COI rate was fixed, while the clock rates for nuclear markers were estimated in relation to COI. The nuclear gene clock rates were given a normal distribution with a median equal to the initial rate. The sigma, or standard deviation, was adjusted to prevent the chain from exploring nuclear clock rates that were faster than the COI rate, as mitochondrial substitution rates are typically faster than that of nuclear genes (Eytan & Hellberg, 2010). As suggested in Heled (2010), a normal distribution was set for the popmean.alltrees prior and the size of three operators were tripled ("EBSP bitflip operator", "EBSP indicator sampler", and "EBSP population sizes").

Method 2 was identical to Method 1 with the exception of the selection of substitution models. All partitions were set to the RBS substitution model. RBS is a reversible-jump based substitution model for nucleotide data (R. Bouckaert et al., 2014). This substitution model does not require a fixed substitution model to be assigned to each partition at the beginning of the analysis. Instead, it allows five different

substitution models to be explored through the run, in order to find the substitution model with the best fit to the dataset (R. Bouckaert, Alvarado-Mora, & Pinho, 2013; R. Bouckaert et al., 2014).

3.2.6 Post-EBSP Construction

After running in BEAST, log files were inspected using Tracer v 1.7.1 (A Rambaut et al., 2018). The results of each run are summarized in Appendix table A-19. Runs were assessed as "Good" or "Poor". "Good" runs were those where key values such as "Prior", "Posterior", "Likelihood", and "sum(indicators.alltrees)" had all converged and their ESS values were above 200. "Poor" runs were those where key parameter values never converged on a stable posterior distribution, and one or more of these key values had ESS values under 100. The most strongly supported EBSP analysis, based on ESS values, was selected and used for the inference of each species' demographic history. The posterior estimate of the number of population size changes provided a test for a rejection of constant population size (Appendix table A-19). Finally, the trees files were uploaded to Rstudio v 0.99.484 (Studio, 2012). The Rscript "plotEBSP", provided with the EBSP tutorial (http://www.beast2.org/files/2016/01/ebsp2-tut.zip), was used to generate and visualize the extended Bayesian skyline plots as well as histograms for the timing of inferred population size change events (Figures 12-21) (Heled, 2010).

3.2.7 Population Dynamics and Vertical Migration

Any species for which we inferred a population change, using both frequency-based statistics and gene tree analyses, was classified as having undergone a population

size change sometime in its evolutionary history. We divided species into two categories; vertical migrators and non-vertical migrators. A chi-squared test was used to test for the significance of the correlation of between inferred population size changes and vertical migration. Information on the migration patterns of two fishes (*Polymixia lowei*, and *Synagrops spinosu*s) was unavailable, so we left these species out of the analysis (Table 9).

3.2.8 Sea Surface Temperature and Population Size Changes

We plotted sea surface temperatures (SST) for the past 500,000 years from the North Atlantic based on foraminifera records (Clark et al., 2006; Ruddiman et al., 1989). The site is located at 41°N and corresponds to the northern extent of the range inhabited by many tropical and polar deep-pelagic species. The date of the onset of population size change inferred from our extended Bayesian skyline plots were indicated on the plot to allow for the comparison of fluctuations in SST and population dynamics in our study species (Figure 22).

3.3 Results

3.3.1 Frequency Based Statistics

Our first set of analyses were frequency-based, and run for both COI and each nuclear marker. The analyses suggested population expansions in a number of species (Tables 3-6). These species included *Chauliodus sloani*, *Cyclothone alba, Diplospinus multistriatus, Ditropichthys storeri Photostomias guernei, Polymixia lowei, Scopelogaudus mizolepis, Sigmops elongates,Sternoptyx pseudobscura, Stomias affinis, and Synagrops spinosus*.

Chauliodus sloani showed the strongest evidence of population expansion, as all three tests for the two genes used (COI and ENC) were significant (Tables 3 and 5). The two largest negative Fs values calculated for any species and marker were for *Chauliodus sloani* COI, -33.567, and ENC, -10.151 (Tables 3 and 5). These Fs values are strong indicators of population expansion (Fu, 1997; Ramos-Onsins & Rozas, 2002). Both of the *Chauliodus sloani* R2 values were very small and positive, further evidence of recent population expansion (Ramos-Onsins & Rozas, 2002).

The frequency-based tests also provide strong evidence that *Sternoptyx pseudobscura* has undergone population changes. Nine of the twelve tests performed on the four markers were significant (Tables 3-6). PLAG and ENC were significant and negative for both Tajima's D and F_s, while significant and positive for R2 (Table 4 and 5). Only F_s was significant for COI, but Tajima's D and Fs were both significant for Myh6 (Tables 3 and 6).

Table 3. Results of COI frequency-based statistics analysis. Tajima's D values that were significant based on the two-tailed test are dark grey. Significant values determined through coalescent simulations are highlighted in light grey.

	COI								
Species	**Tajima's D**	**R2**	**Fs**	**Fragment Length**	**Individuals**	**Segregating Sites**	**Haplotypes**	**Nucleotide Diverstiy**	**Haplotype Diversity**
Bathophilus pawneii	1.210	0.206	1.761	645	10	12	5	0.00831 (+/- 0.00104)	0.822 (+/- 0.097)
Chauliodus Sloani	-2.124	0.027	-33.567	563	97	32	39	0.00341 (+/- 0.00029)	0.859 (+/- 0.031)
Cyclothone alba	-1.831	0.200	-1.008	594	12	5	4	0.00140 (+/- 0.00062)	0.455 (+/- 0.170)
Cyclothone pseudopallida	-0.026	0.133	-0.680	651	14	7	5	0.00297 (+/- 0.00072)	0.756 (+/- 0.130)
Diplospinus multistriatus	-1.141	0.267	-0.476	645	12	1	2	0.00026 (+/- 0.00021)	0.167 (+/- 0.134)
Ditropichthys storeri	-0.796	0.137	-0.865	612	11	6	5	0.00267 (+/- 0.00064)	0.782 (+/- 0.107)
Photostomias guernei	-1.830	0.096	-3.216	651	12	9	7	0.00251 (+/- 0.00071)	0.773 (+/- 0.128)
Polymixia lowei	-1.243	0.075	-8.968	597	19	20	15	0.00683 (+/- 0.00125)	0.959 (+/- 0.036)
Scopelogaus mizolepis	-0.786	0.182	-2.995	642	11	7	7	0.00300 (+/- 0.00051)	0.909 (+/- 0.066)
Sigmops elongatus	-1.141	0.227	-0.476	651	12	1	2	0.00026 (+/- 0.00021)	0.167 (+/- 0.134)
Sternoptyx pseudobscura	-1.149	0.227	-0.537	537	13	1	2	0.00029 (+/- 0.00024)	0.154 (+/- 0.126)
Stomias affinis	-1.673	0.070	-8.668	651	11	17	11	0.00559 (+/- 0.00087)	1.000 (+/- 0.039)
Synagrops spinosus	-1.775	0.151	-1.564	531	13	4	4	0.00116 (+/- 0.00054)	0.423 (+/- 0.423)

Table 4. Results of PLAG frequency-based statistics analysis. Tajima's D values that were significant based on the two-tailed test are dark grey. Significant values determined through coalescent simulations are highlighted in light grey. NA refers to samples for which no data was available.

	PLAG								
Species	**Tajima's D**	**R2**	**Fs**	**Fragment Length**	**Individuals**	**Segregating Sites**	**Haplotypes**	**Nucleotide Diverstiy**	**Haplotype Diversity**
Bathophilus pawneii	-0.395	0.146	-0.070	576	10	4	4	0.00171 (+/- 0.00034)	0.689 (+/- 0.060)
Chauliodus Sloani	NA	NA	NA	NA	NA	NA	NA	NA	NA
Cyclothone alba	-1.591	0.068	-4.890	555	12	7	8	0.00166 (+/- 0.00049)	0.507 (+/- 0.125)
Cyclothone pseudopallida	-0.023	0.137	0.216	555	10	6	5	0.00304 (+/- 0.00062)	0.774 (+/- 0.052)
Diplospinus multistriatus	-0.163	0.126	0.200	516	12	4	4	0.00197 (+/- 0.00041)	0.612 (+/- 0.087)
Ditropichthys storeri	-2.186	0.074	-5.778	561	10	11	9	0.00213 (+/- 0.00065)	0.653 (+/- 0.122)
Photostomias guernei	-1.346	0.086	-2.582	603	12	10	8	0.00274 (+/- 0.00054)	0.739 (+/- 0.088)
Polymixia lowei	-0.248	0.114	0.230	516	12	1	2	0.00044 (+/- 0.00020)	0.228 (+/- 0.102)
Scopelogaus mizolepis	-1.165	0.121	-0.097	495	11	8	5	0.00089 (+/- 0.00089)	0.519 (+/- 0.114)
Sigmops elongatus	-1.494	0.096	-2.383	552	12	3	4	0.00059 (+/- 0.00024)	0.308 (+/- 0.118)
Sternoptyx pseudobscura	-1.993	0.046	-9.189	549	17	10	11	0.00158 (+/- 0.00028)	0.686 (+/- 0.088)
Stomias affinis	NA	NA	NA	NA	NA	NA	NA	NA	NA
Synagrops spinosus	NA	NA	NA	NA	NA	NA	NA	NA	NA

Table 5. Results of ENC frequency-based statistics analysis. Tajima's D values that were significant based on the two-tailed test are dark grey. Significant values determined through coalescent simulations are highlighted in light grey. NA refers to samples for which no data was available.

Species	Tajima's D	R2	Fs	Fragment Length	ENC Individuals	Segregating Sites	Haplotypes	Nucleotide Diverstiy	Haplotype Diversity
Bathophilus pawneii	NA	NA	NA	NA	NA	NA	NA	NA	NA
Chauliodus Sloani	-2.162	0.046	-10.151	660	19	20	15	0.00257 (+/- 0.00043)	0.791 (+/- 0.065)
Cyclothone alba	NA	NA	NA	NA	NA	NA	NA	NA	NA
Cyclothone pseudopallida	NA	NA	NA	NA	NA	NA	NA	NA	NA
Diplospinus multistriatus	-1.863	0.073	-5.836	663	12	8	9	0.00157 (+/- 0.00035)	0.703 (+/- 0.098)
Ditropichthys storeri	NA	NA	NA	NA	NA	NA	NA	NA	NA
Photostomias guernei	NA	NA	NA	NA	NA	NA	NA	NA	NA
Polymixia lowei	-1.319	0.115	-1.142	705	12	6	5	0.00129 (+/- 0.00035)	0.616 (+/- 0.073)
Scopelogaus mizolepis	NA	NA	NA	NA	NA	NA	NA	NA	NA
Sigmops elongatus	NA	NA	NA	NA	NA	NA	NA	NA	NA
Sternoptyx pseudobscura	-2.410	0.059	-6.027	678	16	16	10	0.00166 (+/- 0.00050)	0.532 (+/- 0.107)
Stomias affinis	NA	NA	NA	NA	NA	NA	NA	NA	NA
Synagrops spinosus	-0.414	0.112	-7.083	711	12	8	12	0.00266 (+/- 0.00036)	0.895 (+/- 0.045)

Table 6. Results of MYH frequency-based statistics analysis. Significant values determined through coalescent simulations are highlighted in light grey. NA refers to samples for which no data was available.

	MYH								
Species	**Tajima's D**	**R2**	**Fs**	**Fragment Length**	**Individuals**	**Segregating Sites**	**Haplotypes**	**Nucleotide Diverstiy**	**Haplotype Diversity**
Bathophilus pawneii	NA	NA	NA	NA	NA	NA	NA	NA	NA
Chauliodus Sloani	NA	NA	NA	NA	NA	NA	NA	NA	NA
Cyclothone alba	NA	NA	NA	NA	NA	NA	NA	NA	NA
Cyclothone pseudopallida	NA	NA	NA	NA	NA	NA	NA	NA	NA
Diplospinus multistriatus	NA	NA	NA	NA	NA	NA	NA	NA	NA
Ditropichthys storeri	NA	NA	NA	NA	NA	NA	NA	NA	NA
Photostomias guernei	NA	NA	NA	NA	NA	NA	NA	NA	NA
Polymixia lowei	NA	NA	NA	NA	NA	NA	NA	NA	NA
Scopelogaus mizolepis	NA	NA	NA	NA	NA	NA	NA	NA	NA
Sigmops elongatus	NA	NA	NA	NA	NA	NA	NA	NA	NA
Sternoptyx pseudobscura	-1.346	0.074	-2.209	594	15	3	4	0.00055 (+/- 0.00020)	0.306 (+/- 0.106)
Stomias affinis	-0.477	0.115	0.430	543	11	5	4	0.00213 (+/- 0.00089)	0.333 (+/- 0.124)
Synagrops spinosus	NA	NA	NA	NA	NA	NA	NA	NA	NA

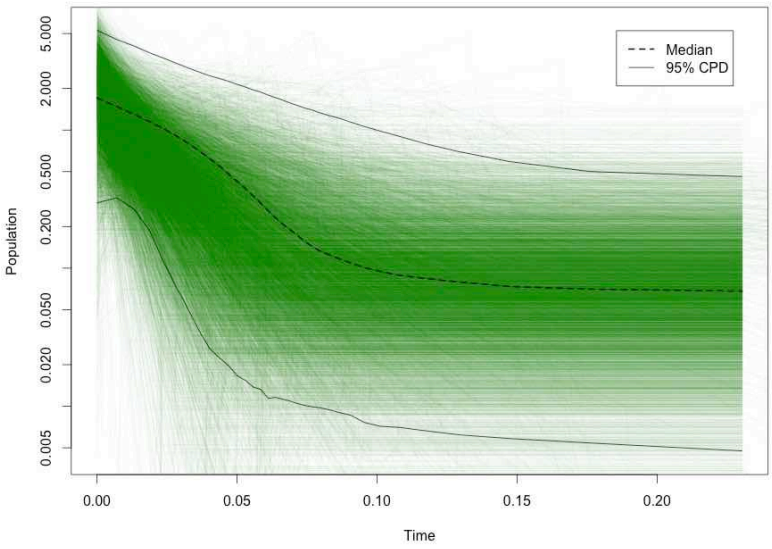

Figure 14. Extended Bayesian Skyline Plot for *Cyclothone alba*. Dates are given in terms of millions of years. The y-axis shows population size on a log-scale.

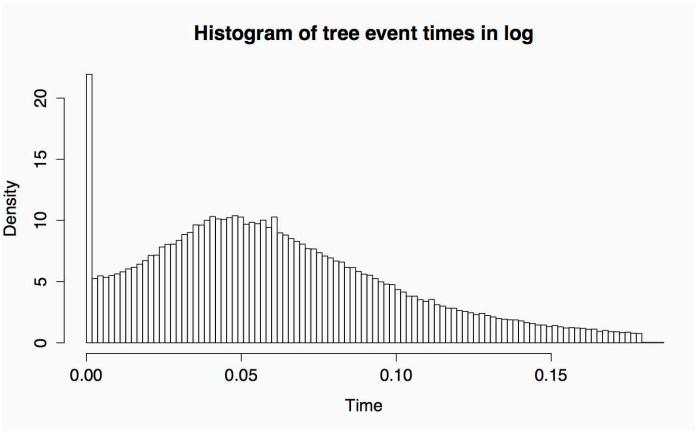

Figure 15. Histogram of tree events for *Cyclothone alba*. Dates are given in terms of millions of years.

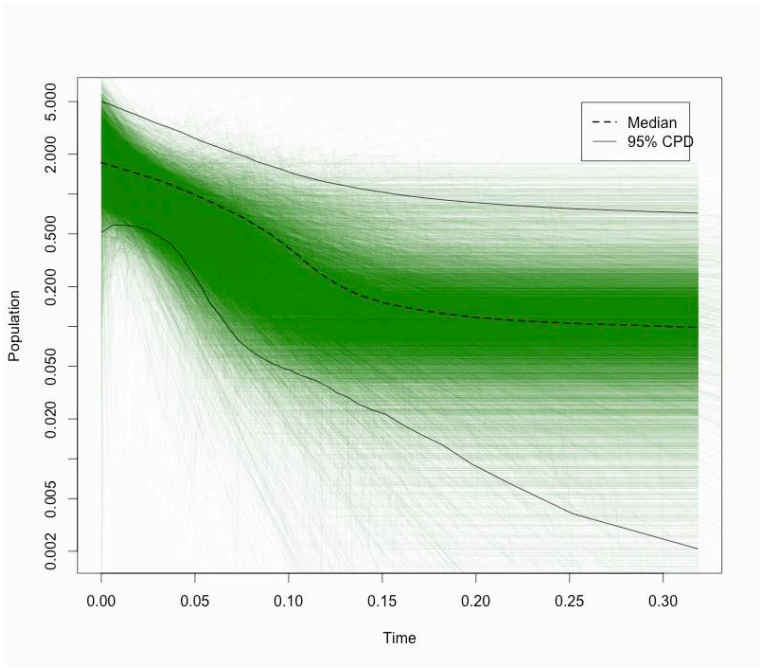

Figure 16. Extended Bayesian Skyline Plot for *Photostomias guernei*. Dates are given in terms of millions of years. The y-axis shows population size on a log-scale.

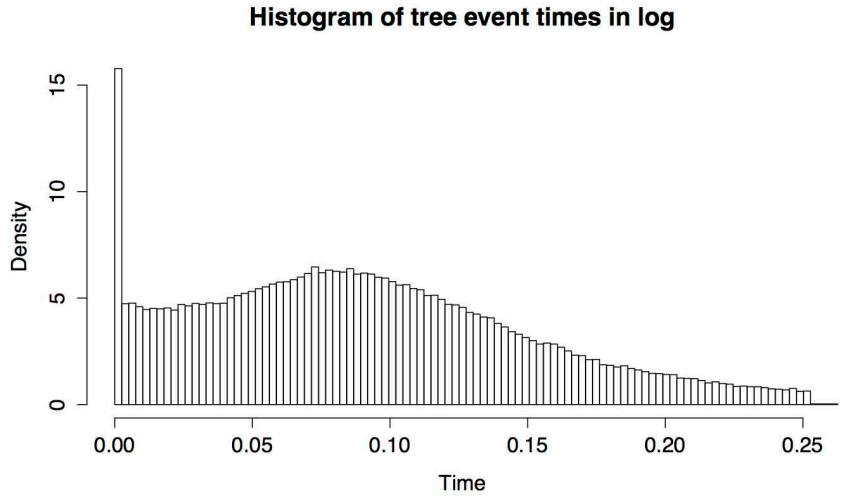

Figure 17. Histogram of tree events for *Photostomias guernei*. Dates are given in terms of millions of years.

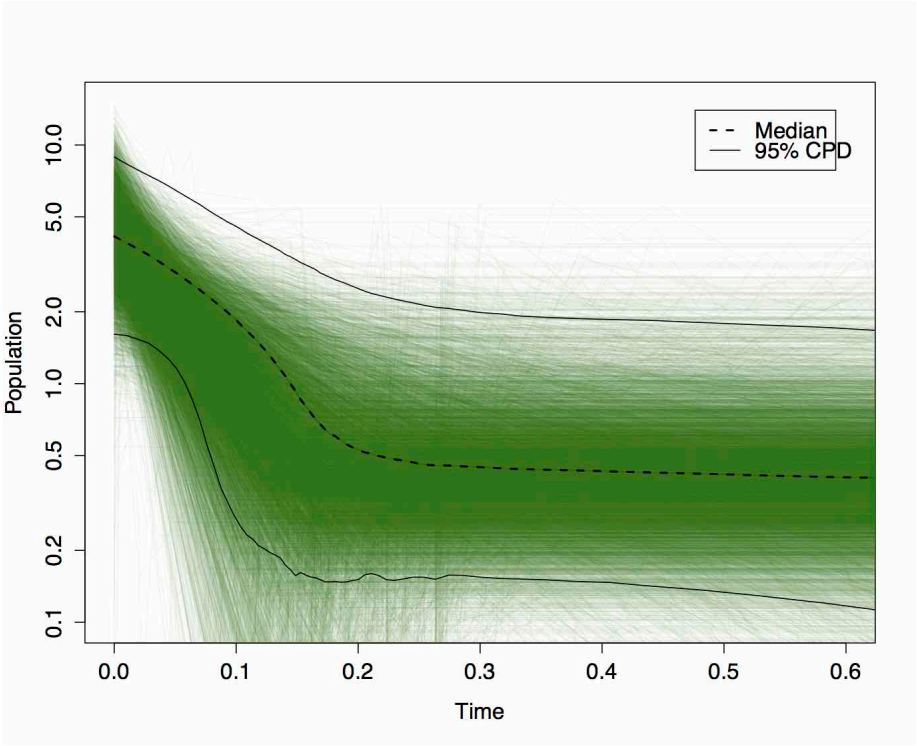

Figure 18. Extended Bayesian Skyline Plot for *Polymixia lowei*. Dates are given in terms of millions of years. The y-axis shows population size on a log-scale.

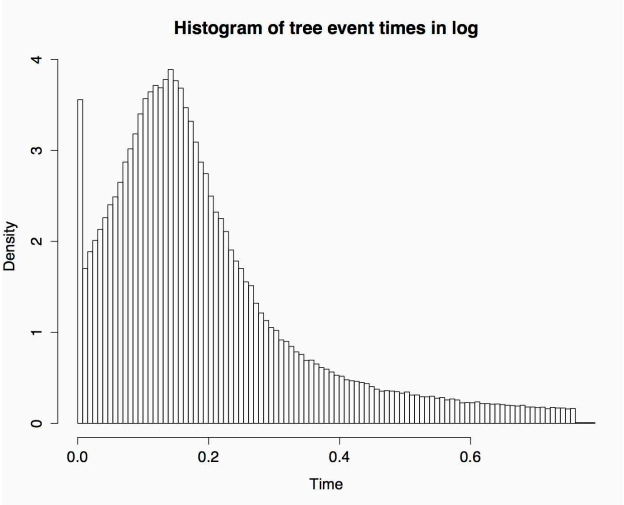

Figure 19. Histogram of tree events for *Polymixia lowei*. Dates are given in terms of millions of years.

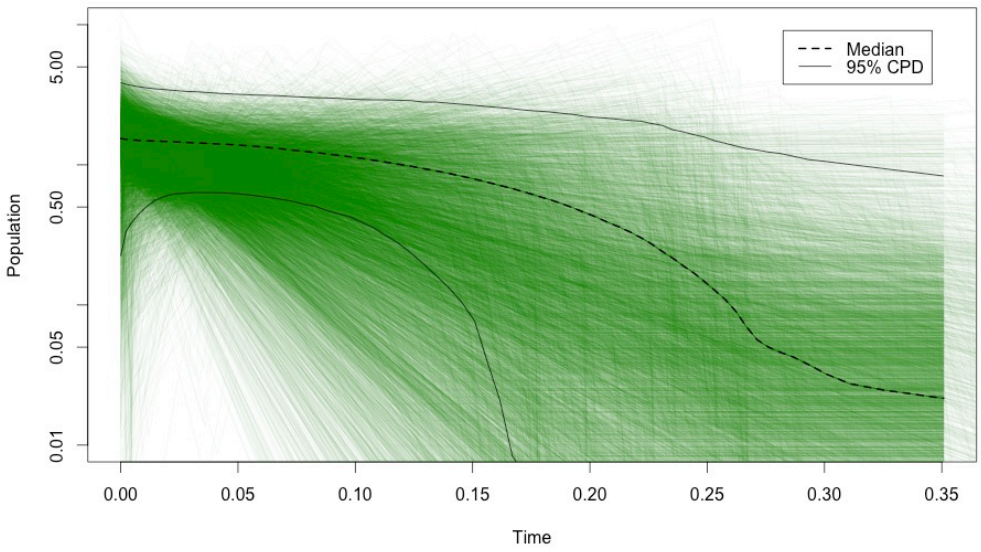

Figure 20. Extended Bayesian Skyline Plot for *Sternoptyx pseudobscura*. Dates are given in terms of millions of years. The y-axis shows population size on a log-scale.

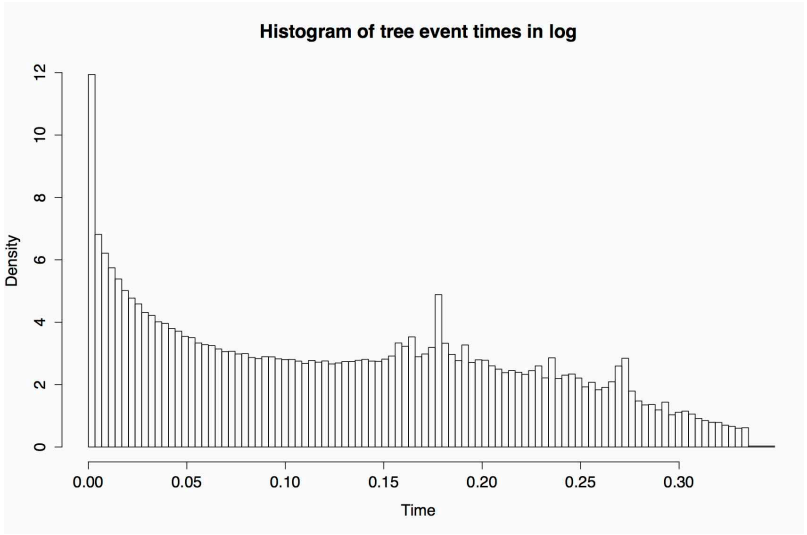

Figure 21. Histogram of tree events for *Sternoptyx pseudobscura*. Dates are given in terms of millions of years.

3.3.6 Vertical Migration and Population Dynamics

In order to determine the significance of vertical migration on demographic history we made use of a chi-squared test. We divided our species into two categories: those that vertically migrate and those that do not (Table 9). Two of the thirteen study species were excluded from this analysis, as information on the vertical migratory habits was unavailable (Appendix Table A-4). The chi-squared test provided low support for this line of inquiry, as we obtained a p-value of 0.8190 (Table 9). It therefore seems unlikely that vertical-migration has a significant effect on population size change dynamics in deep-pelagic fishes.

Table 9. Chi-squared test for significance of vertical migration on the inference of recent population size changes.

	Pop Size Change Inferred	No Pop Size Change Inferred		
Vertical Migrator	4	3	Chi-squared	0.0524
Non Vertical Migrator	2	2	p-value	0.8190

3.3.7 Sea Surface Temperature and Population Size Changes

The dates of inferred population expansion were plotted against published resconstructions of historic sea surface temperature (SST) in the North Atlantic to identify potential links between SST and the demographic histories of our study species (Clark et al., 2006; Ruddiman et al., 1989) (Figure 22). These climate records were utilized, because they came from a site located at ~41°North, the northern boundary for many low-latitude deep-pelagic fishes ranges. Major changes in SST here could impact deep-pelagic larval fish distribution and in turn drive population dynamics. Eight warm periods of SST, when SST was greater than 15 degrees Celsius stand out in the reconstructions of Atlantic SST (Figure 22). The dates of the five population size increases show a clear pattern, coinciding with four of the five most recent warm periods (within ten thousand years in every case). This correlation suggests that periods of warm SST may lead to population expansions in low-latitude deep-pelagic fishes.

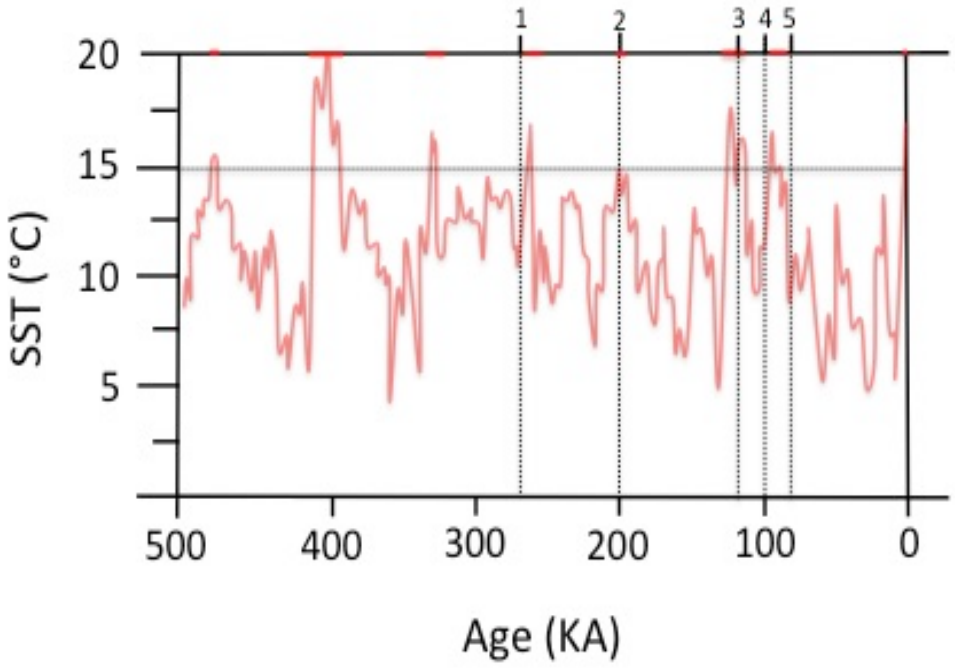

Figure 22. Reconstructed Atlantic SST at ~41°North for the past 500 ky plotted with dates of population size changes. The red plot provides SST estimates from 41 N (Ruddiman et al. 1989). Red lines on the top of the plot indicate periods of time where the North Atlantic site was 15°C or warmer. The numbers on top (1-5) refer to *Sternoptyx pseudobsura*, *Polymixia lowei*, *Photostomias guernei*, *Chauliodus sloani*, and *Cyclothone alba*, respectively.

3.4 Discussion

Historic changes in effective population size are frequently inferred for marine fishes and attributed to major ecological events (Almada et al., 2012; Avise et al., 2000; Eytan & Hellberg, 2010; W. Grant & Bowen, 1998; William Stewart Grant, 2015; Henriques et al., 2014; Robalo et al., 2012). Previous studies however, have largely focused on species inhabiting shallower environments that are more volatile over time in terms of physical conditions such as temperature. Given the relative stability of the deep-pelagic it was therefore possible that the populations of fishes inhabiting this environment would also be stable and no effective population size changes would be inferred. Nonetheless, we were able to uncover evidence of population expansions in five of our thirteen deep-pelagic study species, the most ancient event occurring approximately 270 thousand years ago. These expansions and their timings were based on our EBSPs, which utilized both mitochondrial and nuclear data. The dates of these population expansions coincide closely with periods of warm sea surface temperatures (SST) at 41° North in the Atlantic, a transition zone for many tropical deep-pelagic species. However, migration habit does not appear to predict the occurrence of population size changes

3.4.1 Frequency Based Statistics vs Gene Tree Based Analysis

The frequency-based statistics and gene tree based analysis were largely in agreement. Both sets of analyses made use of COI and all available nuclear data. The frequency-based tests detected population expansions in the five species identified by the gene tree based analysis, as well as an additional six species. The frequency-tests

provided the strongest evidence of demographic changes in four species: Chauliodus sloani, Cyclothone alba, Photstomias guernei, and Sternoptyx pseudobscura. The EBSPs inferred population expansions in every one of those species.

It is not surprising that these tests would not agree in every case. Simulated data sets have shown that frequency-based tests can fail to detect recent population expansion (Ramos-Onsins & Rozas, 2002). Furthermore, different tests perform better in different circumstances. For example, Rozas R2 tends to be the most sensitive test when dealing with small sample sizes, whereas Fu's F_s is the most sensitive when given a large sample size (Ramos-Onsins & Rozas, 2002).

Similarly, the Extended Bayesian Skyline Plot can fail to identify recent population expansions in a variety of circumstances (William Stewart Grant, 2015; Heled & Drummond, 2008). Simulated datasets demonstrate that larger sample sizes increase the sensitivity of EBSP analyses (William Stewart Grant, 2015). The fact that our EBSP did not infer population size changes in the four species identified by the frequency-based test statistics does not necessarily reject population expansion in those species. Rather, it is possible that some of our sample sizes were not sufficient to capture all coalescent events in a species' gene genealogy and the frequency based statistics were more sensitive than the EBSP, which has shown to have a relatively high type-I error rate (Heled and Drummond 2008).

3.4.2 Factors Influencing Deep-Pelagic Fish Population Dynamics

Numerous studies have made use of extended Bayesian skyline plots to infer demographic changes in fish populations in a variety of different environments. These

studies have frequently inferred recent population expansions under 20,000 years in age, roughly coinciding with the end of the last glacial maximum (Eytan & Hellberg, 2010; Henriques et al., 2014; Robalo et al., 2012). In a review of EBSPs in publication, Grant (2015) found that the most commonly reported date of expansion for fishes was under 20,000 years in age. The disparity between the age of these geologically recent population expansions and the expansions uncovered in this study is not unexpected. Many of the species presented in the Grant review are coastal fishes or inhabitants of specialized communities such as coral reefs. There has been a dramatic increase in the availability of shelf habitat since the last glacial maximum that would have led to an increase in carrying capacity of these species (Crandall, Sbrocco, DeBoer, Barber, & Carpenter, 2011; W Stewart Grant, Liu, Gao, & Yanagimoto, 2012).

The amount of deep-pelagic habitat has increased negligibly in comparison, so it is not immediately clear as to what mechanisms would control population dynamics in deep pelagic fishes. Furthermore, the deep-pelagic is thermally stable over time and space, when compared to surface waters (Clark et al., 2009; Levitus et al., 2012; Robison, 2009). It would therefore be possible that the population size of deep-pelagic fishes would be less susceptible to change in response to major global climatic changes than fishes inhabiting shallower waters. We did not find this to be the case however, and uncovered a minimum of five cases of population expansion (identified by both frequency-based statistics and gene tree based analysis) and as many as nine cases, within the past 300,000 years. Similar findings have been found for deep-benthic fish species, as well (Sakuma et al., 2014; Varela et al., 2012).

We identified two potential drivers of population size change in deep-pelagic fishes. Both were based on the obligate use of more variable surface waters by these species. The first focused on vertical migration. Hsieh et al. (2009) reported that the distribution of larvae from species with vertically migrating adults changed more rapidly than the larvae of non-vertically migrating species. They attributed this to short-term changes in surface water conditions. Because vertically migrating adults utilize these shallower waters on a daily basis, if physical conditions (like SST) became intolerable their range would contract and their population would shrink. When surface conditions grew more tolerable, their range would increase and their population would expand. If this were the case, non-vertically migrating fishes would be less susceptible to changes in range than vertical migrators. We did not however, detect any difference in population dynamics between these two groups.

The other mechanism we tested for was a relationship between pelagic larvae and SSTs, as the larvae of most deep-pelagic fishes reside in the upper 200 meters where the effects of climatic changes are more pronounced (Bowlin, 2016; Hsieh et al., 2009; Johnson et al., 2009; Paxton, 1989; Sassa et al., 2004; Smith & Moser, 1988). Two lines of evidence support this hypothesis. The first comes from long-term monitoring efforts in transition zones between tropical and subpolar regions that have shown that physical conditions, such as sea surface temperature (SST), are key predictors of larval community composition. Furthermore, physical changes in these environments alter the larval composition of the community (Ahlstrom, 1969; Netburn & Koslow, 2018; Sassa et al., 2004; Urias-Leyva et al., 2018). Aceves-Medina et al. (2004) found that the

distribution of larvae was congruent with that of the adults. This would suggest that as sea surface conditions change the distribution of larvae is altered, and in turn the range of the adults for a given species.

Further evidence comes from the distribution patterns of deep-pelagic fishes. Deep-pelagic fishes can broadly be classified as tropical or polar species, and tend to have clear latitudinal geographic boundaries to their ranges (Olson, 2001; Pearcy, 1991; Randall, 1981) (See Appendix Table A2 for range description of study species). Within oceanic basins, latitudinal differences in temperature decrease by depth. By 1000 meters the temperature is a near uniform 5 degrees Celsius throughout most of the world's oceans (Helfman et al., 2009; Tyus, 2011). It is therefore noteworthy that even the range of non-vertically migrating bathypelagic groups such as the whale fishes fit this pattern (Paxton, 1989). It seems unlikely that this distribution can be explained by physiological constraints on adults of these species given the relative homogeneity of the environment. Rather, the adult range is constrained to regions with surface waters tolerable to their larvae. If correct, we hypothesized that periods of warm SST in high latitudes would increase the range of tropical deep-pelagic fishes, and lead to population expansions.

Our comparison of reconstructed SSTs for the North Atlantic at 41° N and the dates of inferred population expansion support this hypothesis. We inferred five cases of population expansion with our EBSPs, and all of them appear to coincide with warm periods of SST at this site, a transition zone for many tropical and polar deep-pelagic species (Olson, 2001). This is strong evidence in support of the notion that sea surface conditions constrain the ranges of species living far below them through their larval

phase, and that they have profound impacts on their population sizes. If the tolerances of pelagic larvae dictate species distribution, it would explain why we were unable to detect any difference between vertically migrating and non-vertically migrating adults. The SST conditions present in a region will lead to a pelagic larval community that will mature into adults tolerant to those conditions.

3.4.3 Future Directions

Exploration of the demographic histories of polar mesopelagic and bathypelagic fishes could provide further support for our findings. If periods of warm sea surface temperatures benefit low latitude species, polar species would be expected to experience population bottlenecks during these times. Instead, high-latitude species would only undergo range expansion and a resultant population expansion when sea surface temperatures were low. Repeating this methodology on a set of polar deep-pelagic fish species could demonstrate, whether this is the case.

One of the limitations of this study was sample sizes, both in terms of sample number and number of genes used (William Stewart Grant, 2015; Heled & Drummond, 2008). Collecting large numbers of specimens of deep-pelagic fishes is expensive and labor intensive. A follow up study that utilizes exon capture methods or SNP generation would greatly increase the information available for demographic analyses.

3.5 Conclusions

Insights into the mechanisms that control deep pelagic-fish population dynamics are lacking. Our results demonstrate that despite the long-term stability of the deep-pelagic, the population sizes of the fishes that reside in this habitat are not static in

nature. The dates of expansion we inferred suggest that low latitude deep-pelagic fish species respond positively to an increase in sea surface temperature at high latitudes. As we come to understand the environmental factors that influence demographic changes in these fishes we will better be able to predict how populations of these fishes will behave in the face of future changes in sea surface temperatures.

3.6 References

Aceves-Medina, G., S. Jiménez-Rosenberg, A. Hinojosa-Medina, R. Funes-Rodríguez, R. Saldierna-Martínez, and P. Smith. 2004. Fish larvae assemblages in the Gulf of California. Journal of Fish Biology 65:832-847.

Ahlstrom, E. H. 1969. Mesopelagic and bathypelagic fishes in the California Current region. California Cooperative Oceanic Fisheries Investigations Reports 13:39-44.

Almada, V. C., F. Almada, S. M. Francisco, R. Castilho, and J. I. Robalo. 2012. Unexpected high genetic diversity at the extreme Northern geographic limit of Taurulus bubalis (Euphrasen, 1786). PLoS ONE 7:e44404.

Avise, J. C. 2000. Phylogeography: The History and Formation of Species. Harvard University Press, Cambridge, MA.

Battaglia, P., F. Andaloro, P. Consoli, V. Esposito, D. Malara, S. Musolino, C. Pedà, and T. Romeo. 2013. Feeding habits of the Atlantic bluefin tuna, Thunnus thynnus (L. 1758), in the central Mediterranean Sea (Strait of Messina). Helgoland Marine Research 67:97.

Becquey, S. and R. Gersonde. 2002. Past hydrographic and climatic changes in the Subantarctic Zone of the South Atlantic–The Pleistocene record from ODP Site 1090. Palaeogeography, Palaeoclimatology, Palaeoecology 182:221-239.

Bernatchez, L., J. Dodson, and S. Boivin. 1989. Population bottlenecks: influence on mitochondrial DNA diversity and its effect in coregonine stock discrimination. Journal of Fish Biology 35:233-244.

Bouckaert, R., M. V. Alvarado-Mora, and J. R. Pinho. 2013. Evolutionary rates and HBV: issues of rate estimation with Bayesian molecular methods. Antivir Ther 18:497-503.

Bouckaert, R., J. Heled, D. Kühnert, T. Vaughan, C.-H. Wu, D. Xie, M. A. Suchard, A. Rambaut, and A. J. Drummond. 2014. BEAST 2: a software platform for Bayesian evolutionary analysis. PLoS computational biology 10:e1003537.

Bouckaert, R. R. and A. J. Drummond. 2017. bModelTest: Bayesian phylogenetic site model averaging and model comparison. BMC Evolutionary Biology 17:42.

Bowlin, N. M. 2016. Ontogenetic changes in the distribution and abundance of early life history stages of mesopelagic fishes off California. UC San Diego, San Diego, CA.

Canino, M. F., I. B. Spies, K. M. Cunningham, L. Hauser, and W. S. Grant. 2010. Multiple iceage refugia in Pacific cod, Gadus macrocephalus. Molecular Ecology 19:4339-4351.

Catul, V., M. Gauns, and P. Karuppasamy. 2011. A review on mesopelagic fishes belonging to family Myctophidae. Reviews in Fish Biology and Fisheries 21:339-354.

Clark, P. U., D. Archer, D. Pollard, J. D. Blum, J. A. Rial, V. Brovkin, A. C. Mix, N. G. Pisias, and M. Roy. 2006. The middle Pleistocene transition: characteristics, mechanisms, and implications for long-term changes in atmospheric pCO2. Quaternary Science Reviews 25:3150-3184.

Clark, P. U., A. S. Dyke, J. D. Shakun, A. E. Carlson, J. Clark, B. Wohlfarth, J. X. Mitrovica, S. W. Hostetler, and A. M. McCabe. 2009. The last glacial maximum. Science 325:710-714.

Crandall, E. D., E. J. Sbrocco, T. S. DeBoer, P. H. Barber, and K. E. Carpenter. 2011. Expansion dating: calibrating molecular clocks in marine species from expansions onto the Sunda Shelf following the Last Glacial Maximum. Molecular biology and evolution 29:707-719.

Dulvy, N. K., S. I. Rogers, S. Jennings, V. Stelzenmüller, S. R. Dye, and H. R. Skjoldal. 2008. Climate change and deepening of the North Sea fish assemblage: a biotic indicator of warming seas. Journal of Applied Ecology 45:1029-1039.

Etter, R., M. A. Rex, M. R. Chase, and J. M. Quattro. 2005. Population differentiation decreases with depth in deep-sea bivalves. Evolution 59:1479-1491.

Eytan, R. I. and M. E. Hellberg. 2010. Nuclear and mitochondrial sequence data reveal and conceal different demographic histories and population genetic processes in Caribbean reef fishes. Evolution: International Journal of Organic Evolution 64:3380-3397.

Fu, Y.-X. 1997. Statistical tests of neutrality of mutations against population growth, hitchhiking and background selection. Genetics 147:915-925.

Gaither, M. R., B. W. Bowen, L. A. Rocha, and J. C. Briggs. 2016. Fishes that rule the world: circumtropical distributions revisited. Fish and Fisheries 17:664-679.

Gjøsaeter, J. and K. Kawaguchi. 1980. A review of the world resources of mesopelagic fish. Food & Agriculture Org. FAO, Rome, Italy.

Glenn, T. 2019. PEG Precipitation of PCR products. http://labs.mcdb.lsa.umich.edu/labs/olsen/files/PCR.pdf

Grant, W. and B. Bowen. 1998. Shallow population histories in deep evolutionary lineages of marine fishes: insights from sardines and anchovies and lessons for conservation. Journal of Heredity 89:415-426.

Grant, W. S. 2015. Problems and cautions with sequence mismatch analysis and Bayesian skyline plots to infer historical demography. Journal of Heredity 106:333-346.

Grant, W. S., M. Liu, T. Gao, and T. Yanagimoto. 2012. Limits of Bayesian skyline plot analysis of mtDNA sequences to infer historical demographies in Pacific herring (and other species). Molecular Phylogenetics and Evolution 65:203-212.

Heled, J. 2010. Extended Bayesian skyline plot tutorial. Available from: tutorial.east. bio.ed.ac.uk/Tutorials.

Heled, J. and A. J. Drummond. 2008. Bayesian inference of population size history from multiple loci. BMC Evolutionary Biology 8:289.

Helfman, G., B. B. Collette, D. E. Facey, and B. W. Bowen. 2009. The diversity of fishes: biology, evolution, and ecology. John Wiley & Sons.

Henriques, R., W. M. Potts, C. V. Santos, W. H. Sauer, and P. W. Shaw. 2014. Population connectivity and phylogeography of a coastal fish, Atractoscion aequidens (Sciaenidae), across the Benguela current region: evidence of an ancient vicariant event. PLoS ONE 9:e87907.

Hewitt, G. 2000. The genetic legacy of the Quaternary ice ages. Nature 405:907.

Ho, S. Y. and B. Shapiro. 2011. Skyline-plot methods for estimating demographic history from nucleotide sequences. Molecular Ecology Resources 11:423-434.

Hsieh, C. H., H. J. Kim, W. Watson, E. Di Lorenzo, and G. Sugihara. 2009. Climate-driven changes in abundance and distribution of larvae of oceanic fishes in the southern California region. Global Change Biology 15:2137-2152.

Innan, H., K. Zhang, P. Marjoram, S. Tavaré, and N. A. Rosenberg. 2005. Statistical tests of the coalescent model based on the haplotype frequency distribution and the number of segregating sites. Genetics.

Irigoien, X., T. A. Klevjer, A. Røstad, U. Martinez, G. Boyra, J. Acuña, A. Bode, F. Echevarria, J. I. González-Gordillo, and S. Hernandez-Leon. 2014. Large

mesopelagic fishes biomass and trophic efficiency in the open ocean. Nature communications 5:3271.

Johnson, G. D., J. R. Paxton, T. T. Sutton, T. P. Satoh, T. Sado, M. Nishida, and M. Miya. 2009. Deep-sea mystery solved: astonishing larval transformations and extreme sexual dimorphism unite three fish families. Biology Letters 5:235-239.

Kearse, M., R. Moir, A. Wilson, S. Stones-Havas, M. Cheung, S. Sturrock, S. Buxton, A. Cooper, S. Markowitz, and C. Duran. 2012. Geneious Basic: an integrated and extendable desktop software platform for the organization and analysis of sequence data. Bioinformatics 28:1647-1649.

Lanfear, R., B. Calcott, S. Y. Ho, and S. Guindon. 2012. PartitionFinder: combined selection of partitioning schemes and substitution models for phylogenetic analyses. Molecular biology and evolution 29:1695-1701.

Levitus, S., J. I. Antonov, T. P. Boyer, O. K. Baranova, H. E. Garcia, R. A. Locarnini, A. V. Mishonov, J. Reagan, D. Seidov, and E. S. Yarosh. 2012. World ocean heat content and thermosteric sea level change (0–2000 m), 1955–2010. Geophysical Research Letters 39.

Li, H. 2010. A new test for detecting recent positive selection that is free from the confounding impacts of demography. Molecular biology and evolution 28:365-375.

Maggs, C. A., R. Castilho, D. Foltz, C. Henzler, M. T. Jolly, J. Kelly, J. Olsen, K. E. Perez, W. Stam, and R. Väinölä. 2008. Evaluating signatures of glacial refugia for North Atlantic benthic marine taxa. Ecology 89:S108-S122.

Mix, A. C., E. Bard, and R. Schneider. 2001. Environmental processes of the ice age: land, oceans, glaciers (EPILOG). Quaternary Science Reviews 20:627-657.

Miya, M. and T. Nemoto. 1986. Life history and vertical distribution of the mesopelagic fish Cyclothone alba (family Gonostomatidae) in Sagami Bay, Central Japan. Deep Sea Research Part A. Oceanographic Research Papers 33:1053-1068.

Miya, M. and M. Nishida. 1996. Molecular phylogenetic perspective on the evolution of the deep-sea fish genusCyclothone (Stomiiformes: Gonostomatidae). Ichthyological Research 43:375-398.

Moore, G. and J. Chaplin. 2014. Contrasting demographic histories in a pair of allopatric, sibling species of fish (Arripidae) from environments with contrasting glacial histories. Marine Biology 161:1543-1555.

Moser, H. 1996. The early life stages of fishes in the California Current Region. California Cooperative Oceanic Fisheries Investigations Atlas 33:1505.

Near, T. J., A. Dornburg, R. I. Eytan, B. P. Keck, W. L. Smith, K. L. Kuhn, J. A. Moore, S. A. Price, F. T. Burbrink, and M. Friedman. 2013. Phylogeny and tempo of diversification in the superradiation of spiny-rayed fishes. Proceedings of the National Academy of Sciences 110:12738-12743.

Netburn, A. N. and J. A. Koslow. 2018. Mesopelagic fish assemblages across oceanic fronts: A comparison of three frontal systems in the southern California Current Ecosystem. Deep Sea Research Part I: Oceanographic Research Papers 134:80-91.

Nye, J. A., J. S. Link, J. A. Hare, and W. J. Overholtz. 2009. Changing spatial distribution of fish stocks in relation to climate and population size on the Northeast United States continental shelf. Marine Ecology Progress Series 393:111-129.

Olson, D. B. 2001. Biophysical dynamics of western transition zones: a preliminary synthesis. Fisheries Oceanography 10:133-150.

Otto-Bliesner, B., C. Hewitt, T. Marchitto, E. Brady, A. Abe-Ouchi, M. Crucifix, S. Murakami, and S. Weber. 2007. Last Glacial Maximum ocean thermohaline circulation: PMIP2 model intercomparisons and data constraints. Geophysical Research Letters 34.

Paxton, J. R. 1989. Synopsis of the whalefishes (family Cetomimidae) with descriptions of four new genera. Records of the Australian Museum 41:135-206.

Pearcy, W. G. 1991. Biology of the transition region. NOAA Technical Report NMFS 105:39-55.

Provan, J. and K. Bennett. 2008. Phylogeographic insights into cryptic glacial refugia. Trends in Ecology & Evolution 23:564-571.

Rambaut, A. 2012. FigTree v1. 4.

Rambaut, A., A. Drummond, D. Xie, G. Baele, and M. Suchard. 2018. Posterior summarisation in Bayesian phylogenetics using Tracer 1.7. Systematic biology 67:901-904.

Ramos-Onsins, S. E. and J. Rozas. 2002. Statistical properties of new neutrality tests against population growth. Molecular biology and evolution 19:2092-2100.

Randall, J. E. 1981. Examples of antitropical and antiequatorial distribution of Indo-West-Pacific fishes. Pacific Science 35:197-209.

Robalo, J. I., R. Castilho, S. M. Francisco, F. Almada, H. Knutsen, P. E. Jorde, A. M. Pereira, and V. C. Almada. 2012. Northern refugia and recent expansion in the North Sea: the case of the wrasse Symphodus melops (Linnaeus, 1758). Ecology and Evolution 2:153-164.

Robison, B. H. 2009. Conservation of deep pelagic biodiversity. Conservation Biology 23:847-858.

Rogers, A. R. and H. Harpending. 1992. Population growth makes waves in the distribution of pairwise genetic differences. Molecular biology and evolution 9:552-569.

Rosendahl, S., P. Mcgee, and J. B. Morton. 2009. Lack of global population genetic differentiation in the arbuscular mycorrhizal fungus Glomus mosseae suggests a recent range expansion which may have coincided with the spread of agriculture. Molecular Ecology 18:4316-4329.

Rozas, J., A. Ferrer-Mata, J. C. Sánchez-DelBarrio, S. Guirao-Rico, P. Librado, S. E. Ramos-Onsins, and A. Sánchez-Gracia. 2017. DnaSP 6: DNA sequence polymorphism analysis of large data sets. Molecular biology and evolution 34:3299-3302.

Ruddiman, W. F., M. Raymo, D. Martinson, B. Clement, and J. Backman. 1989. Pleistocene evolution: Northern hemisphere ice sheets and North Atlantic Ocean. Paleoceanography and Paleoclimatology 4:353-412.

Sakuma, K., Y. Ueda, T. Hamatsu, and S. Kojima. 2014. Contrasting population histories of the deep-sea demersal fish, Lycodes matsubarai, in the Sea of Japan and the Sea of Okhotsk. Zoological science 31:375-382.

Sassa, C., K. Kawaguchi, Y. Oozeki, H. Kubota, and H. Sugisaki. 2004. Distribution patterns of larval myctophid fishes in the transition region of the western North Pacific. Marine Biology 144:417-428.

Smith, P. E. and H. G. Moser. 1988. CalCOFI time series: an overview of fishes. CalCOFI Report 29:66-77.

Stewart, J. R., A. M. Lister, I. Barnes, and L. Dalén. 2009. Refugia revisited: individualistic responses of species in space and time. Proceedings of the Royal Society B: Biological Sciences 277:661-671.

Sutton, T. 2013. Vertical ecology of the pelagic ocean: classical patterns and new perspectives. Journal of Fish Biology 83:1508-1527.

Sutton, T. T. and T. L. Hopkins. 1996. Species composition, abundance, and vertical distribution of the stomiid (Pisces: Stomiiformes) fish assemblage of the Gulf of Mexico. Bulletin of Marine Science 59:530-542.

Tajima, F. 1989. Statistical method for testing the neutral mutation hypothesis by DNA polymorphism. Genetics 123:585-595.

Team, R. 2012. RStudio: integrated development environment for R. RStudio Inc, . RStudio Inc, Boston, Massachusetts.

Tyus, H. M. 2011. Ecology and conservation of fishes. CRC press, Boca Raton, FL.

Urias-Leyva, H., G. Aceves-Medina, R. Avendaño-Ibarra, R. J. Saldierna-Martínez, J. Gómez-Gutiérrez, and C. J. Robinson. 2018. Regionalization in the distribution of larval fish assemblages during winter and autumn in the Gulf of California. Latin American Journal of Aquatic Research 46:20-36.

Varela, A. I., P. A. Ritchie, and P. J. Smith. 2012. Low levels of global genetic differentiation and population expansion in the deep-sea teleost Hoplostethus atlanticus revealed by mitochondrial DNA sequences. Marine Biology 159:1049-1060.

Varghese, S. P. S., V.S.; Gulati, D.K. 2013. Ontogenetic and seasonal variations in the feeding ecology of the Indo-Pacific sailfish, Istiophorus platypterus, or the eastern Arabian Sea. Indian Journal of Marine Sciences 42:593-605.

Watterson, G. 1975. On the number of segregating sites in genetical models without recombination. Theoretical population biology 7:256-276.

4. CONCLUSIONS

The deep-pelagic is the largest biome on planet Earth. Despite it size, only one percent of the habitat has been explored and the animal life inhabiting the deep-pelagic is severely underrepresented in global marine biological records. Accordingly, many questions related to the demographic histories and taxonomic relationships of deep-pelagic fishes remain unanswered. We utilized molecular data to infer the demographic histories of 13 species of deep-pelagic fishes and to investigate taxonomic issues related to the family Cetomimidae (the whale fishes).

Taxonomic issues have long plagued family Cetomimidae. Phylogenetic relationships within the family are poorly resolved. The same is true for the relationships between all of the families comprising Stephanoberycoidei. Even the matching of male and female cetomimids has proven extremely difficult, due to striking sexual dimorphism within the family (only one male and female species have been matched prior to this study). Molecular data is a powerful tool that we used to construct two maximum clade credibility trees and perform bGMYC analysis in order better understand whale fish taxonomy.

Our tree for the family Cetomimidae largely agreed with past morphological work. Areas of disagreement regarding morphological analyses included a clade comprising Cetostoma + Ditropichthys, as well as paraphyly within Gyrinomimus with respect to Cetomimus. These results are supported by several previous studies that relied on different markers. Our Stephanoberycoidei tree failed to uncover a previously

proposed monophyletic “cetomimoid” clade, and was only in partial agreement with previous morphological analyses. Instead of a “cetomimoid” clade we identified a clade comprised of Cetomimidae + Barbourisiidae that was sister to Gibberichthyidae + Rondeletiidae. The bGMYC analysis revealed Cetostoma regani to be a cryptic species complex, comprised of two operational taxonomic units that divered ~3.1 Ma ago. We identified two new putative Cetomimus species, as well. Finally, we were able to match all of our male samples to three different female species.

Reconstructions of historic demography shed light on the way the population size of a given species has reacted to past ecological and evolutionary events. By understanding the past we can begin to understand how populations will behave in response to current and future changes to their habitat. Both mitochondrial and nuclear markers were sequenced for 13 low-latitude deep-pelagic fish species representing 8 families. Demographic histories were reconstructed using two sets of analyses: one based on frequency derived summary statistics and the other based on the topologies and branch lengths of gene trees (extended Bayesian skyline plots).

Historic population expansions were inferred for eleven species using frequency-based statistics, while our extended Bayesian skyline plots (EBSPs) detected expansions in five of those species. Our EBSPs provided estimated dates of expansion that ranged from 80 ky ago to 270 ky ago. All of these dates appear to coincide with periods of warm sea surface temperature (SST) at approximately 41° of latitude in the North Atlantic, the northernmost range for many low-latitude deep-pelagic fishes. The influence of SST on deep-sea fish population size is intriguing given the long-term

stability of the environment. It is likely that physiological tolerances of the pelagic larval phase of deep-pelagic fishes constrain range and control population dynamics. In the case of low-latitude deep-pelagic fishes warming SST would allow the larval range to expand toward the poles leading to and increase population size.

APPENDIX

Table A-1. List of mitochondrial COI primers used.

Gene	Primer Name	Primer Sequence
COI	FISH1F	TCAACCAACCACAAAGACATTGGCAC
COI	FISH1R	TAGACTTCTGGGTGGCCAAAGAATCA
COI	FISH2F	TCGACTAATCATAAAGATATCGGCAC
COI	FISH2R	ACTTCAGGGTGACCGAAGAATCAGAA
COI	BOLD_COI_Forward	TTCTCCACCAACCACAARGAYATYGG
COI	BOLD_COI_Reverse	CACCTCAGGGTGTCCGAARAAYCARAA
COI	FISHCOI_F	TCAACYAATCAYAAAGATATYGGCAC
COI	FISHCOI_R	ACTTCYGGGTGRCCRAARAATCA

Table A-2. Samples and accession numbers used to generate the Cetomimidae maximum clade credibility tree.

Number	Genus (Field ID)	Species (Field ID)	Sex (if known)	Source
DPND_2173	*Cetomimus*	*sp.*	Female	Deepend
DPND_2521	*Cetomimus*	*sp.*	Female	Deepend
DPND_2904	*Cetomimus*	*sp.*	Female	Deepend
DPND_4578	*Cetomimus*	*sp.*	Female	Deepend
RIE_364	*Cetomimus*	*sp.*	Female	Deepend
RIE_756	*Cetomimus*	*sp.*	Female	Deepend
DPND_1316	*Cetostoma*	*regani*	Female	Deepend
RIE_232	*Cetostoma*	*regani*	Female	Deepend
RIE_960	*Gyrinomimus*	*sp.*	Female	Deepend
Pisces_P543	*Gyrinomimus*	*parri*	Female	Pisces Cruises
DPND_1525	*Ataxolepis*	*apus*	Male	Deepend
DPND_2798	*Ataxolepis*	*apus*	Male	Deepend
Pisces_P553	*Ataxolepis*	*apus*	Male	Pisces Cruises
DPND_5048	*Cetomimus*	*sp.*	Female	Deepend
DPND_2989	*Ditropichthys*	*storeri*	Female	Deepend
DPND_3302	*Ditropichthys*	*storeri*	Female	Deepend
DPND_3911	*Ditropichthys*	*storeri*	Female	Deepend
DPND_1466	*Ditropichthys*	*storeri*	Female	Deepend
RIE_522	*Ditropichthys*	*storeri*	Female	Deepend
DPND_5635	*Anoplogaster*	*cornuta*	NA	Deepend
AP010881.1	*Cetomimus*	*sp*	Female	Genbank
AP010884.1	*Gyrinomimus*	*myersi*	Female	Genbank
UWNC_12049.1	*Gyrinomimus*	*sp.*	Female	Genbank
AP002936.1	*Danacetichthys*	*galathenus*	Female	Genbank
NC_12047.1	*Procetichthys*	*kreffti*	Female	Genbank

Table A-3. Samples and accession numbers used to generate the Stephanoberycoidei maximum clade credibility tree.

Number	Genus (Field ID)	Species (Field ID)	Source
RIE_756	*Cetomimus*	*sp.*	Deepend
DPND_1316	*Cetostoma*	*regani*	Deepend
RIE_960	*Gyrinomimus*	*bruuni*	Deepend
Pisces_P543	*Gyrinomimus*	*parri*	Pisces Cruises
RIE_522	*Ditropichthys*	*storeri*	Deepend
AP010884.1_	*Gyrinomimus*	*myersi*	Genbank
AP002936.1_	*Danaceticthys*	*galathenus*	Genbank
DPND_1383	*Melamphaes*	*sp*	Deepend
JF492951.1_	*Beryx*	*decadactylus*	Genbank
KF489520.1_	*Centroberyx*	*druzhinini*	Genbank
DPND_2511	*Scopelogadus*	*mizolepis*	Deepend
RIE_172	*Poromitra*	*megalops*	Deepend
RIE_63	*Scopeloberyx*	*opisthopterus*	Deepend
DPND_1991	*Anoplogaster*	*cornuta*	Deepend
KF929557.1_	*Acanthochaenus*	*luetkenii*	Genbank
DPND_1947	*Gibberichthys*	*pumilus*	Deepend
DPND_4011	*Barbourisia*	*rufa*	Deepend
RIE_773	*Rondeletia*	*bicolor*	Deepend
NC_12047.1	*Procetichthys*	*kreffti*	Genbank
DPND_1983	*Polymixia*	*lowei*	Deepend

Table A-4. Life History Trait Data. Vertical migration refers to habits of adults not larvae or juveniles

Species	Family	Order	Diel Vertical Migrators	Max Length (cm)	Upper Depth of occurrence	Lower Depth of occurrence	Total Depth Range	References
Bathophilus pawneei	Stomiidae	Stomiiformes	Yes	12.4	0	1500	1500	McEachran & Fechhelm (1998)
Chauliodus sloani	Stomiidae	Stomiiformes	Yes	30	0	1800	1800	McEachran & Fechhelm (1998); Clarke (1983)
Cyclothone alba	Gonostomatidae	Stomiiformes	No	3.4	300	600	300	McEachran & Fechhelm (1998); Miya & Nemoto (1986)
Cyclothone pseudopallida	Gonostomatidae	Stomiiformes	No	5.8	300	900	600	McEachran & Fechhelm (1998); Miya & Nemoto (1986)
Ditropichthys storeri	Cetomimidae	Stephanoberyciformes	No	12.8	650	2150	1500	McEachran & Fechhelm (1998); Pacton (1989)
Diplospinus multistriatus	Gempylidae	Perciformes	Yes	33	100	1000	900	McEachran & Fechhelm (1998); Levya-Cruz et al. (2016)
Polymixia lowei	Polymixiidae	Polymixiiformes		19.8	82	660	578	McEachran & Fechhelm (1998); Moore et al. (2003)
Scopelogadus mizolepis	Melamphaidae	Stephanoberyciformes	Yes	7.4	268	1250	982	McEachran, Fechhelm & Clarke (1983); Willis & Pearson (1982); Keene, Gibbs & Krueger (1987)
Sigmops elongatus	Gonostomatidae	Stomiiformes	Yes	27.5	50	1200	1150	McEachran & Fechhelm (1988); Lancraft et al. (1988); Gartner (1993)
Sternoptyx pseudobscura	Sternoptychidae	Stomiiformes	No	5.5	800	1500	700	McEachran & Fechhelm (1998)
Stomias affinis	Stomiidae	Stomiiformes	Yes	20.4	850	50	-800	McEachran & Fechhelm (1998); Sutton & Hopkins (1996)
Synagrops spinosus	Acropomatidae	Perciformes		13	72	412	340	McEachran & Fechhelm (1998)
Photostomias guernei	Stomiidae	Stomiiformes	Yes	13.5	15	800	785	McEachran & Fechhelm (1998); Clarke (1974)

Table A-5. Range Description for Study Species.

Species	Range Description	Oceans Inhabited	Latitudes Inhabited	Citations	Notes
Bathophilus pawneii	Circumglobal; Tropical	Atlantic, Indian, Pacific	36°N-34°S	Agustin 2018	
Chauliodus sloani	Circumglobal; Tropical and Polar	Atlantic, Indian, Pacific	50°N-50°S	Mundy 2005	Less common but records exist from individuals as far as 70°N-56°S (Priede 2017)
Cyclothone alba	Circumglobal; Tropical	Atlantic, Indian, Pacific	40°N-40°S	Miya & Nemoto 1986	
Cyclothone pseudopallida	Circumglobal; Tropical and Polar	Atlantic, Indian, Pacific	65°N–30°S	Mundy 2005	
Diplospinus multistriatus	Circumglobal; Tropical	Atlantic, Indian, Pacific	40°N-40°S	Mundy 2005	
Ditropichthys storeri	Circumglobal; Tropical	Atlantic, Indian, Pacific	48°N-43°S	Paxton 1989	
Photostomias guernei	Non circumglobal; Tropical	Atlantic	40°N-3°N	Kenaley 2009	
Polymixia lowei	Non circumglobal; Tropical	Atlantic	40°N-34°S	Lachner 1955; Haimovici 1994	
Scopelogadus mizolepis	Circumglobal; Tropical	Atlantic, Indian, Pacific	40°N-22°S	Mundy 2005	
Sigmops elongatus	Circumglobal; Tropical and Polar	Atlantic, Indian, Pacific	65°N–35°S	Torres 2018	
Sternoptyx pseudobscura	Circumglobal; Tropical	Atlantic, Indian, Pacific	40°N-40°S	Mundy 2005; Zammaro & Loris 1999	One record from 42°N and 47°N
Stomias affinis	Circumglobal; Tropical	Atlantic, Indian, Pacific	35°N-39°S	Priede 2017	
Synagrops spinosus	Non circumglobal; Tropical	Atlantic	36°N-34°S	Haimovici 1994	

Table A-6. Table of nuclear introns that were tested and rejected. These primers failed to amplify anything or amplified multiple sequences for the majority species in this study.

Gene	Primer Name	Primer Sequence
14867E1	14867E1-FOR	CCACAARTACAAGGCCAAGAGRAACTG
	14867E1-REV	GTTCTCCTTSTCCTGSACGGTCTT
36298E1	36298E1-FOR	GATCCTGAGGGAYTCCCAYGGTGT
	36298E1-REV	GGGCCAGGACTCTCYTGGTCTTGTAGT
55378E1	55378E1-FOR	ATGARGAAAATGAGGCCAACTTGCT
	55378E1-REV	GCCACCTGKGTATTGATTATAGCTGAG
4174E20	4174E20-FWD	CTYTCGCTGGCTTTGTCTCAAATCA
	4174E20-REV	CTTTTACCATCKCCACTRAAATCCAC
L8Ex	L8Ex2F	CAYATTGACTTCGCTGARCG
	L8Ex3R	TTGCCGCAGTAGATRAACTG
P0Ex	P0ExAF	ATGATGCGYAARGCCATCCG
	P0ExBR	GYAAGRTCCTCCTTGGTGAA
S8Ex	S8Ex4F	GGCMGSAAGAAGGGAGCCAA
	S8Ex5R	TGCWGGAACTGCTCCTCCAG
19231E4	19231E4-F	CGGARGACTACGGACGTGATTTGAC
	19231E4-R	CTCCYTCCAGTGSTCCACAAACT
59107E2	59107E2-F	GGAGATGGGYGTGGACTGGTCYCT
	59107E2-R	ATTGTAGATCTCVTCCACCACCTGRAT
40245E5	40245E5-F	CTGAGGAGGAYGGCTGGGARTTYGT
	40245E5-R	ACCATCAGCTTCACCACCTGCTC
1777E4	1777E4-F	AGGAGYTGGTGAACCAGAGCAAAGC
	1777E4-R	AGATCRGCCTGAATSAGCCAGTT
25073E1	25073E1-F	GTACTCTCKGTACATGTTGTGRGTKCC
	25073E1-R	GAAGGTGAARAACTTTGGBATCTGG
Gpd	Gpd2F	GCCATCAATGACCCCTTCATCG
	Gpd3R	TTGACCTCACCCTTGAAGCGGCCG
GnRH3	GnRH3F	GCCCAAACCCAAGAGAGACTTAGACC
	GnRH3R	TTCGGTCAAAATGACTGGAATCATC
A-Enol	EnolF_731	TGGACTTCAAATCCCCCGATGATCCCAGC
	EnolR_912	CCAGGCACCCCAGTCTACCTGGTCAAA
Alpha-tropomyosin	ATROP_F	GAGTTGGATCGCGCTCAGGAGCG
	ATROP_R	CGGTCAGCCTCCTCAGCAATGTGCTT

Table A-7. List of nuclear exon primers used to generate extended Bayesian skyline plots.

Gene	**Primer Name**	**Primer Sequence**
ENC	Perc_ENC_F	TTCCTRGAGAGAAACCTTCACC
ENC	Perc_ENC_R	GAYGGAGARGCNGGGAGGCAGCC
PLAG	Perc_PLAG_F	CATGAYCCYAACAARGARGCCTT
PLAG	Perc_PLAG_R	TGRCARCCCATGCCCATAGCTG
MYH	Perc_MYH_F	ACYAARAGRGTYATYCAGTACT
MYH	Perc_MYH_R	CCRAKGGMRTAGTAGACYTGRTC

Table A-8. List of Calibrations used to generate the Stomiiformes tree. Adapted from Near et al. (2013).

Prior	Mean	Sigma		Species
Chauliodus	16	2	Monophyletic	*Chauliodus sloani* *Chauliodus macouni* *Chauliodus dane*
Gonostomatidae	46	1.9	Monophyletic	*Cyclothone microdon* *Sigmops bathyphilus* *Cyclothone pseudopallida* *Sigmops elongatus* *Cyclothone alba*
Gonostomatidae/Sternoptychidae	53	2	Monophyletic	*Argyropelecus gigas* *Argyropelecus affinis* *Cyclothone microdon* *Polyipnus spinifer* *Sigmops bathyphilus* *Sternoptyx diaphana* *Cyclothone pseudopallida* *Polyipnus clarus* *Sigmops elongatus* *Cyclothone alba* *Sternoptyx pseudobscura*
Neonesthes/Astronesthes	33	4	Don't enforce monophyly	*Neonesthes capensis* *Astronesthes similus*
Sternoptychidae	45	3	Monophyletic	*Argyropelecus gigas* *Argyropelecus affinis* *Polyipnus spinifer* *Sternoptyx diaphana* *Polyipnus clarus* *Sternoptyx pseudobscura*
Sternoptyx/Argyropelecus	11	1	Monophyletic	*Argyropelecus affinis* *Argyropelecus gigas* *Sternoptyx diaphana* *Sternoptyx pseudobscura*

Table A-8. Continued.

Prior	Mean	Sigma		Species
				Stomias affinis
				Bathophilus pawneei
				Chauliodus sloani
				Malacosteus niger
Stomiidae	50	2.5	Monophyletic	*Stomias boa*
				Photostomias goodyeari
				Chauliodus macouni
				Neonesthes capensis
				Chauliodus dane
				Bathophilus proximus
Stomiidae	50	2.5	Monophyletic	*Astronesthes similus*
				Photostomias goodyeari
				Stomias affinis
				Bathophilus pawneei
				Chauliodus sloani
				Argyropelecus gigas
				Argyropelecus affinis
				Malacosteus niger
				Cyclothone microdon
				Stomias boa
				Polymetme thaeocoryla
				Chauliodus macouni
Stomiiformes	69	2	Monophyletic	*Neonesthes capensis*
				Chauliodus dane
				Polyipnus spinifer
				Bathophilus proximus
				Sternoptyx diaphana
				Cyclothone pseudopallida
				Astronesthes similus
				Polyipnus clarus
				Sigmops elongatus
				Cyclothone alba
				Sternoptyx pseudobscura
				Photostomias goodyeari

Table A-9. List of Calibrations used to generate the Stephanoberyciformes tree. Adapted from Near et al. (2013).

Prior	Mean	Sigma		Species
Barbourisiidae	27	1	Monophyletic	*Acanthochaenus luetkenii* *Barbourisia rufa*
Berycidae/Melamphaidae	39	2.5	Monophyletic	*Beryx decadactylus* *Centroberyx druzhinni* *Melamphaes sp.* *Scopelogadus mizolepis* *Poromitra crassiceps* *Poromitra megalops* *Scopeloberyx opisthopterus* *Scopelogadus beanii*
Trachichthyiformes	96.1	0.7	Monophyletic	*Acanthochaenus luetkenii* *Barbourisia rufa* *Beryx decadactylus* *Centroberyx druzhinni* *Melamphaes sp.* *Cetostoma regani* *Scopelogadus mizolepis* *Ditropichthys storeri* *Gyrinomimus grahami* *Gyrinomimus bruuni* *Poromitra megalops* *Anoplogaster cornuta* *Cetostoma sp* *Scopeloberyx opisthopterus* *Rondeletia loricata* *Sargocentron cornutum* *Scopelogadus beanii*

Table A-9. Continued.

Prior	Mean	Sigma		Species
Cetomimidae	21	1	Monophyletic	*Cetostoma regani* *Ditropichthys storeri* *Gyrinomimus grahami* *Gyrinomimus bruuni* *Cetostoma sp* *Acanthochaenus luetkenii* *Barbourisia rufa*
"“Cetomimoid” + Stephanoberycidae	32	0.7	Monophyletic	*Cetostoma regani* *Ditropichthys storeri* *Gyrinomimus grahami* *Gyrinomimus bruuni* *Cetostoma sp* *Rondeletia loricata* *Acanthochaenus luetkenii* *Barbourisia rufa*
Cetomimidae and Barbourisiidae	28	1	Monophyletic	*Cetostoma regani* *Ditropichthys storeri* *Gyrinomimus grahami* *Gyrinomimus bruuni* *Cetostoma sp* *Acanthochaenus luetkenii* *Barbourisia rufa*
Stephanoberyciformes	54	2	Monophyletic	*Beryx decadactylus* *Centroberyx druzhinni* *Melamphaes sp.* *Cetostoma regani* *Scopelogadus mizolepis* *Ditropichthys storeri* *Gyrinomimus grahami*

Table A-9. Continued

Prior	Mean	Sigma		Species
Stephanoberyciformes continued				*Gyrinomimus bruuni* *Poromitra megalops* *Cetostoma sp* *Scopeloberyx opisthopterus* *Rondeletia loricata* *Scopelogadus beanii* *Acanthochaenus luetkenii* *Barbourisia rufa* *Beryx decadactylus* *Centroberyx druzhinni* *Melamphaes sp.* *Cetostoma regani* *Scopelogadus mizolepis*
Stephanoberyciformes and Holocentridae	92	1.3	Monophyletic	*Ditropichthys storeri* *Gyrinomimus grahami* *Gyrinomimus bruuni* *Poromitra megalops* *Cetostoma sp* *Scopeloberyx opisthopterus* *Rondeletia loricata* *Sargocentron cornutum* *Scopelogadus beanii*
Poromitra	NA	NA	Monophyletic	*Poromitra crassiceps* *Poromitra megalops*

Table A-10. List of Calibrations used to generate the Gempylidae tree. Adapted from Near et al. (2013).

Prior	Mean	Sigma		Species
Bramidae	15	0.7	Monophyletic	*Brama dussumieri* *Taractes asper* *Taractes rubescens*
Gempylidae/Bramidae	26	0.7	Monophyletic	*Brama dussumieri* *Paradiplospinus gracilis* *Diplospinus multistriatus* *Taractes asper* *Taractes rubescens*
Gempylidae/Trichiuridae/Bramidae	27	0.7	Monophyletic	*Brama dussumieri* *Paradiplospinus gracilis* *Diplospinus multistriatus* *Taractes asper* *Taractes rubescens* *Assurger anzac* *Trichiurus lepturus*
Gempylidae/Trichiuridae/Bramidae/ Peprilus	30	0.1	Monophyletic	*Brama dussumieri* *Paradiplospinus gracilis* *Diplospinus multistriatus* *Taractes asper* *Taractes rubescens* *Assurger anzac* *Trichiurus lepturus* *Peprilus paru*
Gempylidae	NA	NA	Monophyletic	*Paradiplospinus gracilis* *Diplospinus multistriatus*

Table A-10. Continued.

Prior	Mean	Sigma		Species
Scombriformes	34	0.6	Monophyletic	*Brama dussumieri* *Paradiplospinus gracilis* *Diplospinus multistriatus* *Taractes asper* *Taractes rubescens* *Assurger anzac* *Trichiurus lepturus* *Peprilus paru* *Thunnus albacares* *Psenes maculatus*
Scombroidei	32	0.7	Monophyletic	*Brama dussumieri* *Paradiplospinus gracilis* *Diplospinus multistriatus* *Taractes asper* *Taractes rubescens* *Assurger anzac* *Trichiurus lepturus* *Peprilus paru* *Psenes maculatus*
Trichiuridae	27	1.8	Monophyletic	*Assurger anzac* *Trichiurus lepturus*

Table A-11. List of Calibrations used to generate the Polymixiiformes tree. Adapted from Near et al. (2013)

Prior	Mean	Sigma		Species
Amphredoderoidei	44	1.8	Monophyletic	*Aphredoderus sayanus* *Chologaster cornuta*
Percopsiformes	58	1.7	Monophyletic	*Aphredoderus sayanus* *Chologaster cornuta* *Percopsis omiscomaycus*
Percopsiformes/Polymixiiformes	127.8	0.5	Monophyletic	*Aphredoderus sayanus* *Chologaster cornuta* *Polymixia lowei* *Polymixia japonica* *Percopsis omiscomaycus*
Polymixiiformes	8	1	Monophyletic	*Polymixia lowei* *Polymixia japonica*

Table A-12. List of Calibrations used to generate the Acropomatidae tree. Adapted from Near et al. (2013)

Prior	Mean	Sigma		Species
Acropomatidae/Ostracoberyx	37	1.8	Monophyletic	*Acropoma japonicum* *Synagrops bellus* *Synagrops spinosus* *Doederlenia berycoides* *Ostracoberyx dorgenys* *Malakichthys elegans*
Howella/Acropomatidae/Ostracoberyx	38	1.8	Monophyletic	*Acropoma japonicum* *Synagrops bellus* *Synagrops spinosus* *Doederlenia berycoides* *Malakichthys elegans* *Howella brodei*
Howella	NA	NA	Monophyletic	*Howella sherbourni* *Howella atlantica* *Howella zina* *Howella brodei* *Howella sherbourni* *Howella atlantica* *Howella zina*
Acropomatidae	NA	NA	Monophyletic	*Acropoma japonicum* *Synagrops bellus* *Synagrops spinosus* *Doederlenia berycoides* *Malakichthys elegans*

Table A-13. Samples used to generate the secondarily calibrated Stomiiformes tree.

Number	Genus	Species	Source
RIE_1171	*Polyipnus*	*clarus*	DEEPEND
RIE_278	*Sigmops*	*elongatus*	DEEPEND
RIE_506	*Photostomias*	*guernei*	DEEPEND
RIE_349	*Cyclothone*	*alba*	DEEPEND
RIE_238	*Cyclothone*	*pseudopallida*	DEEPEND
RIE_415	*Sternoptyx*	*pseudobscura*	DEEPEND
RIE_577	*Stomias*	*affinis*	DEEPEND
RIE_71	*Sternoptyx*	*diaphana*	DEEPEND
RIE_1051	*Astronesthes*	*similus*	DEEPEND
MG856583.1	*Bathophilus*	*proximus*	GenBank
KY033761.1	*Sigmops*	*bathyphilus*	GenBank
KU893054.1	*Polyipnus*	*spinifer*	GenBank
KF929724.1	*Chauliodus*	*danae*	GenBank
KF768171.1	*Neonesthes*	*capensis*	GenBank
JQ354039.1	*Chauliodus*	*macouni*	GenBank
GU071725.1	*Photostomias*	*goodyeari*	GenBank
GQ860359.1	*Sigmops*	*bathyphilus*	GenBank
FJ918933.1	*Polymetme*	*thaeocoryla*	GenBank
EU148335.1	*Stomias*	*boa*	GenBank
EU148136.1	*Cyclothone*	*microdon*	GenBank
DPND_4220	*Argyropelecus*	*affinis*	DEEPEND
DPND_1835	*Argyropelecus*	*gigas*	DEEPEND
DPND_4568	*Malacosteus*	*niger*	DEEPEND
DPND_1556	*Chauliodus*	*sloani*	DEEPEND
DPND_1336	*Bathophilus*	*pawneei*	DEEPEND

Table A-14. Samples used to generate the secondarily calibrated Trachichthyiformes, Holocentridae, and Stephanoberyciformes tree.

Number	Genus	Species	Source
RIE_425	*Anoplogaster*	*cornuta*	DEEPEND
RIE_172	*Poromitra*	*megalops*	DEEPEND
RIE_63	*Scopeloberyx*	*opisthopterus*	DEEPEND
RIE_441	*Cetostoma*	*sp*	DEEPEND
Pisces_P558	*Gyrinomimus*	*bruuni*	Pisces
KP267663.1	*Centroberyx*	*druzhinini*	GenBank
JQ354324.1	*Rondeletia*	*loricata*	GenBank
JQ354300.1	*Poromitra*	*crassiceps*	GenBank
JQ354000.1	*Barbourisia*	*rufa*	GenBank
JF492951.1	*Beryx*	*decadactylus*	GenBank
FJ237588.1	*Sargocentron*	*cornutum*	GenBank
FJ164637.1	*Gyrinomimus*	*grahami*	GenBank
EU148314.1	*Scopelogadus*	*beanii*	GenBank
EU148067.1	*Acanthochaenus*	*luetkenii*	GenBank
DPND_2130	*Cetostoma*	*regani*	DEEPEND
DPND_4130	*Ditropichthys*	*storeri*	DEEPEND
DPND_1383	*Melamphaes*	*sp*	DEEPEND
DPND_2511	*Scopelogadus*	*mizolepis*	DEEPEND

Table A-15. Samples used to generate the secondarily calibrated Polymixiiformes tree**.**

Number	Genus	Species	Source
KX145224.1	*Percopsis*	*omiscomaycus*	GenBank
HQ557552.1	*Chologaster*	*cornuta*	GenBank
JN024804.1	*Aphredoderus*	*sayanus*	GenBank
KF930291.1	*Polymixia*	*japonica*	GenBank
DPND_1983	*Polymixia*	*lowei*	DEEPEND

Table A-16. Samples used to generate the secondarily calibrated Gempylidae tree.

Number	Genus	Species	Source
AB205444.1	*Psenes*	*maculatus*	GenBank
DQ835957.1	*Thunnus*	*albacares*	GenBank
EU263815.1	*Assurger*	*anzac*	GenBank
EU263823.1	*Trichiurus*	*lepturus*	GenBank
GU440550.1	*Taractes*	*asper*	GenBank
JN641062.1	*Paradiplospinus*	*gracilis*	GenBank
KY372189.1	*Taractes*	*rubescens*	GenBank
EU400170.1	*Taractes*	*asper*	GenBank
DPND_3230	*Brama*	*dussumieri*	DEEPEND
DPND_4576	*Peprilus*	*paru*	DEEPEND
RIE_882	*Diplospinus*	*multistriatus*	DEEPEND

Table A-17. Samples used to generate the secondarily calibrated Acropomatidae tree.

Number	Genus	Species	Source
DQ648437.1	*Acropoma*	*japonicum*	GenBank
KP266851.1	*Doederleinia*	*berycoides*	GenBank
KY033633.1	*Howella*	*brodiei*	GenBank
KY033904.1	*Howella*	*sherborni*	GenBank
KY371711.1	*Malakichthys*	*elegans*	GenBank
KU943423.1	*Howella*	*zina*	GenBank
KU892849.1	*Ostracoberyx*	*dorygenys*	GenBank
DPND_1874	*Synagrops*	*spinosus*	DEEPEND
DPND_1495	*Synagrops*	*bellus*	DEEPEND
DPND_2153	*Howella*	*atlantica*	DEEPEND

Table A-18. Initial nuclear rates**.** Taken from the trees constructed for our study species and their sister species.

Inferred From EBSP Runs						
		PLAG		ENC		MYH
Species	PLAG	95%HPD	ENC	95%HPD	MYH	95%HPD
Bathophilus pawneii	0.00177	[0.00027, 0.00370]				
Chauliodus Sloani			0.00090	[0.00047, 0.00134]		
Cyclothone alba	0.00577	[0.00178, 0.01970]				
Cyclothone pseudopallida	0.00519	[0.00046, 0.01020]				
Diplospinus multistriatus	0.00885	[0.00259, 0.01600]	0.01010	[0.00333, 0.01780]		
Ditropichthys storeri	0.00102	[0.00060, 0.00146]				
Photostomias guernei	0.01344	[0.00707, 0.02020]				
Polymixia lowei	0.00100	[0.00012, 0.00219]	0.00237	[0.00079, 0.00424]		
Scopelogaus mizolepis	0.00272	[0.00053, 0.00544]				
Sigmops elongatus	0.00226	[0.00046, 0.00423]				
Sternoptyx pseudobscura	0.00229	[0.00134, 0.00323]	0.00412	[0.00278, 0.00549]		
Stomias affinis					0.00188	[0.00019, 0.00424]
Synagrops spinosus			0.01260	[0.00466, 0.02090]		
Mean	0.00443	[0.00152, 0.00864]	0.00602	[0.00241, 0.00995]	0.00188	[0.00019, 0.00424]

Table A-19. Summary of EBSP Runs. **"**Good" (Green) refers to runs where key traces converged and all ESS values < 200. "Bad" (Red) refers to runs where one or more key traces failed to converge, and at least one ESS value was > 200.
* Best Run for each species

Study Species	Method 1	Method 2	Reject Constant Pop	Date Change Begins
Bathophilus pawneii	Bad	Good*	No [0,3]	NA
Chauliodus Sloani	Good	Good*	Yes [1,3]	~100 ky ago
Cyclothone alba	Good	Good*	Yes [1,3]	~80 ky ago
Cyclothone pseudopallida	Good	Good*	No [0,3]	NA
Diplospinus multistriatus	Good*	Good	No [0,3]	NA
Ditropichthys storeri	Good*	Bad	No [0,3]	NA
Photostomias guernei	Good	Good*	Yes [1,3]	~120 ky ago
Polymixia lowei	Good*	Good	Yes [1,3]	~200 ky ago
Scopelogaus mizolepis	Good*	Bad	No [0,3]	NA
Sigmops elongatus	Bad	Bad	No [0,3]	NA
Sternoptyx pseudobscura	Good*	Good	Yes [1,3]	~270 ky ago
Stomias affinis	Good*	Good	No [0,3]	NA
Synagrops spinosus	Bad	Good*	No [0,3]	NA

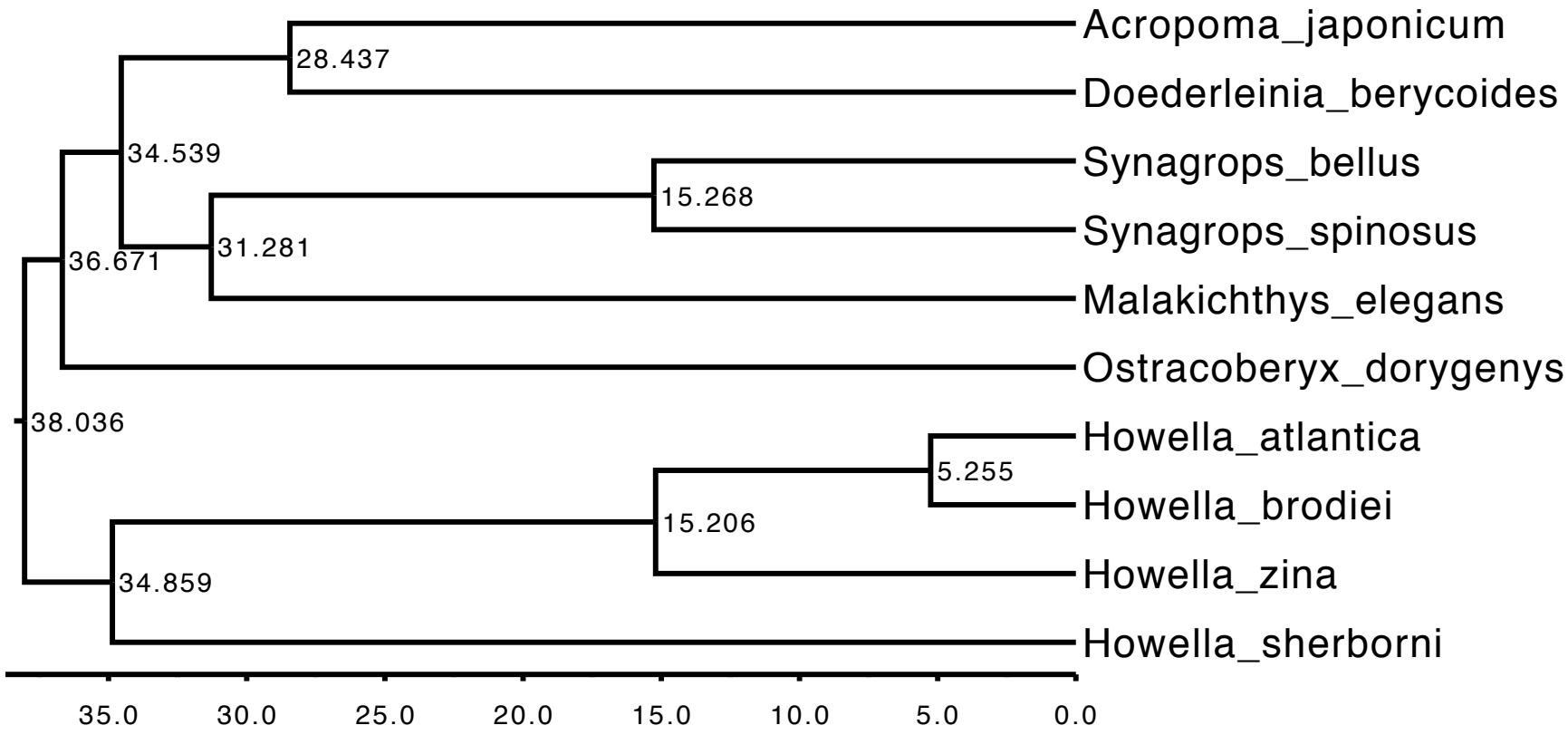

Figure A-1. Clock Calibration Tree 1 (Acropomatidae). Dates are given in terms of millions of years

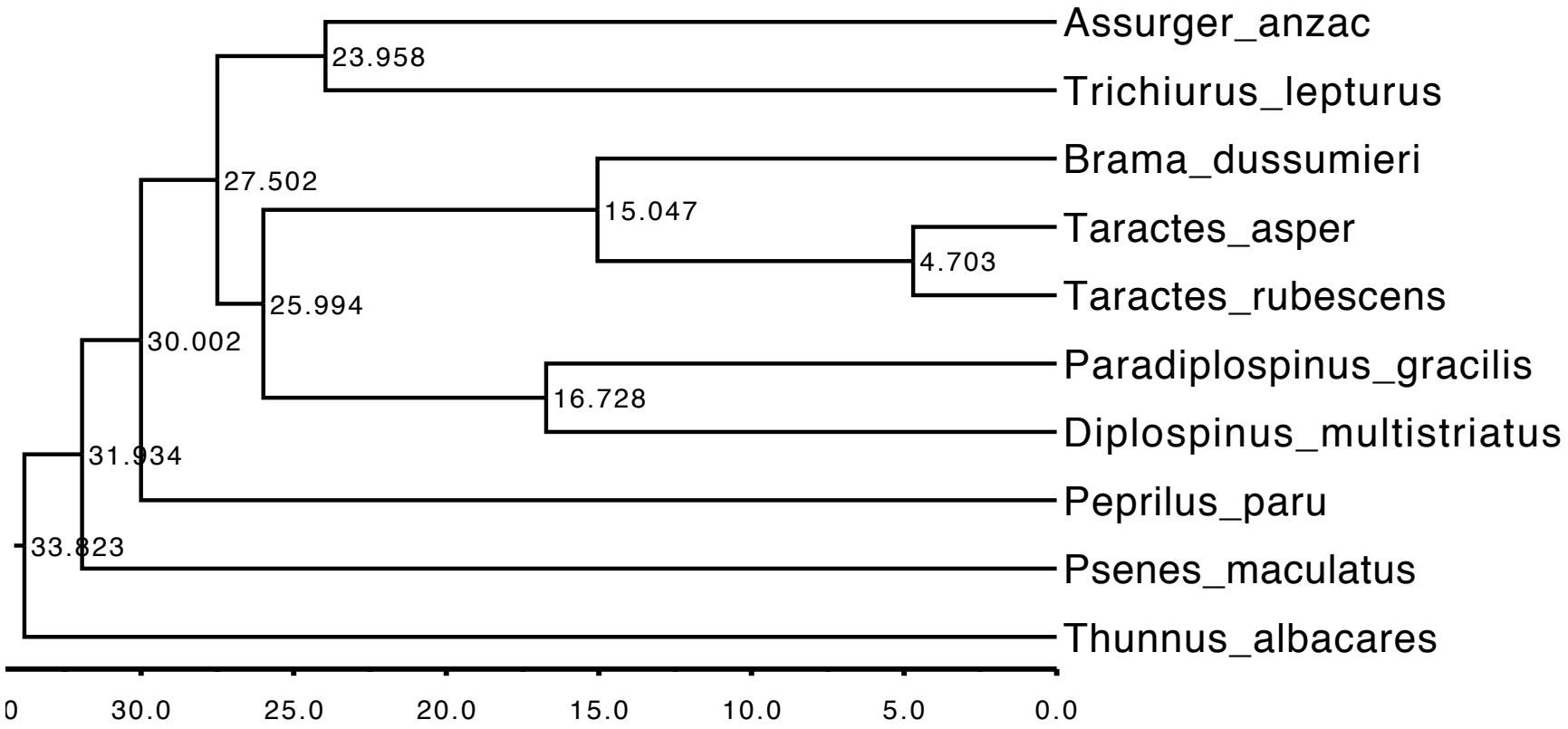

Figure A-2. Clock Calibration Tree 2 (Gempylidae). Dates are given in terms of millions of years.

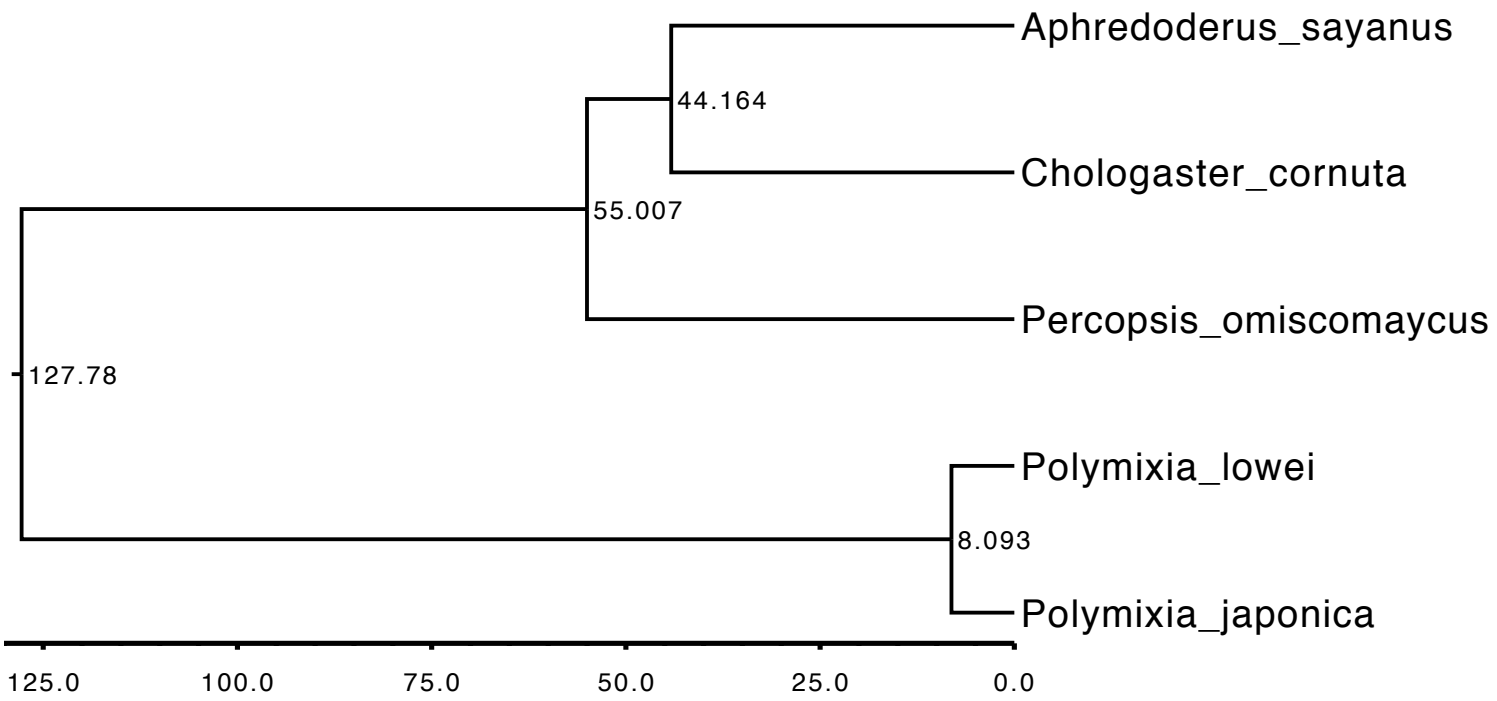

Figure A-3. Clock Calibration Tree 3 (Polymixiiformes). Dates are given in terms of millions of years.q

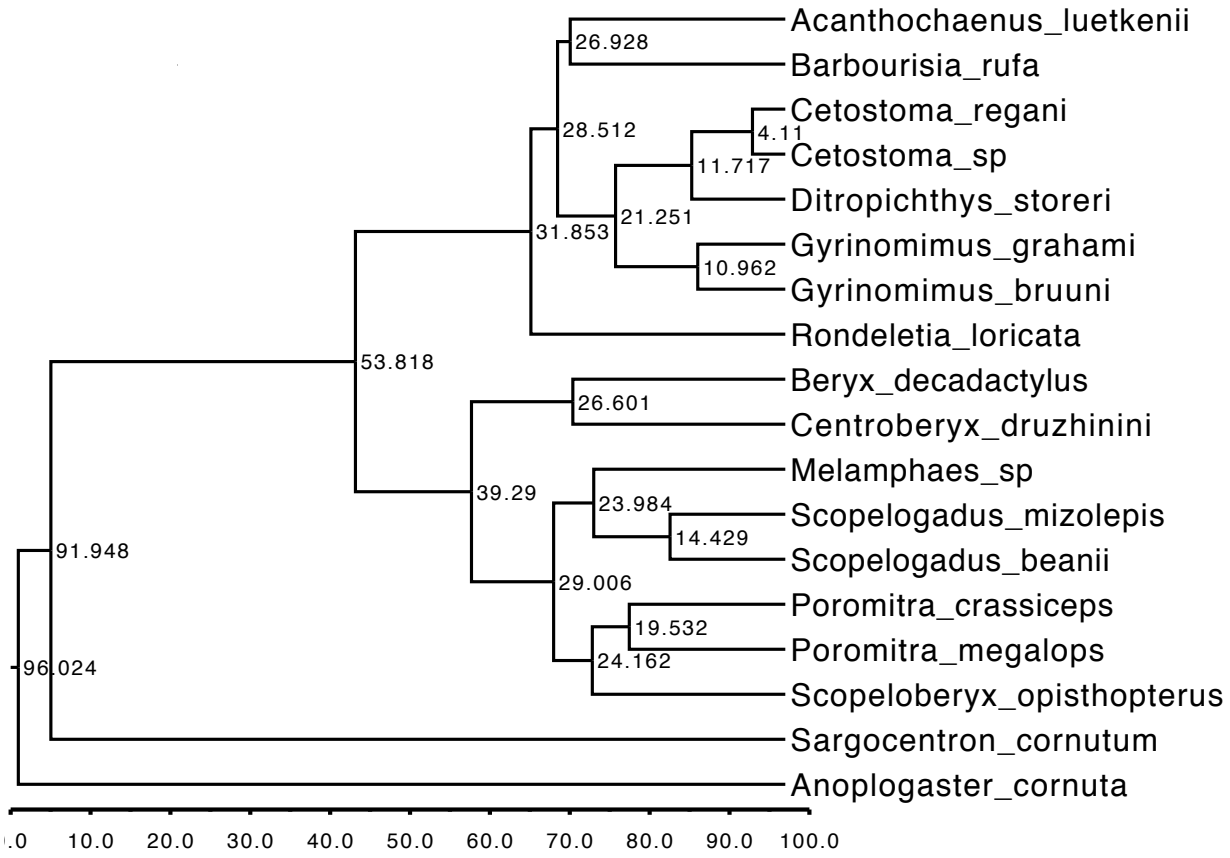

Figure A-4. Clock Calibration Tree 4 (Stephanoberyciformes). Dates are given in terms of millions of years.

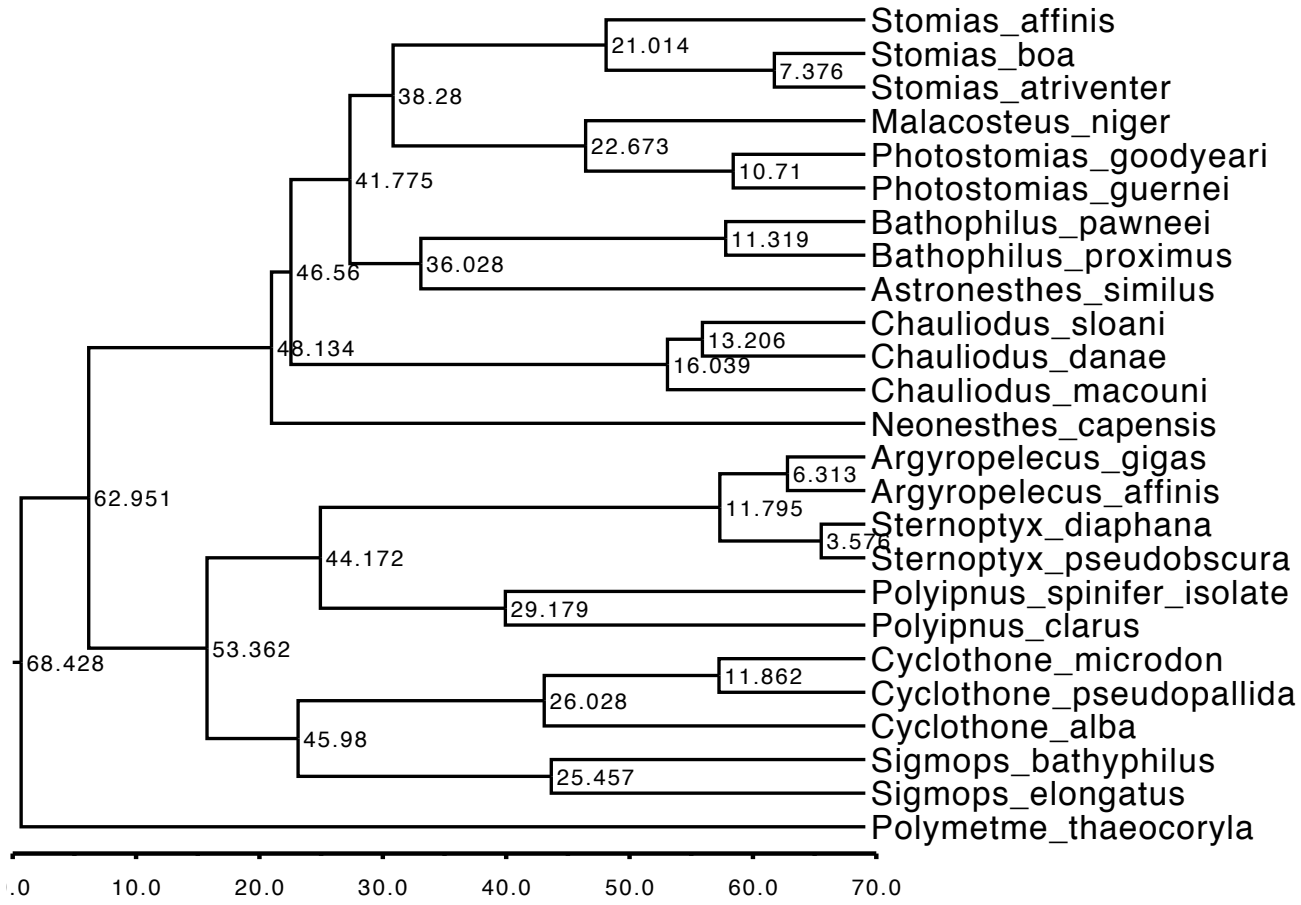

Figure A-5. Clock Calibration Tree 5 (Stomiiformes). Dates are given in terms of millions of years.

Table A-20. COI Consensus Sequences for every species. Polymorphic sites are highlighted in grey.

Species	Base Pair #	Consensus Sequence
Bathophilus pawneii	1 - 80	CTAGTATTTGGCGCCTGAGCTGGAATAGTCGGCACCGCCTTAAGCTTACTCATCCGAGCAGAGCTTAGTCAGCCAGGTGC
	81 - 160	TCTTCTGGGYGATGACCAGATCTACAACGTTATCGTTACRGCCCATGCTTTTGTAATAATTTTCTTCATAGTGATGCCAA
	161 - 240	TTATAATYGGAGGCTTTGGGAACTGGCTTATCCCTCTTATGATTGGGGCCCCTGACATGGCTTTCCCMCGAATGAACAAC
	241 - 320	ATGAGCTTCTGGCTCCTSCCTCCGTCATTTTTACTYCTGCTTGCCTCTTCTGGTGTAGAAGCAGGGGCAGGAACAGGGTG
	321 - 400	GACCGTCTATCCYCCTCTAGCTGGAAACCTGGCTCACGCCGGGGCATCCGTAGACCTAACGATCTTTTCTTTRCACCTAG
	401 - 480	CAGGGGTATCTTCTATTTTAGGGGCAATCAACTTCATCACGACAATTATTAACATGAAACCGCCAGCGATTTCTCAATAC
	481 - 560	CAGACACCCCTCTTTGTGTGGTCCGTTCTGATTACTGCGGTTCTTCTGYTACTCTCRCTGCCAGTGCTAGCGGCAGGGAT
	561 - 640	CACTATGCTCCTTACAGACCGCAACCTGAACACGACATTTTTTGACCCCGCAGGGGGAGGRGAYCCAATTCTGTACCAGC
	641 - 720	ACTTG
Chauliodus sloani	1 - 80	ACCCTTTACTTAATCTTCGGTGCYTGAGCCGGAATASTTGGCACCGCACTAAGCCTGTTAATTCGAGCAGARCTCAGCCA
	81 - 160	ACCCGGCGCCTTCATRGGCGNYGAYCAAATTTATAATGTCATCGTYACAGCACATGCCTTCGTAATAATTTTCTTTATGG
	161 - 240	TRATRCCCATCATGATCGGGGGYTTCGGAAACTGACTWGTRCCCCTAATGATCGGRGCCCCWGATATAGCCTTCCCMCGA
	241 - 320	ATAAACAACATGAGCTTCTGGCTCCTCCCTCCCTCATTTCTTCTTCTRCTCGCCTCTTCTGGRGTTGAAGCTGGGGCCGG
	321 - 400	AACCGGRTGAACTGTATACCCRCCCCTCTCAGGAAACCTTGCCCACGCTGGTGCCTCCGTYGACCTCACAATTTTCTCCC
	401 - 480	TCCACCTAGCAGGGATTTCTTCTATTCTGGGGGCAATTAATTTYATYACCACAATTTATAAYATGAARCCTGCYGGCATR
	481 - 560	TCTCARTAYCAGGCCCCCCTRTTCGTGTGGTCYGTTCTYATCACTGCCGTCCTTCTCCTTCTCTCCCTYCCCGTCTTAGC
	561 - 640	CGCCGGTATYACYATGCTCCTCACAGACCGAAACCTCAACACA
Cyclothone alba	1 - 80	CTCATCCGGGCTGAATTAAACCAACCCGGGGCTTTATTGGGGGATGACCAGATTTACAACGTAATTGTAACTGCTCACGC
	81 - 160	CTTTGTYATGATCTTTTTTATGGTAATGCCAATCATGATTGGAGGCTTTGGCAACTGGCTTATCCCTCTCATGCTYGGAG
	161 - 240	CACCTGAYATGGCGTTYCCTCGGATAAATAACATGAGCTTTTGACTTCTTCCCCCCTCTTTTTTTCTGCTGCTAGCTTCA
	241 - 320	GCTGGTGTAGAAGCAGGGGCCGGCACAGGATGAACAGTCTACCCTCCTCTGGCAAGCAACTTAGCTCATGCTGGGGCCTC
	321 - 400	TGTAGACCTTACAATCTTCTCCCTTCACCTAGCGGGTGTTTCCTCAATTTTAGGGGCTATTAATTTTATTACAACCATTA
	401 - 480	TCAATATGAAACCCCCAGCTTCCACACAATACCAAACGCCTCTCTTTGTCTGAGCAGTGCTGATTACTGCCGTCCTACTA
	481 - 560	CTCCTCTCACTTCCAGTGTTAGCTGCAGGCATCACTATGCTACTCACAGACCGTAACCTCAACACCTCCTTTTTTGACCC
	561 - 640	TGCTGGGGGCGGTGACCCCATCYTCTACCAACAC
Cyclothone pseudopallida	1 - 80	CTTTACTTTATCTTTGGGGCCTGAGCCGGCATRGTCGGCACAGCCTTAAGCCTTCTCATTCGAGCCGAGCTCAACCAACC
	81 - 160	CGGCGCCCTTCTGGGCGACGACCAAGTCTACAACGTTATCGTTACCGCCCACGCCTTTGTAATGATCTTTTTTATGGTCA
	161 - 240	TGCCAATCATGATTGGCGGKTTTGGCAACTGACTAATTCCYCTGATGCTAGGGGCCCCTGACATGGCTTTCCCTCGGATG
	241 - 320	AACAACATAAGCTTTTGACTACTTCCCCCCTCCTTTTTYCTCTTGCTAGCCTCAGCTGGCGTAGARGCAGGCACAGGCAC
	321 - 400	AGGCTGAACTGTGTACCCCCCTCTGGCCAGCAACCTGGCCCATGCCGGAGCCTCCGTAGACCTAACCATCTTCTCCCTTC
	401 - 480	ACCTTGCCGGTGTCTCTTCGATCCTYGGCGCAATCAACTTCATCACCACGATTATTAACATGAAACCCCCCGCCTCAACC
	481 - 560	CAATATCAGACCCCCCTCTTCGTCTGAGCTGTTCTAATTACTGCCGTTCTCCTTCTCCTCTCTCTRCCCGTCTTGGCCGC
	561 - 640	GGGCATCACAATGCTTCTGACTGACCGGAACTTAAACACCTCCTTTTTCGACCCTGCCGGGGGGGGCGACCCGATCCTCT
	641 - 720	ACCAACACCTG

Table A-20. Continued.

Species	Base Pair #	Consensus Sequence
Diplospinus multistriatus	1 - 80	TATATAGTATTTGGTGCATGAGCTGGGATAGTAGGTACAGCCCTAAGCCTCCTTATTCGAGCTGAACTAAGTCAACCAGG
	81 - 160	TGCCCTCCTTGGAGATGACCAGATCTATAACGTAATCGTTACAGCACATGCCTTCGTAATGATTTTCTTTATAGTAATGC
	161 - 240	CCATTATGATCGGAGGGTTCGGAAACTGATTAATTCCCCTAATGATCGGGGCCCCCGATATGGCTTTCCCCCGTATAAAC
	241 - 320	AATATGAGCTTTTGACTCCTCCCCCCCTCGTTCCTTCTTCTGCTAGCTTCTTCAGGAGTCGAATCTGGGGCCGGAACAGG
	321 - 400	ATGAACAGTTTATCCGCCTCTCGCAGGCAACTTAGCCCACGCAGGCGCATCCGTAGACTTAACCATTTTTTCTCTRCACT
	401 - 480	TGGCAGGGATCTCCTCAATTCTTGGGGCAATTAACTTCATCACTACAATTATTAACATAAAACCTGCCGCCATCTCGCAG
	481 - 560	TACCAAACCCCACTGTTTGTCTGAGCAGTTCTTATTACTGCCGTTCTTCTCCTTCTCTCCCTCCCAGTTCTTGCTGCTGG
	561 - 640	CATTACAATGCTACTTACAGACCGAAACCTTAACACAACTTTCTTTGACCCCGCGGGGGGAGGAGACCCAATCTTGTATC
	641 - 720	AACAC
Ditropichthys storeri	1 - 80	GGAACAGCCTTAAGCCTTCTTATTCGAGCAGAGTTAAGCCAGCCTGGGGCTCTCCTGGGGGATGACCAAATCTACAATGT
	81 - 160	AATTGTTACTKCACAMGCCTTCGTAATAATTTTCTTTATAGTAATACCAATTATAATTGGGGGATTCGGAAATTGATTAG
	161 - 240	TTCCTTTAATAATCGGRGCCCCTGATATAGCATTCCCCCGGATAAATAATATAAGTTTCTGACTTCTCCCCCCCTCTTTT
	241 - 320	TTACTACTTCTAGCCTCCTCGGGGGTTGAAGCAGGTGCCGGAACAGGTTGAACAGTATACCCCCCCCTTGCAGGAAACCT
	321 - 400	AGCCCACGCAGGGGCTTCAGTAGATTTAACCATTTTTTCCTTACACTTGGCAGGTGTGTCSTCAATTCTAGGGGCTATTA
	401 - 480	ACTTYATTACAACCATTATTAATATAAAACCTCCAGCCATTTCACAATATCAGACCCCCCTTTTTGTTTGATCCGTTTTA
	481 - 560	GTGACAGCYGTTCTTCTTCTTCTTTCCTTACCCGTTCTTGCAGCGGGCATTACCATACTACTAACTGACCGCAACCTAAA
	561 - 640	TACAACCTTCTTTGACCCCGCTGGGGGGGGAGACCCCATTCTTTATCAACAC
Photostomias guernei	1 - 80	TTGTACCTAGTGTTTGGTGCATGAGCTGGGATAGTTGGAACTGCACTTAGTCTCCTYATTCGAGCAGAGCTGGGCCAGCC
	81 - 160	GGGCGCTCTTCTRGGGGATGACCAGATCTATAACGTTATCGTGACAGCACATGCTTTTGTCATAATCTTTTTTATGGTGA
	161 - 240	TGCCCATCATAATCGGGGGGTTCGGAAACTGACTGATTCCGCTTATGATCGGGGCACCCGACATAGCTTTCCCCCGAATG
	241 - 320	AAYAACATGAGTTTCTGGCTTCTACCGCCCTCCTTCCTTCTCTTGCTTGCATCATCTGGTGTTGAAGCCGGGGCTGGTAC
	321 - 400	RGGTTGGACRGTTTATCCTCCGCTTGCYGGAAATCTTGCGCATGCTGGGGCGTCCGTTGATTTGACGATTTTCTCGCTCC
	401 - 480	ATCTGGCGGGCATTTCCTCTATTTTAGGGGCAATTAATTTTATCACTACGATTATTAATATGAAGCCTCCGRCYATCTCT
	481 - 560	CAATACCAGACCCCCTTATTCGTCTGGGCGGTTCTTATTACTGCTGTTCTTCTTCTTTTGTCRCTTCCTGTCCTCGCTGC
	561 - 640	GGGCATTACTATGCTATTAACAGACCGGAATCTAAACACAACATTCTTCGACCCTGCGGGCGGCGGGGACCCCATCCTGT
	641 - 720	ACCAGCACCTA
Polymixia lowei	1 - 80	GCTTGAGCCGGCATRGTCGGCACAGCCCTAAGTCTCCTCATCCGGGCAGAACTAAGTCAACCCGGGGCCCTGCTAGGRGA
	81 - 160	TGATCAAATCTACAACGTCATTGTTACGGCACATGCCTTTGTAATAATTTTCTTTATAGTAATACCAATTATGATTGGTG
	161 - 240	GRTTTGGTAACTGACTYATCCCMCTAATGATYGGAGCACCCGAYATAGCATTTCCTCGRATAAACAACATAAGCTTTTGA
	241 - 320	CTACTCCCCCCTTCATTCCTHCTGCTATTAGCCTCTTCCGGCGTAGAAGCGGGGGCTGGTACAGGATGAACTGTMTAYCC
	321 - 400	RCCYCTTGCAGGTAATYTRGCACACGCTGGTGCCTCAGTTGACTTAACCATTTTCTCCCTTCATTTAGCAGGTGTCTCCT
	401 - 480	CAATTCTTGGAGCCATCAACTTTATTACAACTATTATTAACATRAAACCCCCAGCTATYTCCCAATACCAAACACCCYTG
	481 - 560	TTTGTATGATCAGTTTTAATTACCGCTGTTCTTCTACTGCTCTCCCTACCYGTCCTTGCAGCTGGYATTACCATGCTATT
	561 - 640	AACAGACCGAAATCTAAACACCACCTTCTTTGACCCT

Table A-20. Continued.

Species	Base Pair #	Consensus Sequence
Scopelogadus mizolepis	1 - 80	TTAGTATTCGGTGCCTGAGCCGGCATAGTCGGCACCGCCCTCAGCCTCTTAATTCGAGCAGAGTTAAGTCAACCGGGGGC
	81 - 160	ACTTCTAGGCGACGACCAAATTTATAATGTTATTGTTACCGCACACGCTTTCGTAATAATTTTCTTTATAGTYATACCAG
	161 - 240	TYATRATTGGCGGGTTCGGTAACTGACTCGTCCCCCTTATGATTGGGGCCCCAGATATGGCCTTTCCCCGAATAAATAAC
	241 - 320	ATAAGCTTCTGGCTTCTCCCGCCCTCTTTTCTCCTCCTCCTATCCTCTTCCGCAGTAGAAGCAGGGGCTGGCACTGGATG
	321 - 400	AACCGTGTATCCCCCGCTTGCAAGCAATCTGGCACATGCGGGCGCCTCAGTAGAYCTAACAATTTTTTCCCTCCACTTAG
	401 - 480	CGGGGGTCTCTTCTATCCTCGGGGCCATCAATTTTATCACAACCATCATCAACATAAAACCTCCCGCCACTACACAGCAC
	481 - 560	CAAACRCCCCTGTTTGTTTGATCCGTCCTAATTACAGCCATCCTCCTRCTTCTTTCTCTGCCCGTACTTGCAGCAGGGAT
	561 - 640	TACAATACTGCTAACAGACCGCAACCTCAATACAACYTTCTTTGACCCTGCAGGAGGGGGCGACCCTATTCTATACCAAC
	641 - 720	AC
Sigmops elongatus	1 - 80	CTTTATCTAATTTTTGGTGCTTGGGCCGGAATAGTTGGAACAGCCCTAAGCCTACTAATCCGAGCAGAGCTGAGTCAGCC
	81 - 160	CGGCACCCTGCTGGGTGATGACCAGATTTTTAATGTTATCGTTACAGCACATGCCTTCGTAATGATCTTTTTTATAGTAA
	161 - 240	TACCAGTTATAATTGGGGGTTTCGGGAATTGACTAATCCCTCTAATAATTGGAGCCCCTGATATAGCATTCCCCCGAATA
	241 - 320	AACAACATAAGCTTCTGACTCCTTCCCCCCTCTTTTCTCCTCTTGCTTGCCTCCTCAGGRGTTGAAGCCGGAGCCGGGAC
	321 - 400	AGGATGAACAGTCTACCCTCCCCTCTCCAGCAACTTAGCCCACGCAGGAGCTTCAGTTGACCTAACTATCTTCTCCCTCC
	401 - 480	ACCTTGCAGGAGTCTCCTCAATCCTCGGGGCAATTAACTTTATCACCACAATTATTAACATAAAACCCCCTGCCACCTCC
	481 - 560	CTGTACCAAACCCCCCTCTTCATCTGAGCCGTCCTTGTTACAGCCGTCCTCCTCCTCCTCTCACTCCCAGTCTTAGCCGC
	561 - 640	TGGAATCACCATACTTCTGACTGATCGAAACCTAAACACAACATTCTTTGACCCAGCAGGAGGAGGAGACCCCATCCTCT
	641 - 720	ATCAACATCTC
Sternoptyx pseudobscura	1 - 80	GATCAAATTTATAATGTTATTGTAACCGCGCATGCGTTTGTAATGATTTTCTTTATAGTCATGCCTATTATGATTGGGGG
	81 - 160	ATTTGGTAATTGGCTAATCCCTCTTATAATTGGTGCACCTGATATGGCTTTCCCTCGAATAAATAATATGAGTTTCTGAC
	161 - 240	TTCTTCCNCCATCCTTCYTACTCCTGTTGGCNTCATCAGGCGTGGAGGCTGGNGCTGGAACNGGTTGGACTGTTTATCCG
	241 - 320	CCTCTCGCTGGNAATTTAGCTCATGCGGGGGCATCTGTTGATTTAACCATCTTCTCTCTACATTTAGCAGGGATTTCTTC
	321 - 400	AATTTTGGGGGCCATTAATTTTATTACCACTATTGTTAATATAAAGCCTGCGGGCATGTCTCAGTATCAAACGCCTCTTT
	401 - 480	TTGTATGAGCTGTTCTTGTTACCGCTGTTCTTCTTCTCTTATCTCTTCCAGTATTGGCTGCGGGAATTACAATACTTTTA
	481 - 560	ACGGATCGAAATTTAAATACAACATTTTTTGACCCGGCGGGAGGAGGAGATCCTATT
Stomias affinis	1 - 80	CTCTATCTGGTATTYGGTGCTTGAGCTGGGATGGTCGGCACAGCTTTAAGCCTGCTTATTCGGGCAGAGCTAAGTCAACC
	81 - 160	CGGCGCCCTCCTAGGCGACGACCAAATCTATAACGTTATCGTYACTGCGCACGCCTTCGTAATAATTTTCTTCATAGTAA
	161 - 240	TGCCCCTCATGATYGGTGGCTTCGGAAACTGACTAATCCCCCTAATGATTGGCGCCCCCGACATGGCTTTCCCCCGAATG
	241 - 320	AATAACATGAGCTTTTGGCTCCTTCCCCCTTCATTCCTCCTCCTTCTTGCCTCTTCTGGCGTGGAAGCCGGGGCCGGGAC
	321 - 400	AGGCTGAACCGTCTACCCYCCTCTGGCCGGYAACCTAGCCCACGCRGGRGCCTCCGTAGACCTGACAATTTTTTCCCTTC
	401 - 480	ACYTAGCAGGTRTCTCTTCCATTCTTGGGGCAATCAACTTCATCACCACAATTATTAATATGAAGCCCCCAGCCATCTCY
	481 - 560	CAATATCAGACACCCCTCTTTGTCTGATCTGTCCTRATCACSGCTGTCCTTCTTCTCCTGTCCCTGCCGGTTCTGGCTGC
	561 - 640	CGGAATTACAATGCTTCTYACAGAYCGRAACTTAAATACRACATTCTTTGACCCGGCAGGGGGAGGAGACCCCATYCTCT
	641 - 720	ACCAACACCTG

Table A-20. Continued.

Species	Base Pair #	Consensus Sequence
Synagrops spinosus	1 - 80	GGGGATGACCARAYCTATAACGTAATTGTTACAGCCCATGCATTNGTAATAATCTTTTTTATAGTGATACCCATCATAAT
	81 - 160	TGGAGGTTTCGGAAACTGACTTCTACCTCTAATAATTGGGGCCCCTGRCATAGCATTCCCCCGAATAAACAACATAAGCT
	161 - 240	TCTGGCTGCTCCCCCCTTCTTTTCTTCTCCTCNTAGCATCCTCCGGAGTARAGGCAGGCGCTGGCACTGGGTGGACAGTA
	241 - 320	TACCCCCCCCTGGCTAGCAACCTCGCCCACGCAGGAGCCTCAGTCGACTTAACAATCTTCTCCCTCCACCTGGCCGGTGT
	321 - 400	CTCCTCAATCCTTGGGGCCATTAATTTTATTACAACTACTATCAACATGAAGCCCCCAGCTATCTCACAATATCAAACCC
	401 - 480	CCCTCTTCGTGTGGGCTGTCTTGATTACCGCTGTCCTTCTTCTCTTATCCCTTCCGGTCCTTGCAGCCGGCATCACAATA
	481 - 560	CTATTGACAGACCGAAACCTTAACACCACCTTCTTTGACCCCGCAGGAGGA

Table A-21. PLAG Consensus Sequences for every species. Polymorphic sites are highlighted in grey.

Species	Base Pair #	Consensus Sequence
Bathophilus pawneli	1 - 80	AAGTGCGAGGAGTGCGGCAAGCACTACAACACCAAGCTGGGCTACAAGCGTCACGTGGCCATGCACTCGGCCACGGCGGG
	81 - 160	GGATCTGACCTGCAAGGTCTGCCTGCAGAGCTACGAGAGCACGCCKGCGCTGCTGGAGCACCTCAAGAGCCACTCCGGGA
	161 - 240	AGTCGNCGGGCGGCGCCAAGGAGAAGAAGCACCCGTGNGACCACTGTGACCGCCGCTTCTACACGCGCAAGGACGTCAGG
	241 - 320	CGCCACATGGTGGTGCACACCGGCCGCAAGGACTTYCTGTGCCAGTACTGTGCCCAGCGCTTCGGCAGGAAGGACCACCT
	321 - 400	GACGCGGCACGTGAAGAAGAGCCACTCNCAGGAGCTGCTGAAGATCAAGGCGGAGCCGGCGGACATGCTGGGGCTNCTGG
	401 - 480	GCTCCGGCTCGCCGCCCTGCGCCGTCAAGGAGGAGCTTAGCCCCATGATGTGCAGCATGGGTCCCTCCAAGGACCCCCTG
	481 - 560	ATGGCCAAGCCCTTCCCCAGCGGGACTCCYTTCCCCATGGGCATGTACAACCCYCANCACCTGCAAGCCATGTCCGGCCC
	561 - 640	CGGGGGGGCCCACCAC
Cyclothone alba	1 - 80	CGGCACGTCGCCATGCACTCTGCCACGGCGGGCGACCTCACCTGCAAGGTGTGCCTGCAGAGCTACGAGAGCACGCCCGC
	81 - 160	GCTCCTGGAGCATCTGAAGAGCCACTCGGGGAAGTCGTCGGGCGGCGCCAAGGAGAAGAAGCACCCGTGYGACCACTGCG
	161 - 240	ACCGCCGCTTCTACACGCGCAAGGACGTCAGACGGCACATGGTGGTGCACACCGGCCGCAAGGACTTCCTSTGCCAGTAC
	241 - 320	TGCGCCCAGCGCTTTGGCAGGAAGGACCATCTGACACGGCATGTGAAGAARAGCCACTCGCAGGAGCTGCTGAAGATCAA
	321 - 400	GTCGGAGCCTCCGGACATGCTGGGGTTGCTGGGCTCCGGATCRCCACCCTGCMCCRTCAAAGAGGAGCTCAGCCCCATGA
	401 - 480	TGTGCAGCATGGGTCCATCCAAGGACCCCCTGATGGCCAAGCCTTTCCCCAGCGGAACCCCCTTCCCCATGGGTATGTAC
	481 - 560	AACCCCCACCACCTGCAGGCCATGTCTGGCCCTGGGGSRGGGCATCACCCTTCTCTTATGCCTGGTTCCCTGTCT
Cyclothone pseudopallida	1 - 80	CGGCAYGTCGCCATGCACTCGGCCACGGCGGGYGACCTCACCTGCAAGGTGTGCCTGCAGAGCTACGAGAGCACNCCCGC
	81 - 160	GCTCNTGGAGCACCTGAAGAGCCACTCGGGGAAGTCGTCGGGNGGCGCCAAGGAGAAGAAGCACCCGTGCGACCAYTGCG
	161 - 240	ACCGCCGCTTCTACACGCGCAAGGACGTCAGACGCCACATGGTGGTGCACACYGGCCGCAAGGACTTCCTGTGCCAGTAC
	241 - 320	TGCGCCCAGCGCTTCGGCAGGAAGGACCATCTGACTCGGCATGTGAAGAAGAGCCACTCGCAGGAGCTGCTGAAGATCAA
	321 - 400	GGCTGAGCCTCCGGACATGCTGGGTCTGYTGGGCTCCGGCTCGCCGCCCTGCCCCGTCAAAGAGGAGCTCAGCCCCATGA
	401 - 480	TGTGCAGCATGGGTCCCTCCAAGGACCCCCTGATGGCCAAGCCTTTCCCCAGCGGAACCCCCTTCCCCATGGGCATGTAC
	481 - 560	AACCCCCACCACYTGCAGGCCATGTCTGGCCCTGGAGGGGGGCACCACCCCTCTCTAATGCCCGGTTCCCTGTCT
Diplospinus multistriatus	1 - 80	TACAACACCAAGCTGGGCTACAAGCGCCATGTGGCCATGCACTCCGCCACGGCAGGGGANCTCACCTGTAAAGTGTGCAT
	81 - 160	GCAGAGCTACGAGAGCACTCCTGTCCTCCTGGAGCATCTCAAGAGCCACTCGGGGAAGTCGTCCGGCGGAGCCAAGGAGA
	161 - 240	AAAAACACCCGTGNGACCACTGCGACCGCCGTTTCTACACACGGAAGGATGTGAGACGGCACATGGTGGTCCACACYGGC
	241 - 320	CGCAAGGACTTCCTKTGCCAGTACTGYGCCCAGCGCTTYGGCAGGAAGGACCACCTGACCCGCCACGTGAAGAAGAGCCA
	321 - 400	CTCGCAGGAGCTGCTAAAGATCAAGACNGAGCCTCCCGACATGTTGGGTCTTTTAGCCTCGGGGTCACCNCCTTGCTCCG
	401 - 480	TGAAGGAGGAGCTCAGCCCCATGATGTGCGGCATGGGTCCCAACAAAGACCCCATGATGGGCAAACCNTTCCCCAGTGGN
	481 - 560	GCCCCTTTTCCAATGGGTATGTACAACCCCCACCAC

Table A-21. Continued.

Species	Base Pair #	Consensus Sequence
Ditropichthys storeri	1 - 80	AAGCGCCATGTGGCCATGCACTCTGCCACGGCAGGGGACCTTACCTGTAAAGTGTGCATGCAGAGCTTCGAGAGCACGCC
	81 - 160	KGTGCTCCTGGAGCACCTCAAGAGCCACTCAGGGAAGTCCTCRGGTGGCGCSAAGGAGAAAAAACACCCATGTGACCACT
	161 - 240	GCGACCGTCGCTTCTACACTCGGAAGGATGTAAGACGGCACATGGTGGTCCATACAGGYCGAAAGGACTTCCTGTGCCAG
	241 - 320	TACTGCGCCCAGCGCTTTGGCAGGAAGGACCACCTGACACGGCATGTRAAGAAGAGCCACTCGCAGGAGCTGCTGAAGAT
	321 - 400	CAAGACAGAGCCTCCGGATATGTTAAGTCTTTTAGGTTCTGGYTCRCCACCTTGTTCNGTCAAGGAGGAGCTTAGNCCCA
	401 - 480	TGATGTGYAGCATGGGTCCCAACAAAGACCCCATGATGGGCAAACCTTTCCCCAGCGGAACCCCYTTCCCGATGGGCATG
	481 - 560	TATAACCCCCAYCATCTCCAGGCCATGTCCAATTCTGGRGTGGGTCATCCCCACCCCTCCCTGATGCCTAGTCCCCTGTC
Photostomias guernei	1 - 80	AAGTGTGAGGAGTGCGGCAAGCACTACAACACCAAGCTGGGCTACAAGCGNCACGTGGCCATGCACTCNGCCACNGCNGG
	81 - 160	GGACCTGACCTGCAAGGTGTGCCTGCAGAGCTACGAGAGCACGCCGGCNCTGCTGGAGCACCTGAAGAGCCACTCCGGGA
	161 - 240	AGTCGTCNGCNGGNACCAAGGAGAAGAAGCACCCATGNGACCACTGNGACCGCCGCTTCTACACNCGCAAGGACGTGAGG
	241 - 320	CGCCACATGGTGGTGCACACCGGCCGCAAGGACTTCCTGTGCCAGTACTGCGCCCAGCGNTTCGGNAGGAAGGACCACCT
	321 - 400	GACACGGCATGTGAAGAAGAGCCACTCGCAGGAGCTGNTGAAGATYAAGGCRGAGCCGNCRGACATGCTGGGGCTGCTGG
	401 - 480	GCTCYGGCTCRCCRCCNTGTGCYRTCAAGGAGGAGCTCAGCCCCATGATGTGCAGNATGGGTCCCTCCAAGGACCCCCTG
	481 - 560	ATGGCCAAGCCCTTCCCCAGYGGAACTCCCTTCCCCATGGGCATGTACAAYGCCCACCACCTGCAGGCCATGTCCAGCCC
	561 - 640	CGNNGGNNCCCACCACCCNTCGCTGATGCCCGGCTCCCTGTCC
Polymixia lowei	1 - 80	GGCTACAAGCGCCATGTGGCCATGCACTCTGCCACGGCGGGGGACCTCACCTGCAAGGTGTGCATGCAGAGCTACGAGAG
	81 - 160	CACGCCGGTGCTNCTGGAGCACCTGAAGAGCCACTCGGGGAAGTCCACGGGCGGCGCCAAGGAGAAAAAGCACCCGTGCG
	161 - 240	ATCACTGCGACCGTCGCTTCTACACCCGGAAGGATGTCAGGCGGCACATGGTGGTCCACACGGGCCGAAAGGACTTCCTG
	241 - 320	TGCCAGTACTGCGCCCAGCGCTTTGGCCGGAAGGACCACCTGACGCGCCACGTCAAGAAGAGCCACTCGCAGGAGTTGCT
	321 - 400	GAAGATCAAGACGGAGCCTCCGGACATGTTAGGTCTCYTAGGTTCTGGCTCTCCGCCTTGCTCTGTCAAGGAGGAGCTTA
	401 - 480	GCCCTATGATGTGCAGCATGGGTCCCAACAAGGACCCCATGATGGGCAAACCCTTCCCCAGTGGGACCCCCTTCCCCATG
	481 - 560	GGCATGTACAACCCCCACCACCTCCAGGCCATGTCC
Scopelogadus mizolepis	1 - 80	CGACATGTGGCCATGCACTCGGCCACGGCGGGGGACCTCACCTGCAAAGTGTGCATGCAGAGCTACGAGAGCACGCCCGT
	81 - 160	GCTGCTGGAGCACCTCAAGAGCCACTCGGGGAAATCCTCGGGGGGCGCMAAGGARAAGAAGCACCCGTGCGACCACTGYG
	161 - 240	ACCGCCGCTTCTACACCCGCAAGGATGTGMGACGGCACATGGTGGTCCACACGGGCCGAAAGGACTTCCTGTGCCAGTAC
	241 - 320	TGCGCCCAGCGCTTTGGCAGGAAGGACCACCTGACGCGGCACGTCAAGAAGAGCCACTCGCAGGAGCTGCTGAAGATCAA
	321 - 400	RACGGAGCCTCCGGATATGTTAGGGCTTTTAGGGTCCNGKTCCCCACCTTGCTCYGTCAAGGAGGAGCTCAGCCCTATGA
	401 - 480	TGTGCAGCATGGGTCCCAACAAAGACCCTATGATGGGCAAGCCCTTYCCCAGCGGGACCCCCTTCCCGATGGGCATGTAC
	481 - 560	AACCCTCACCACCTC

Table A-21. Continued.

Species	Base Pair #	Consensus Sequence
Sigmops elongatus	1 - 80	GGCTACAAGCGCCATGTGGCCATGCACTCGGCCACGGCAGGTGACCTCACCTGCAAGGTGTGCCTGCAGAGCTACGAGAG
	81 - 160	CACGCCGGCCCTCCTGGAGCACCTGAAGAGCCACTCCGGGAARTCCTCRGGCGGCGCCAAGGAGAAGAAGCACCCGTGCG
	161 - 240	ACCACTGCGACCGCCGCTTCTACACGCGCAAGGACGTCAGACGCCACATGGTGGTGCACACCGGCCGCAAGGACTTCCTG
	241 - 320	TGCCAGTACTGCGCCCAGCGCTTTGGCAGGAAGGACCATCTGACACGGCACGTGAAGAAGAGCCACTCGCAGGAGCTGCT
	321 - 400	GAAGATCAAGGCGGAGCCTCCGGACATGCTGGGGCTGCTGGGGTCCGGCTCGCCGCCCTGCTCTGTCAAAGAGGAGCTCA
	401 - 480	GCCCCATGATGTGCAGCATGGGTCCCTCCAAGGACCCCCTGATGGCCAAGCCTTTCCCCAGCGGGACCCCCTTCCCYATG
	481 - 560	GGCATGTACAACCCCCACCACTTGCAGGCCATGTCCGGCCCTGGGGGGGCCCACCACCCCTCCCTGATGCCC
Sternoptyx pseudobscura	1 - 80	CGCCACGTGGCCATGCACTCGGCCACGGCCGGAGACCTCACCTGCAAGGTGTGCCTGCAGAGCTACGAGAGCACGCCGGC
	81 - 160	CYTGCTGGAGCACCTGAAGAGCCACTCYGGGAAGTCGTCCGGCGGCGCCAAGGAGAAGAAGCACCCGTGCGACCACTGCG
	161 - 240	ACCGCCGCTTCTACACRCGCAAGGACGTCCGGCGCCACATGGTGGTGCACACCGGCCGCAAGGACTTCCTGTGCCAGTAC
	241 - 320	TGCGCCCAGCGCTTTGGCAGGAAGGACCAYCTGACGCGGCAYGTGAAGAAGAGCCACTCRCAGGAGCTGCTGAAGATCAA
	321 - 400	GGCRGAGCCTCCGGACATGCTGGGGCTGTTGGGGTCCRGCTCGCCACCCTGCTCCGTCAAGGAGGAGCTCAGCCCCATGA
	401 - 480	TGTGCAGCATGGGTCCCTCCAAGGACCCGCTGATGGCCAAGCCTTTCCCCAGCGGGACCCCCTTCCCCATGGGCATGTAY
	481 - 560	AACCCCCACCACTTGCAGGCCATGTCCGGCCCSGGGGGGGGSCACCACCCCTCCCTGATGCCCGGCTCC

Table A-22. ENC Consensus Sequences for every species. Polymorphic sites are highlighted in grey.

Species	Base Pair #	Consensus Sequence
Chauliodus sloani	1 - 80	AAGNTGTCCGAGCTSTCCTGGRGCATGTGCCTNNGNAANTTTCCCGCCATTTGCAAGACNGAGGACTTYCTGCAGTTGCC
	81 - 160	CAAAAACATGGCGGTGCAGCTGCTGTCTCACGAGGAGCTGGAGACGGAGGACGAGAGGCTGGTGTAYGAGGCCGCTCTCR
	161 - 240	GCTGGATCAACYACGACCTGGAGAGGCGSCACTGCCAYCTGCCRGAGCTGCTGAGAACCGTCCGTCTGGCCTTGCTGCCC
	241 - 320	GCCATCTTCCTCATGGAGAACGTCTCCACGGAGGAGCTGATCAACGGCCAGGCCAAGAGCAAGGAGGTGGTGGACGAGGC
	321 - 400	CATCCGCTGCAAGCTGAGGATCCTGCAGAACGASGGCGTGGTSACCAGCCCGCTGGCCAGGCCCAGGAAGACNAGCCAYG
	401 - 480	CCCTCTTCCTRCTGGGCGGCCAGACCTTCATGTGCGANAAACTCTACCTGGTGGACCAGAAGGCCAAGGAGATYATCCCC
	481 - 560	AAGGCGGACATMCCYAGCCCCAGGAAGGAGTTCAGNGCCTGCGCCATYGGCTGCAAGGTSTACATCACTGGAGGCAGGGG
	561 - 640	CTCTGAGAACGGAGTCTCCAAGGACGTKTGGGTGTACGACACGTCCCACGAGGAGTGGTCGAARGCGGCTCCCATGCTCA
	641 - 720	TCGCCCGGTTCGGCCACGGC
Diplospinus multistriatus	1 - 80	ACCAAGCTGTCAGAGCTGTCTTGGGGCATGTGTCTCAGCAACTTCCCTGCTATTTGCAAGACAGAGGACTTCCTCCAACT
	81 - 160	GCCCAAAGATATGGTGGTGCAGCTTTTGTCACACGAGGAGCTGGAGACAGAAGATGAGAGACTGGTTTATGAAGCTGCCC
	161 - 240	TGAACTGGATCAACTANGACCTGGAAAGGAGGCACTGTCACCTTCCAGAGCTACTGAGAACGGTCCGTCTTGCCCTGCTG
	241 - 320	CCCGCCATCTTTCTAATGGAGAATGTCTCRACAGAAGAGCTGATCAATGCCCAGGCCAAGAGCAAGGAGCTRGTGGACGA
	321 - 400	GGCTATCCGCTGTAAGCTGAAGATCCTGCAGAATGACGGYGTTGTTAACAGCCCATGTGCTCGACCGAGAAAAACCAGCC
	401 - 480	ATGCTCTCTTTCTCCTGGGAGGGCAGACTTTCATGTGTGACAAGTTGTAYCTGGTGGACCAAAAGGCCAAAGAGATCATC
	481 - 560	CCCAAGGCGGACATTCCCAGCCCCAGGAAGGAGTTYAGCGCCTGTGCCATCGGCTGTAARGTGTACATCACAGGTGGGAG
	561 - 640	AGGCTCHGAGAATGGCGTGTCCAAAGATGTATGGGTCTATGACACCGTCCAYGAGGAATGGTCCAAAGCGGCGCCCATGC
	641 - 720	TCATCGCCAGGTTYGGCCATGGC
Polymixia lowei	1 - 80	CTGTTGCTGTCTGATGCCCACCAGTGTACCAAATTATCAGAGCTCTCCTGGGGCATGTGCCTCAGCAACTTCCCTGCTAT
	81 - 160	TTGCAAGACAGAAGACTTCCTCCAACTGCCCAAAGACATGGTGGTGCAGCTTYTGTCTCACGAGGAGCTGGAGACAGAAG
	161 - 240	ATGAAAGACTGGTTTATGAGGCTGCTCTTAACTGGGTCAACTATGACCTGGAAAGGAGGCACTGCMACCTTCCAGAGCTG
	241 - 320	TTGAGAACAGTTCGCCTGGCMCTGCTTCCTGCCATCTTCCTTATGGAGAATGTCTCCACAGAAGAGCTGATCAATGCCCA
	321 - 400	GGCCAAGAGCAAGGAGCTGGTGGATGAGGCCATCCGCTGCAAGCTGAAGATCTTGCAGAATGATGGTGTNGTTAACAGCC
	401 - 480	CCTGTGCCCGGCCANGAAAAACCAGCCACGCTCTCTTTCTGCTGGGAGGGCAGACCTTCATGTGCGACAAGCTGTACCTG
	481 - 560	GTGGACCAGAAGGCCAAAGAGATCATCCCCAAGGCTGACATCCCCAGCCCCAGGAAGGAGTTCAGCGCCTGYGCCATCGG
	561 - 640	CTGCAAGGTTTACATCACAGGCGGRAGAGGCTCNGAGAATGGCGTGTCGAARGACGTGTGGGTCTATGATACCGTCCACG
	641 - 720	AGGAATGGTCCAAGGCGGCRCCCATGCTCATTGCCAGGTTTGGTCACGGGTCTGCCGAGCTGAAA

Table A-22. Continued.

Species	Base Pair #	Consensus Sequence
Sternoptyx pseudobscura	1 - 80	TGTGCCAAGCTGTCTGAGCTGTCCTGGGGSATGTGCCTCAGCAACTTCCCCGCAATCTGCAAGACMGAGGACTTCCTGCA
	81 - 160	GTTGCCCAAAGACATGGCGGTCCAACTGCTGTCTCACGAGGAGCTGGAGACCGAGGACGAGAGRCTGGTCTAYGAGGCCG
	161 - 240	CCCTCAACTGGGTCAACTAYGACCTGGAGAGGCGTCACTGCCATTTGCCGGAGCTGCTGAGAACYGTCCGTCTGGCCTTG
	241 - 320	YTGCCCGCCATCTTCCTCATGGAGAACGTGTCCACRGAGGAGCTGATCAAYGCCCAGACCAAGAGCAAGGAGCTGGTGGA
	321 - 400	CGAGGCCATTCGCTGCAAGCTGAGGATCCTGCAGAACGAGGGTGTGGTCAACAGCCCACTGGCCCGRCCCAGGAAGACCA
	401 - 480	GCCACGCTCTCTTCYTGYTSGGYGGCCAGACCTTCATGTGTGACAAACTCTACCTGGTGGACCAGAAGGCCAAGGAGATY
	481 - 560	ATCCCCAAGGCRGACATCCCCAGCCCCAGGAAGGAGTTCAGCGCCTGCGCCATYGGCTGCAAGGTCTACATCACCGGAGG
	561 - 640	CAGAGGCTCYGAGAACGGCGTGTCCAAAGAYGTCTGGGTCTACGATACGTCCCACGAGGAGTGGTCGAAGGCGGCTCCCA
	641 - 720	TGCTCATCGCCCGGTTYGGCCACGGATCCGCGGAACTC
Synagrops spinosus	1 - 80	TTGTCTGANGCYCAYCAGTGCACCAAGCTGTCNGAGCTCTCCTGGGGCATGTGCCTCAGCAACTTTCCCGCTATTTGCAA
	81 - 160	GACGGAGGACTTCCTCCAACTGCCCAAAGATATGGTGGTGCAGCTTTTGTCACACGAGGAGCTNGAGACAGAAGAYGAGA
	161 - 240	GACTGGTTTATGARGCTTCCCTTAACTGGATCAACTATGACCTGGAGAAGAGGCACTGCCACCTTCCAGAGCTCCTGAGA
	241 - 320	ACGGTCCGTCTGGCCCTGCTGCCGGCCATCTTCCTCATGGAGAACGTTTCTACAGARGAGCTGATCAATGCCCAGGCCAA
	321 - 400	GAGCAANGARCTGGTGGATGAAGCTATCCGCTGTAAGCTGAAGATCCTGCAGAACGATGGCGTCGTTAACAGNCCGTGTG
	401 - 480	CTCGACCAAGAAAAACCAGCCATGCCCTCTTTCTTCTGGGAGGGCAGACTTTCATGTGNGACAAGTTGTACCTGGTGGAC
	481 - 560	CAGAAAGCCAAAGAGATCATCCCCAAAGCCGACATTCCCAGCCCCAGNAAGGAGTTCAGCGCCTGCGCCATCGGCTGTAA
	561 - 640	GGTGTACATCACTGGTGGGAGAGGCTCRGAGAAYGGCGTNTCCAAAGATGTGTGGGTCTACGACACCGTCCACGAGGAAT
	641 - 720	GGTCGAAGGCGGCACCCATGCTCATNGCCAGGTTCGGCCACGGCTCTGCAGAGCTGAAACACTGCCTCTAC

Table A-23. MYH Consensus Sequences for every species. Polymorphic sites are highlighted in grey.

Species	Base Pair #	Consensus Sequence
Sternoptyx pseudobscura	1 - 80	GCAGTTCCTGGAGCAAAGARGGATCCCAGCAAGGGAACCTTGGAGGATCAAATCATCCAGGCTAACCCTGCCCTGGAGGC
	81 - 160	TTTTGGTAATGCSAAAACATTGAGAAATGACAACTCATCACGCTTTGGCAAATTCATCCGGATTCACTTCGGAACCAGTG
	161 - 240	GCAAGTTGTCCTCTGCAGACGTAGAGACTTATCTTCTGGAAAAGTCACGTGTTACATTTCAGCTCAAGTCAGAGAGGAAC
	241 - 320	TACCATATCTTCTTCCAGATCTTGTCCAATCAAAAGCCAGAGCTGTTGGACATGCTTTTAATCACCAACAATCCATATGA
	321 - 400	CTACTCCTTCATCTCCCAAGGAGAGGTAACAGTAGCATCCATCAATGATTCTGAGGAGTTGTTAGCCACTGACAGTGCAT
	401 - 480	TCGATGTGCTTGGCTTTACTCAAGAGGAGAAAATGGGGATCTACAAATTGACAGGTGCAATCATGCATTACGGTAACATG
	481 - 560	AAGTTCAAGCAAAAGCAGCGCGAGGAGCAGGCAGAGCCTGACGGCACTGAGGCTGCTGACAAAGCAGCTTACCTAATGGG
	561 - 640	GCTGAACTCTGCAGATCTAGCRAAAGGACTCTGC
Synagrops spinosus	1 - 80	GATCAAATCATCCAGGCTAACCCTGCCCTGGAGGCTTTNGGCAATGCCAAAACATTGAGAAATGACAACTCGTCACGCTT
	81 - 160	TGGTAAATTCATCCGGATTCACTTTGGAAACACTGGCAAGTTGTCCTCTGCAGACATAGAGACTTACCTTCTGGAAAAGT
	161 - 240	CACGAGTCACCTTTCAGCTCAAGTCTGAGAGGAACTATCATATCTTCTTCCAGATCTTGTCCAATCAAAAGCCAGAGCTG
	241 - 320	TTGGACATGCTGTTAATCACCAACAATCCATATGACTACTCYTACATCTCCCAAGGAGAGGTAACAGTAGCATCCATCAA
	321 - 400	TGATTCTGAGGAGTTGTTAGCCACTGACAGTGCATTTGACGTGCTTGGCTTTACTCAAGAGGAGAAAATGGGAGTCTACA
	401 - 480	AGTTGACAGGTGCAATCATGCATTACGGCAACATGARGTTCAAGCAAAAGCAGCGNGAGGAGCAGGCAGAGCCTGATGGC
	481 - 560	ACTGAGGCTGCTGACAAGTCMGCTTACCTWATGGGGCTGAACTCTGCAGATCTARTCAAGGGG